

**ELECTRICAL STUDIES OF METHACRYLIC ACID HYDROGELS
MOLECULARLY IMPRINTED WITH HYDROCORTISONE**

By
Carlos M. Ortega-Fuentes

A thesis submitted in partial fulfillment of the requirements for the degree of

MASTER OF SCIENCE

IN

ELECTRICAL ENGINEERING

UNIVERSITY OF PUERTO RICO
MAYAGUEZ CAMPUS
2008

Approved by:

José Rosado Román, Ph.D.
Member, Graduate Committee

Date

Gerson Beauchamp Báez, Ph.D.
Member, Graduate Committee

Date

Eduardo J. Juan García, Ph.D.
President, Graduate Committee

Date

Madeline Torres Lugo, Ph.D.
Representative of Graduate Studies

Date

Isidoro Couvertier, Ph.D.
Chairperson of the Department

Date

Abstract

Electrical studies of cross-linked methacrylic acid hydrogels molecularly imprinted with hydrocortisone were conducted by means of electrical resistivity estimates. A factorial experimental design method was followed to investigate the effect of several factors (hydrogel morphologies, solution pH, hydrocortisone concentration and signal frequency) and interactions between them in the electrical resistance of the hydrogels. It was possible to identify and sort by significance the factors that had the most effect in the electrical response of the hydrogels. Of the studied factors the solution pH had the most significant effect on the electrical response of hydrogels while frequency was the least significant. In average, the response of every combination tested at saturation levels of hydrocortisone concentration (0.24 mg/ml) for the molecularly imprinted group more than doubled the response of the non-imprinted group. Sensitivity and selectivity studies were performed with favorable outcomes at intermediate concentrations (0.12 mg/ml) of hydrocortisone in solution. Finally, this study presents a methodology which can be employed to characterize the electrical response of hydrogels that, when combined with statistical fundamentals, could aid in finding an optimum operating region for an application while reducing the number of testing iterations.

Resumen

La caracterización eléctrica de hidrogeles entrecruzados de ácido metacrílico con impresión molecular con hidrocortisona fue efectuada a través de estimados de resistencia eléctrica. Un diseño de experimento factorial fue desarrollado con el fin de investigar el efecto de varias variables (morfología de los hidrogeles, pH de la solución, concentración de hidrocortisona y frecuencia de la señal) e interacciones entre las mismas en la resistencia eléctrica de los hidrogeles. Fue posible identificar y ordenar por significancia las variables que tuvieron mayor efecto en la respuesta eléctrica de los hidrogeles. El valor de pH resultó ser el factor más significativo en la respuesta eléctrica de los hidrogeles, mientras que la frecuencia fue el factor menos significativo. En promedio la respuesta de los hidrogeles con impresión molecular fue al menos el doble que las del grupo de control en todas las pruebas efectuadas a niveles de saturación de hidrocortisona (0.24 mg/ml) en solución. Estudios de sensibilidad y selectividad fueron efectuados con resultados favorables a concentraciones intermedias (0.12 mg/ml) en solución de hidrocortisona. Finalmente, este estudio presenta una metodología que puede ser utilizada para caracterizar la respuesta eléctrica de hidrogeles que al ser combinada con fundamentos estadísticos puede ayudar a encontrar un punto de operación óptimo para una aplicación mientras se reduce el número de iteraciones durante la fase experimental.

To my wife Rhaiza Vélez for her unconditional support.

Acknowledgments

I would to thank everybody that in some way or another supported the conclusion of this work. First of all I would like to thank my wife Rhaiza Vélez for all her love and constant support all these years. Lorena Padró, the best research partner someone could ask for. Thank you for not only being my research partner on all those long nights and weekends at the lab after work, but most importantly for being a true friend. Your guidance as well as the many technical discussions we shared at the lab were invaluable for the completion of this work. I would also like to thank my thesis advisor Eduardo J. Juan for giving me the opportunity to work under his guidance. Special thanks to Madeline Torres for allowing me the opportunity to work at her research laboratory in addition to all her technical and documentation support. I also want to thank the rest of my graduate committee members, Gerson Beauchamp and Jose Rosado for their collaboration to make this work a better one. Finally, I would like to thank Luis Serrano at IAS for always being flexible with my work schedule to allow me to complete my academic responsibilities. Without the support of all of you this chapter would not have come to an end, thank you.

Table of Contents

List of tables.....	viii
List of figures	ix
1. Introduction.....	1
2. Theoretical Background and Literature Review	5
2.1 Biosensors.....	5
2.2 Principles of biosensors based on molecularly imprinted polymers	7
2.2.1 Molecular imprinting technology fundamentals	7
2.2.2 Developing molecularly imprinted hydrogels.....	11
2.3 Molecularly imprinted hydrogels as sensing devices.....	13
2.3.1 Hydrogels fundamentals.....	13
2.3.2 Electrical properties of hydrogels.....	16
2.3.3 Electrical conductivity studies in hydrogels	19
2.3.4 Electrical studies of molecularly imprinted polymers	22
2.4 Factor Analysis	27
3. Objectives.....	30
4. Materials and Methods.....	31
4.1 Experimental Design	31
4.1.1 Electrical resistance of MAA-TEGDMA hydrogels.....	31
4.1.2 Electrical resistance of MIP's as function of hydrocortisone concentration.....	33
4.1.3 Selectivity of MIP's to an analog template molecule.....	35
4.2 Experimental components and setup.....	36
4.2.1 Silver/Silver Chloride (Ag/AgCl) Electrodes.....	36
4.2.2 Instrumentation amplifier development	38
4.2.3 Graphical user interface development	41
4.2.4 Experimental setup	42
4.3 Hydrogel synthesis.....	45
4.4 Hydrogel swelling procedure	45
4.5 Electrical studies of MAA crosslinked hydrogels	47

4.5.1 Electrical characterization experiments.....	47
4.5.2 MIP's sensitivity experiments.....	49
4.5.3 MIP's selectivity experiments.....	51
5. Results and Discussion	53
5.1 Virtual Instrument Validation.....	53
5.2 MAA-TEGDMA hydrogels electrical studies.....	56
5.2.1 Experimental protocol.....	56
5.2.2 Non-molecularly imprinted MAA-TEGDMA hydrogels	61
5.2.3 Molecularly imprinted MAA-TEGDMA hydrogels.....	63
5.3 Factor analysis of electrical resistivity of MAA-TEGDMA hydrogels.....	66
5.3.1 Analysis of variance: MAA-TEGDMA Reference hydrogels resistivity versus composition, pH, concentration and frequency	66
5.3.2 Analysis of variance: MAA-TEGDMA molecularly imprinted hydrogels resistivity versus composition, pH and concentration	73
5.3.3 Comparison of non-imprinted and molecularly imprinted hydrogels resistivity as function of composition, pH and template concentration	77
5.4 Sensitivity studies of molecularly imprinted MAA-TEGDMA hydrogels	79
5.5 Selectivity studies of molecularly imprinted MAA-TEGDMA hydrogels	85
5.6 Swelling and electrical resistivity correlation of MAA-TEGDMA hydrogels.....	88
6. Conclusions	92
7. References	94
8. Appendix	97

List of tables

1: General characteristics of molecularly imprinted polymers [4]	9
2: Biological active species that can be immobilized on and within hydrogels [19].....	12
3: General arrangement for a two factor factorial design [42]	29
4: Analysis of variance for a general two factor fixed effects model.....	29
5: Factors and levels taken into consideration during first stage of experiments for the electrical characterization of MAA-TEGDMA hydrogels.....	32
6: Factors and levels taken into consideration during second stage of experiments for the electrical characterization of MAA-TEGDMA hydrogels	34
7: Factors and levels taken into consideration during third stage of experiments for the electrical characterization of MAA-TEGDMA hydrogels	35
8: Glutaric acid hydroxide buffer guide.....	47
9: Concentration of hydrocortisone in buffer solution for MIP's sensitivity experiments.....	50
10: Concentration of fluorescein sodium salt in buffer solution for MIP's selectivity experiments	51
11: Summary of validation results of virtual instrument using a controlled setup in which resistance values were known <i>a priori</i>	55
12: General linear model: hydrogels resistivity versus hydrogel composition, solution pH, concentration and frequency	66
13: Factors and levels used in analysis of variance of molecularly imprinted MAA-TEGDMA hydrogels resistivity.....	73
14: Least Squares Means for Hydrogels Resistivity (ohms*cm).....	77
15: Pearson correlation coefficients – electrical resistivity and swelling of MAA-TEGDMA hydrogels (non-imprinted and molecularly imprinted) by pH levels.	91

List of figures

1: Generalized medical instrumentation system. Dashed lines in the diagram represent optional elements in the system [2].....	1
2: Schematic representation of a conceptual biosensor. The recognition of a particular molecule is converted to an electrical signal [13].	5
3: Biosensors transduction mechanisms and device types [15].....	6
4: Imprinting Process. (A): Solution mixture of template, functional monomer(s) Cross-linking monomer, solvent and initiator. (B): The pre-polymerization complex is formed via covalent or non-covalent chemistry. (C): The formation of the network. (D): Wash step where original template is removed. (E): Rebinding of template. (F): In less cross-linked systems, movement of the macromolecular chains will produce areas of differing affinity and specificity [16].....	8
5: Applications of imprinted hydrogels. (A) Intelligent release. (B) Targeted Drug Delivery, (C) Micro-fluidic Devices [18].....	10
6: The three major components (physical, polymer and biological) of a biosensor based on MIP's [19].....	11
7: Schematic of MIP preparation using a non-covalent approach [14].	13
8: Hydrogel structure which includes its polymeric chains, cross-links, fluid filled regions and ions [29].	15
9: Apparatus for measuring specific resistances of membranes, (A) Vacik and Kopecek 1975 [32], (B) Gu and Justiz 2002 [37].	18
10: (A) Hydrogel Impedance as a function of the excitation frequency. Numbers on the plots denote the diameter of the membranes. Error bars represent ± 2 SD. (B) Hydrogel phase as function of the excitation voltage. Numbers denote the excitation frequency [23].	20
11: Swelling kinetics of hydrogels with immobilized glucose oxidase measured (bars) and estimated from conductivity measurements (straight lines) at several glucose concentrations. Error bars represent ± 3 SD [23].	21
12: Influence of the herbicide concentration in solution of the sensor response. ■ triazine, □ simazine, ♦ atrazine [39].	24
13: (A) The difference in the responses (MIP and ref-MIP based) of the conductometric sensors as function of the mass of benzyltriphenylphosphonium chloride added. (B) The response time of a MIP based conductometric sensor. The response was recorded after the addition of 2000 μg of benzyltriphenylphosphonium chloride [41].	25
14: (A): Responses to atrazine as function of the cross-linking agent (TEDMA) concentration: (1) MIP Membrane; (2) Reference membrane. Measurements were carried out in 25 mmol dm^{-3} potassium phosphate buffer (pH 7.5) containing 35 mmol dm^{-3} NaCl. (B): Responses to atrazine as a function of porogen (Chloroform) concentration [40].	26

15: Design of experiment used in first stage of experiments to analyze the contribution of the identified factors in the electrical conductivity of MAA-TEGDMA hydrogels.	33
16: Design of experiment used in second stage of experiments to assess the relation between the electrical resistance of MIP's and template molecule concentration.	34
17: Design of experiment used in final stage of experiments to assess the selectivity of MIP's to an analog template molecule.	35
18: Equivalent electrode circuit in contact with an electrolyte. E_{hc} is the half cell potential, R_d and C_d make up the impedance associated with the electrode-electrolyte interface and polarization effects, and R_s is the series resistance associated with interface effects and due to resistance in the electrolyte [2].....	36
19: Impedance as function of frequency for A_g electrodes coated with an electrolytically deposited A_gC_l layer. The electrodes area is 0.25 cm^2 . Numbers attached to curves indicate number of mA*s for each deposit [2].....	37
20: Ag/AgCl electrodes used in experiments of the electrical characterization of MAA-TEGDMA hydrogels.	38
21: Analog Devices instrumentation amplifier AD620 connection diagram [44].....	39
22: (A) Circuit schematic of instrumentation amplifier used in the experiments. Voltage gains of 1, 2, 5 and 10 V/V and DC offset compensation. (B) Actual instrumentation amplifier used in the experiments.	40
23: User interface controls and indicators used to setup and monitor the experiments respectively.....	41
24: From top to bottom, time domain acquired voltage signals across control resistance and sample membrane, amplitude and phase spectrum of acquired signals.	42
25: Experimental setup diagram.....	43
26: Actual experimental setup used to perform the experiments. (A) Water pump (Master Flex – Cole-Parmer Instrument Company), (B) Heater (Precision 180 Series Water Bath), (C) Electrodes and Diffusion Cells, (D) Electric circuit board with current control resistance, (E) Custom made differential amplifier, (F) Data acquisition board (National Instruments BNC-2090), (G) Personal Computer.....	44
27: Hydrogels after circular disks have been sliced in order to equilibrate them in glutaric acid hydroxide buffer at several pH values.	46
28: Flowchart of electrical characterization of hydrogels experiments.	49
29: Flowchart of sensitivity experiments performed on MIP's as function of template molecule concentration under equilibrium conditions.	50
30: Flowchart of selectivity experiments performed on MIP's with hydrocortisone to analog molecule fluorescein sodium salt under equilibrium conditions.....	52

31: Experimental setup used to determined error induced by the instrumentation and virtual instrument.....	54
32: Experimental setup used to estimate MAA-TEGDMA hydrogels resistance.....	54
33: Estimated resistances from a simulation run in order to determine the error induced by the virtual instrument and instrumentation. Three replicates were performed taking three samples at each frequency interval (100 – 5kHz, $\Delta f = 100\text{Hz}$). Each of the values plotted represents an average of three sampled data points.....	55
34: Estimated currents (mA) for glutaric acid sodium hydroxide buffer pH 3.2 and buffer + non-MIP MAA-TEGDMA (17:1) hydrogels. Buffer + hydrogel trials produced a lower net current in the system than that of the buffer trials.....	57
35: Sample replicates of MAA-TEGDMA electrical studies. From top to bottom, left to right: (a) estimated electrical resistance of glutaric acid sodium hydroxide buffer pH 3.2; (b) estimated electrical resistance of buffer + hydrogel samples; (c) estimated electrical resistance of hydrogels calculated offline; (d) estimated hydrogels resistivity calculated offline. Each data point represents the mean value of 3 samples for a total of 150 samples per replicate.....	59
36: Sample plot of electrical studies on MAA-TEGDMA (17:1) hydrogels equilibrated at pH 3.2. (Top) Buffer phase as function of frequency, (Middle) Buffer + Hydrogel phase as function of frequency, (Bottom) estimated hydrogel phase calculated offline as the difference between curves Middle and Top. Each data point represents the average from 3 replicates (n = 9), error bars do not show in plot due to their small magnitude compared to the scale.	60
37: Estimated electrical resistivity as function of pH and hydrocortisone concentration for MAA-TEGDMA non-imprinted. Vertical bars represent the average value from 3 replicates (n = 450) while error bars represent the mean standard deviation.....	62
38: Estimated electrical resistivity as function pH and hydrocortisone concentration for MIP MAA-TEGDMA hydrogels. Vertical bars represent the average value from 3 replicates (n = 450) while error bars represent the mean standard deviation.....	64
39: Normalized estimated resistivity of MAA-TEGDMA non-imprinted and imprinted with hydrocortisone as function of buffer pH (3.2, 4.8 and 5.4), hydrogel composition (17:1 and 39:1), hydrocortisone concentration (0 mg/ml and 24 mg/ml) and input signal frequency (100 – 5000 Hz). Each block represents the mean value (3 replicates, n = 450) for each of the 24 combinations studied stacked in a normalized resistivity value per pH tested.	65
40: Main effects plot of the factors taken into consideration during electrical studies of reference MAA-TEGDMA hydrogels. Data points represent the mean value for each of the levels studied within the main factors.....	67
41: Interactions plot of the factors and levels taken into consideration during electrical studies of reference MAA-TEGDMA hydrogels. Data points represent the mean value for each of the combinations studied.	67

42: Four in one plot of residuals of analysis of variance of the electrical resistivity of reference MAA-TEGDMA hydrogels, n = 1800.	68
43: Normal probability plot at 95% confidence interval of standardized residuals of analysis of variance of reference MAA-TEGDMA hydrogels.	68
44: Pareto chart of standardized effects up to two way interactions for non-MIP MAA-TEGDMA hydrogels. Effects to the right of vertical line are considered statically significant.	70
45: Modified (frequency less) main effects plot of the factors taken into consideration during electrical studies of reference MAA-TEGDMA hydrogels. Data points represent the mean value for each of the levels studied within the main factors.	71
46: Modified (frequency less) interaction plot of the factors and levels taken into consideration during electrical studies of reference MAA-TEGDMA hydrogels. Data points represent the mean value for each of the combinations studied.	71
47: Four in one plot of residuals of analysis of variance of the electrical resistivity of reference MAA-TEGDMA hydrogels without frequency as a factor, n = 24.	72
48: Normal probability plot at 95% confidence interval of standardized residuals of analysis of variance of reference MAA-TEGDMA hydrogels (frequency less).	73
49: Pareto chart of standardized effects up to two way interactions for MIP MAA-TEGDMA hydrogels. Effects to the right of vertical line are considered statically significant.	74
50: Modified (frequency less) main effects plot of the factors taken into consideration during electrical studies of molecularly imprinted MAA-TEGDMA hydrogels. Data points represent the mean value for each of the levels studied within the main factors.	75
51: Modified (frequency less) interaction plot of the factors and levels taken into consideration during electrical studies of molecularly imprinted MAA-TEGDMA hydrogels. Data points represent the mean value for each of the combinations studied.	75
52: Four in one plot of residuals of analysis of variance of the electrical resistivity of molecularly imprinted MAA-TEGDMA hydrogels without frequency as a factor, n = 24.	76
53: Normal probability plot at 95% confidence interval of standardized residuals of analysis of variance of molecularly imprinted MAA-TEGDMA hydrogels (frequency less).	76
54: Least squares mean resistivity delta between high level (0.24 mg/ml) and low level (0.0 mg/ml) concentration of hydrocortisone in solution per tested group and level.	78
55: Distribution of estimated resistance of glutaric acid sodium hydroxide buffer at pH 3.2 for all tested combinations of 17:1 hydrogels during first stage of experiments. Bars 1 - 4 from left to right represent the average resistance value for each of the sample (n = 450) while 5 th bar is the average of all samples (n = 1800). Error bars represent the mean standard deviation.	81
56: Estimated electrical resistivity for MAA-TEGDMA (17:1 molar ratio) non-imprinted and molecularly imprinted as function of hydrocortisone concentration. Data points represent	

mean value for each replicate (n = 3) at an excitation signal frequency of 2.5 KHz in a glutaric acid sodium hydroxide buffer pH 3.2.	83
57: Evaluation of change in electrical resistivity of MAA-TEGDMA (17:1 molar ratio) non-imprinted and molecularly imprinted as function of hydrocortisone concentration. Delta values were calculated as the difference in electrical resistivity at each concentration value and the baseline value of resistivity $C_0 = 0$ mg/ml. Data points represent mean value (n = 3) at an excitation signal frequency of 2.5 KHz in a glutaric acid sodium hydroxide buffer pH 3.2.....	84
58: Estimated electrical resistivity for MAA-TEGDMA (17:1) molecularly imprinted with hydrocortisone as function of Fluorescein Sodium Salt concentration. Data points represent mean value for each replicate (n = 3) at an excitation signal frequency of 2.5 KHz in a glutaric acid sodium hydroxide buffer pH 3.2.	86
59: Evaluation of change in electrical resistivity of MAA-TEGDMA (17:1) molecularly imprinted with Hydrocortisone as function of Fluorescein Sodium Salt concentration. Delta values were calculated as the difference in electrical resistivity at each concentration value and the baseline value of resistivity at $C_0 = 0$ mg/ml. Data points represent mean value (n = 3) at an excitation signal frequency of 2.5 KHz in a glutaric acid sodium hydroxide buffer pH 3.2.....	87
60: Evaluation of change in electrical resistivity of MAA-TEGDMA (17:1) molecularly imprinted with hydrocortisone as function of Hydrocortisone and Fluorescein Sodium Salt concentration. Delta values were calculated as the difference in electrical resistivity at each concentration value and the baseline value of resistivity at $C_0 = 0$ mg/ml. Data points represent mean value (n = 3) at an excitation signal frequency of 2.5 KHz in a glutaric acid sodium hydroxide buffer pH 3.2.....	88
61: Estimated resistivity and equilibrium swelling [45] of MAA-TEGDMA non-imprinted and imprinted with hydrocortisone as function of glutaric acid sodium hydroxide buffer pH value. Resistivity data points represent the average value from 3 replicates (n = 450) while swelling value represent the average value from 3 replicates. Errors bars represent the mean standard deviation.	89
62: Scatter plot of electrical resistivity and swelling of reference and molecularly imprinted MAA-TEGDMA (17:1 and 39:1 molar ratio) hydrogels at three different glutaric acid sodium hydroxide buffer pH values (3.2, 4.8 and 5.4). Electrical resistivity data points correspond to average of 3 samples taken at an input signal frequency of 2.5 KHz for each replicate.	90
63: Scatter plot of MAA-TEGDMA hydrogels (non-MIP and MIP) resistivity versus swelling grouped by pH.	91

1. Introduction

Advance on clinical devices is indispensable to improve the accuracy and efficiency of patients' diagnosis [1]. Medical instrumentation plays a key role in the clinical process and it is used by medical practitioners to diagnose, treat and monitor patients' welfare. A generalized medical instrumentation system diagram is presented in Figure 1. The sensor element is one of the most important components of these systems and their main function is to convert a physical quantity into another form, usually an electrical signal that is proportional to the information of interest. In the case of sensors used to measure biological agents the term biosensor is commonly employed and their development is of significant importance on the medical instrumentation industry [2].

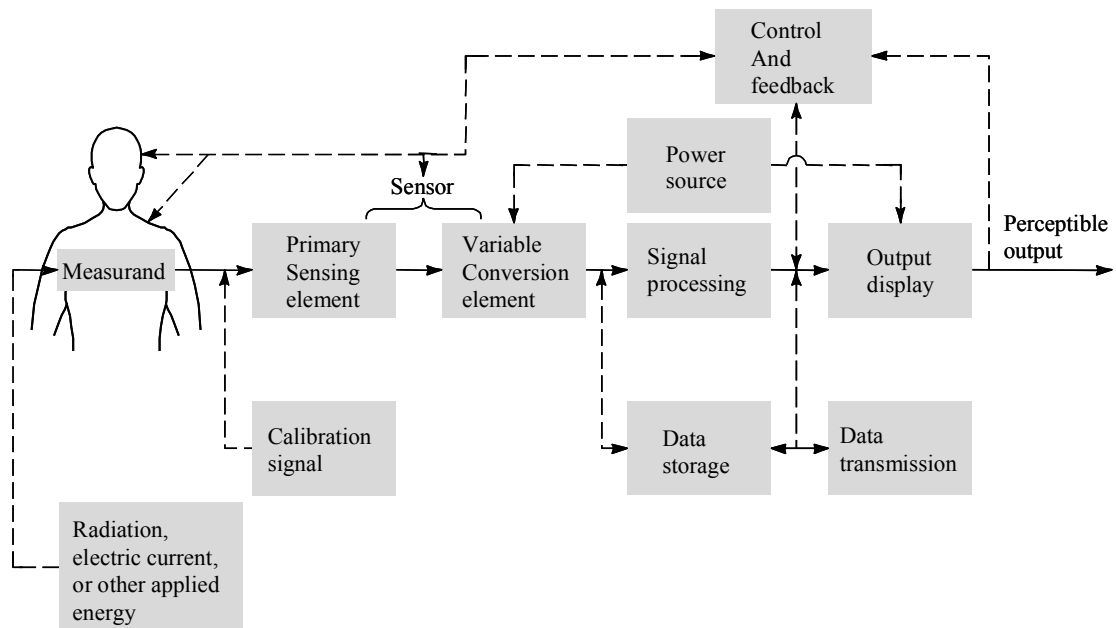


Figure 1: Generalized medical instrumentation system. Dashed lines in the diagram represent optional elements in the system [2]

Biosensors are typically composed of three main elements: a transducer that converts a reaction of interest into an electrical signal, a biological component responsible for the recognition of a target compound and an interface component that integrates the biological component with the transduction method. The response of biosensors is a function of the affinity and specificity of their recognition element. Biosensors based on molecular imprinting technique (MIT) have been one of the studied alternatives towards the development of high affinity and specificity materials with numerous successful applications [3]. Several of the advantages of molecularly imprinted polymers (MIP's) which make them suitable as sensing devices are their low cost, storage endurance, and physical and chemical stability when compared to their biological counterparts [4].

Despite the fact that molecular imprinting technology shows great promise, several factors were identified by Piletsky and co-workers as critical for successful design of the next generation of sensors based on molecularly imprinted polymers [3, 5] (2001-2002): (a) development of transducers with high sensitivities capable of monitoring the binding process between the receptor sites and template molecule, transforming it into a processable signal; (b) development of imprinted polymers capable of interacting with the template-analyte under the required conditions and required affinity and specificity; and (c) integration of the MIP with the transducer. Piletsky and co-workers [3] (2002) also highlighted that even though numerous successful examples of the development of MIP electrochemical sensors exist, the commercial market for the product is still considerably low. This is attributed to: (a) development and validation of a general protocol for MIP design; (b) development of MIP's capable of effectively functioning in water; (c)

need for a substantial increase in polymer affinity and improvement of the ratio between specific and non-specific binding; (d) development of effective immobilization protocols.

The foundation for a non-invasive biosensor based on molecularly imprinted hydrogels with hydrocortisone using a conductometric transduction method was the main interest in this research. Hydrocortisone is a synthetic form of Cortisol, a corticosteroid hormone released by the adrenal glands shown to have a direct relation to stress levels in individuals [6]. The American Institute of Stress has reported that many health problems in the United States are due to stress related diseases [7]. Typically, Cortisol levels in individuals are measured by means of invasive blood test exams. Electrical characterization of Methacrylic Acid Tetra(ethyleneglycol) Dimethacrylate (MAA-TEGDMA) hydrogels imprinted with hydrocortisone as function of several measurable factors will be the basis for the future biosensor development. For this, an analysis of variance of the electrical resistance of the hydrogels as function of the following factors and levels were taken into consideration: (a) hydrogel morphology (functional monomer to cross-linker ratio), (b) hydrogel variant (non-imprinted versus molecularly imprinted hydrogels), (c) liquid medium pH (3.2, 4.8, 5.4) , (d) concentration of template molecule in solution (none and saturated) and (e) input voltage signal frequency (frequency sweep from 100-5kHz, $\Delta f = 100$ Hz). This analysis will allow a better understanding of the electrical properties of hydrogels in general and the principles that govern them. Additionally, it will also permit future biosensor performance optimization due to the comprehension of how the different studied factors or interaction between them affects sensor operation.

Understanding how the electrical properties of the MAA-TEGDMA hydrogels are altered as function of the factors and levels mentioned above would be instrumental in a future development and design of a hydrogel-based biosensor used for the assessment of concentration of Cortisol utilizing molecularly imprinted polymers. Relevance of this particular future biosensor development resides in the fact that aside from being released into the bloodstream as a result of stress or agitated states [8], abnormal levels of Cortisol have been associated with the following conditions [6]: (a) Cushing's syndrome, (b) Addison's disease, (c) increase in blood pressure, (d) clinical depression, (e) suppression of immune system, (f) damage to cells in the hippocampus and (g) hyperglycemia. Therefore, being able to correctly quantify Cortisol concentration levels could provide valuable information regarding the physiological state of an individual. Medical practitioners can take advantage of this tool to monitor patients' Cortisol levels that can aid them in the prevention and diagnosis of diseases.

2. Theoretical Background and Literature Review

2.1 Biosensors

Biosensors are “devices that incorporate a biological or biochemical recognition system in conjunction with a transducer, yielding an electrical signal proportional to the analyte concentration” [9]. Development of biosensors that allow fast, accurate, simple and inexpensive ways of measuring a wide variety of analytes fuels a vast research industry [10, 11]. The principal parameters that describe biosensors performance are selectivity, sensitivity, stability, re-usability and response time. A broad range of applications exists for biosensors which include: clinical diagnostics, food and agricultural processes, measurement of environmental pollutants, detection of warfare agents and bio-process control [9, 10, 12]. Figure 2 shows a schematic of a typical biosensor.

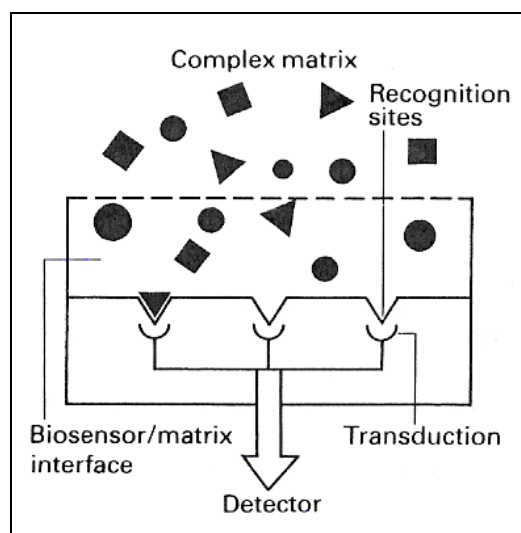


Figure 2: Schematic representation of a conceptual biosensor. The recognition of a particular molecule is converted to an electrical signal [13].

Several types of transducers are common in the development of biosensors in which the transduced parameter mainly depends on the type of bio-analytical event concerned [14]. Some of the most common types of biosensors transduction principles include: (a) potentiometric (operate in almost zero current flow to measure the difference in potential between a working and a reference electrode), (b) amperometric (operate at a fixed voltage to measure the current generated or consumed by oxidation/reduction), (c) conductometric (total electrical resistance is measured to the flow of an alternate current), (d) mass (resonant frequency of bulk material is measured) and (e) thermal (generation or consumption of heat of an analyte and recognition component is measured) [10]. Figure 3 shows several of the most common transduction parameters for biosensors classified by either electrochemical or electromagnetic device type.

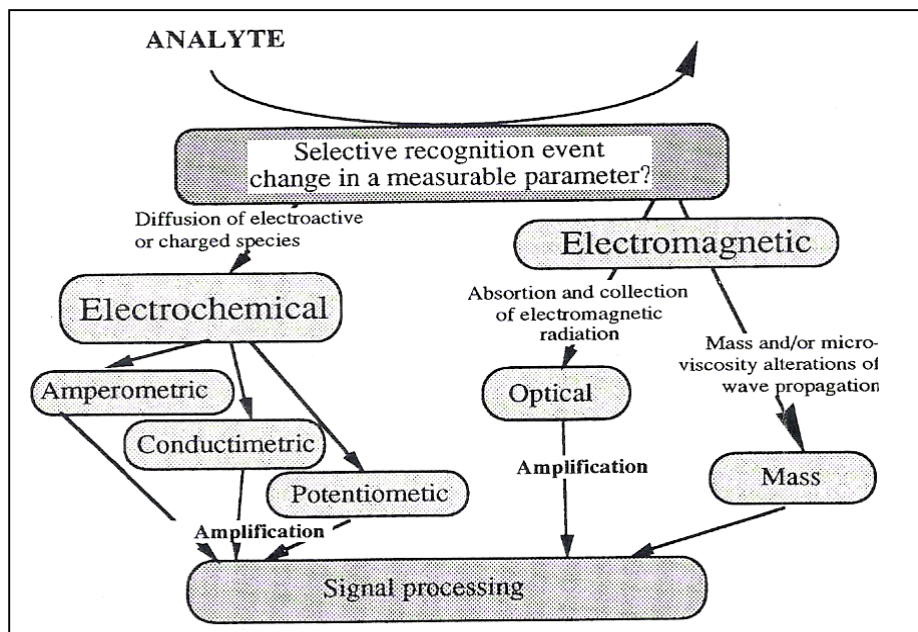


Figure 3: Biosensors transduction mechanisms and device types [15].

2.2 Principles of biosensors based on molecularly imprinted polymers

2.2.1 Molecular imprinting technology fundamentals

The laboratories of Wulff and Klotz in 1972 independently reported the preparation of organic polymers with predetermined ligand selectivities giving birth to modern molecular imprinting technology (MIT) [10]. MIT, a novel and still under development area of study mimics nature by making artificial locks for molecular keys in a process similar to nature's (a) enzyme/substrate binding, (b) protein/receptor interactions and (c) complementary RNA or DNA hybridization [4, 16]. The principle of MIT is based on the cross-linking polymerization in the presence of binding site monomers around a molecule that acts as a template. The molecule is incorporated during the polymer synthesis as a template and later on removed, thus leaving a three dimensional physical and chemical imprint of itself. After removal of the template, an imprint of specific shape and with functional groups capable of chemical interactions remains in the polymer [17]. The complete process of a typical molecular imprinting process is illustrated in Figure 4.

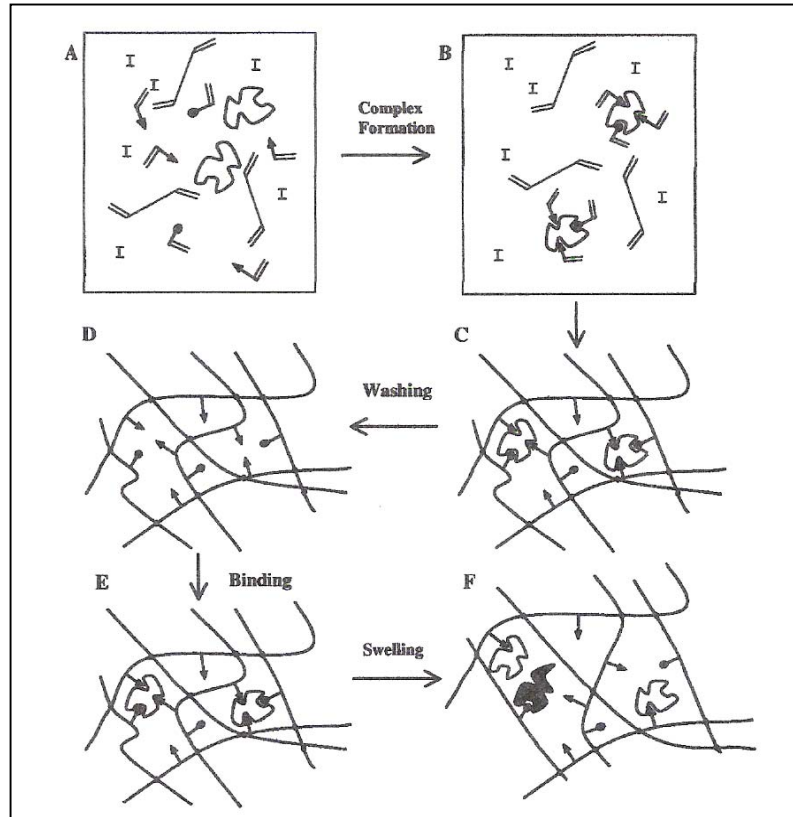
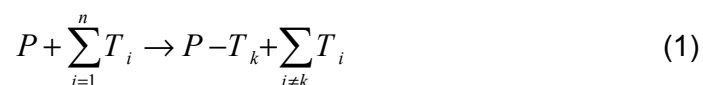


Figure 4: Imprinting Process. (A): Solution mixture of template, functional monomer(s) Cross-linking monomer, solvent and initiator. (B): The pre-polymerization complex is formed via covalent or non-covalent chemistry. (C): The formation of the network. (D): Wash step where original template is removed. (E): Rebinding of template. (F): In less cross-linked systems, movement of the macromolecular chains will produce areas of differing affinity and specificity [16].

The recognition process can be represented as a chemical reaction as:



where the polymer P specifically recognizes the target T_k from a mixture of molecules $T_i (i=1, n)$ and forms a polymer/target complex. These targets can be classified by size and shape as: (a) small molecules with sizes scaling to that of the repeating units in the polymer (such as sugars molecules and amino acids, (b)

large molecules (such as various proteins in their native state) and (c) large molecules with loose shapes (such as synthetic hetero-polymers) [16]. Table 1 presents a summary of the general characteristics of molecularly imprinted polymers.

Table 1: General characteristics of molecularly imprinted polymers [4]

Feature	Characteristics
Physical stability	Resistant against mechanical stress, high pressures and temperatures
Chemical stability	Resistant against acids, bases, various organic solvents and metal ions
Storage endurance	Several years without loss of performance
Capacity	0.1 – 1 mg print molecule/g polymer in enantioselective chromatography
Recovery yield	> 99%
Binding strength	nM range

These characteristics have allowed a broad and diverse field of applications for molecularly imprinted polymers that can be classified in four main categories [4]: (a) separation and isolation, (b) antibody and receptor mimics in immunoassay-type analyses, (c) enzyme mimics in catalytic applications and (d) biosensor-like devices. Figure 5 presents three examples of applications of imprinted hydrogels used for intelligent release, targeted drug delivery and micro fluid devices.

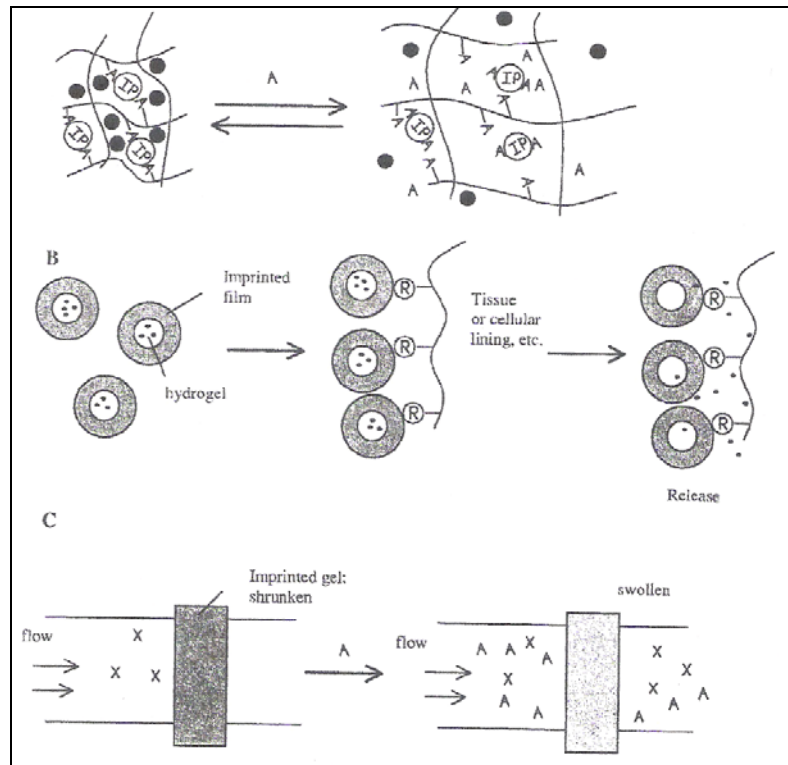


Figure 5: Applications of imprinted hydrogels. (A) Intelligent release. (B) Targeted Drug Delivery, (C) Micro-fluidic Devices [18].

Of these developed MIP based applications biosensors have been studied as alternate sensing devices and multiple applications have been developed [3]. They consist of an electrochemical sensor that contains immobilized molecules or cells in its surface. These biological species are contained on or within a membrane that acts as recognition element interfacing between the bio-molecular or cellular system and the physical sensor components. This physical component is responsible for the conversion of a chemical signal into an electrical one. Examples of commonly used conversion components include: optical fibers, piezo-electric crystals, semi-conductors and electrode systems. Of these physical conversion components electrodes systems are one of the most commonly used.

In essence, electrode systems produce a net charge change on their surface that is used as the transduction mechanism. Figure 6 presents a schematic of the three major components of a biosensor based on polymers with molecular recognition capability.

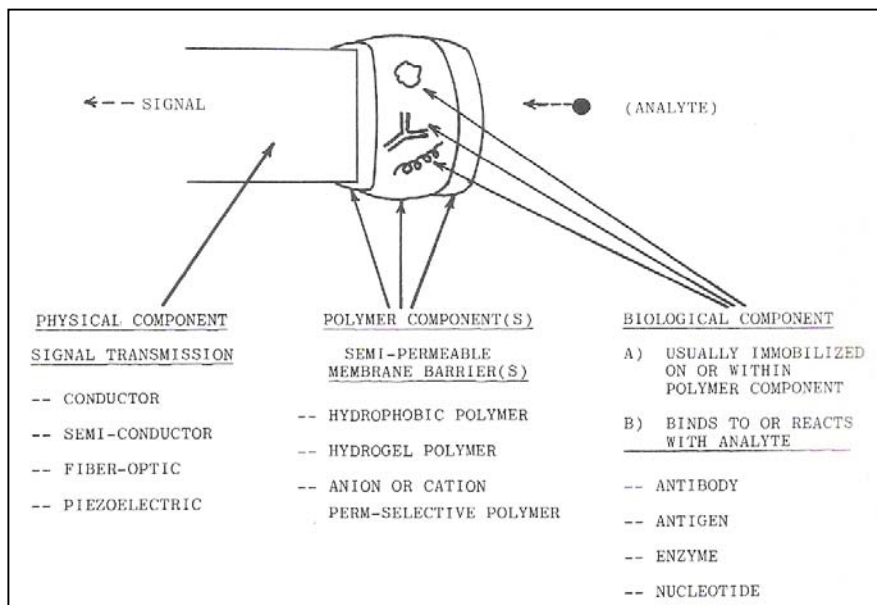


Figure 6: The three major components (physical, polymer and biological) of a biosensor based on MIP's [19].

2.2.2 Developing molecularly imprinted hydrogels

The most straightforward technique to prepare hydrogels with molecular recognition ability is to directly immobilize biological active species on the polymer surface [18]. Hydrogels exhibit good tissue biocompatibility and may interact less strongly with immobilized species than more hydrophilic materials. Thus, molecules and cells immobilized on or within hydrogels may be more likely to retain their biological activity for longer periods of time [19]. Several methods can be used to prepare hydrogels for the immobilization of bio-molecules and cells

such as: (a) bulk polymerization, (b) grafting to a support, and (c) conversion of existing polymers. Table 2 presents samples of immobilized biological active species within hydrogels and their corresponding applications.

Table 2: Biological active species that can be immobilized on and within hydrogels [19]

Species	Applications
Enzymes	Therapeutic agents and reactors, biosensors, artificial organs, red blood cells substitutes, industrial reactors
Antibodies and antigens	Immunoassays, therapeutics and diagnostics, biosensors
Antithrombogenic agents	Artificial organs, blood compatible surfaces
Drugs	Drug delivery systems, drug mechanism studies
Hormones	Biosensors
Cells and organelles	Bioreactors, artificial organs, biosensors
Amino acids	Peptide synthesis
DNA	DNA probe assays

However, a more traditional method of preparing hydrogels with molecular recognition ability is by using a synthetic approach. Since bio-molecules for specific targets are not always available or may lack long term stability the synthetic approach for the development of polymers with recognition ability is widely used. Traditionally, MIP's are highly cross-linked networks with limited movement of the memory sites in the presence of swelling phenomena among other processes [18]. This is a significant difference in regards to its biological counterparts where bio-molecules possess enough mobility and the recognition process occurs usually as conformation adaptation is experienced [16]. A schematic for the preparation of MIP's is presented in Figure 7 using a non-covalent approach. The procedure consists of mixing the functional and cross-linking monomers, radical initiator and imprint molecule in a proper solvent to allow the formation of complexes between the functional monomers and the imprint molecule. The functional monomers are held in place by the polymerization

procedure and once the imprint molecule is extracted the MIP contains the recognition ability for the specific molecule of interest.

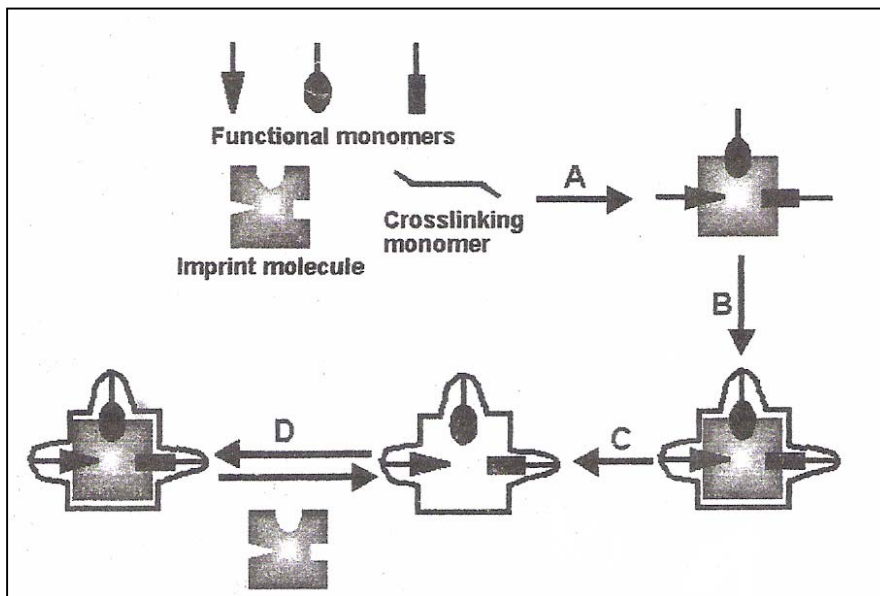


Figure 7: Schematic of MIP preparation using a non-covalent approach [14].

2.3 Molecularly imprinted hydrogels as sensing devices

2.3.1 Hydrogels fundamentals

Hydrogels are defined as polymeric materials that exhibit the ability to swell in water and retain a significant amount of water within its structure without dissolving [19]. Typically, the mass fraction of polymer is much lower than the mass fraction of water, occupying only 5-10% of the volume while providing structural stability that prevents fluid from flowing away [20]. Hydrogels consist of three-dimensional networks of polymer chains and water that fills the space between macromolecules [21]. The three dimensional water-swollen structure of hydrophilic homopolymers or copolymers are cross-linked chemically and/or physically [22]. Also, most hydrogels are considered to be biocompatible due their

ability to resemble natural tissue as consequence of their high water content and special surface properties [19]. One major disadvantage of hydrogels is their relatively low mechanical strength, which can be improved by means of cross-linking, formation of interpenetrating networks and/or crystallization. Due to their nature, a great deal of interest has been focused on the study of their chemical, mechanical and electrical properties. Sample studies of their properties and applications include, equilibrium swelling kinetics [23, 24], electronically controllable micro-valves based on smart hydrogels [25, 26] and evaluation of hydrogels conductivity for micro-sensor development [27, 28]. Hydrogels can be classified by several characteristics which include their structure, cross-links, ionic charges and/or preparation method [18, 19]. Figure 8 shows a schematic of a hydrogel structure. Classification of hydrogels based on structure is divided as follows: (a) amorphous or non-crystalline, (b) semi-crystalline and, (c) hydrogen bonded hydrogels. The non-crystalline structure is often used on hydrogels utilized for biomedical applications. Higher mechanical strength and dimensional stability can be achieved usually by using semi-crystalline hydrogels produced by heat treatment of non-crystalline hydrogels above their glass transition temperature.

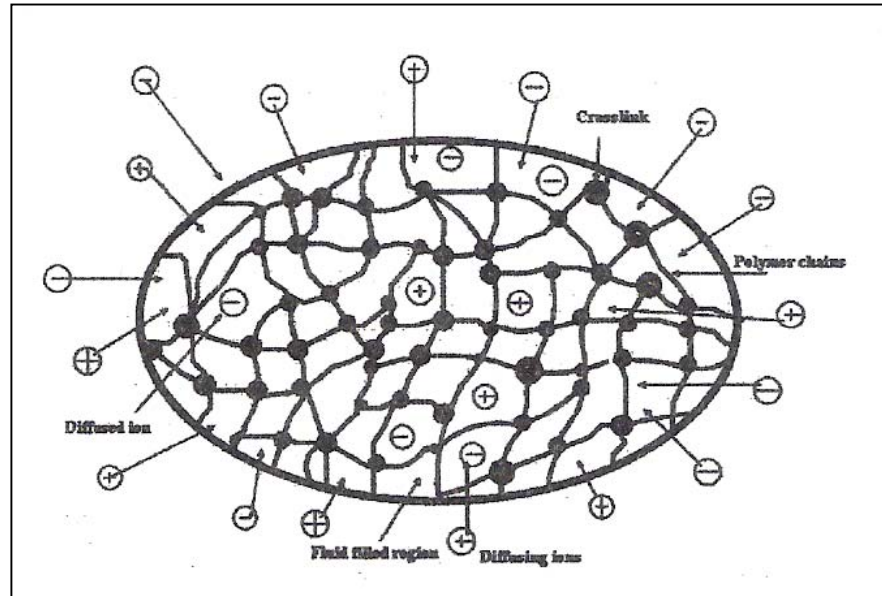


Figure 8: Hydrogel structure which includes its polymeric chains, cross-links, fluid filled regions and ions [29].

In terms of cross-links or monomer that has two or more attachment possibilities to the functional monomer [4] can be formed by several methods such as: reaction of one or more monomers, hydrogen bonds and van der Waals interactions. In terms of preparation procedure, hydrogels can be classified as: homopolymers (one type of hydrophilic monomer), copolymers (two types of monomers and at least one hydrophilic), multi-polymers (more than three types of monomers) or interpenetrating polymeric networks (IPNs). Finally, classification based on ionic charges can be distributed as: neutral, anionic, cationic and amphiphilic.

A key characteristic that allows hydrogels to have numerous biomedical applications is their ability to absorb aqueous solutions without losing their shape and mechanical strength, properties that are usually found in many natural constituents of a human body, like muscles, tendons, cartilage, etc. [21]. Hydrogels also exhibit good biocompatibility in contact with blood, body fluids and

tissues. Peppas and Huang [16] (2002) highlighted two main factors that allow hydrogels to have numerous applications due to their ability to: control the diffusion on molecules in or through them and amplify the microscopic events occurring at the mesh chain level into macroscopic phenomena. Several factors have shown to cause changes at the microscopic level of hydrogels that are translated into a macroscopic level due to a phase transition between its swollen and collapsed states including: light, temperature, solution pH, magnetic field, radiation, solvent composition, electric field, stress and existence of specific molecules in solution [16, 29]. Hydrogels also possess numerous applications in medicine and pharmaceuticals. Some of its most important applications are materials for blood compatible applications, contact lenses, artificial tendons and controlled drug release devices [22, 30]. A wide scope of biomedical applications have been developed using hydrogels including: membranes for artificial kidneys, materials for parts of an artificial liver, carriers for artificial pancreas, linings for artificial hearts, sutures, artificial skin and wound coverings, ophthalmologic applications aside contact lenses, maxillofacial reconstruction, dental uses, reconstruction of vocal cords, augmentation and post-mastectomic mammoplasty, reconstruction of sexual organs, and articular cartilage replacement [30].

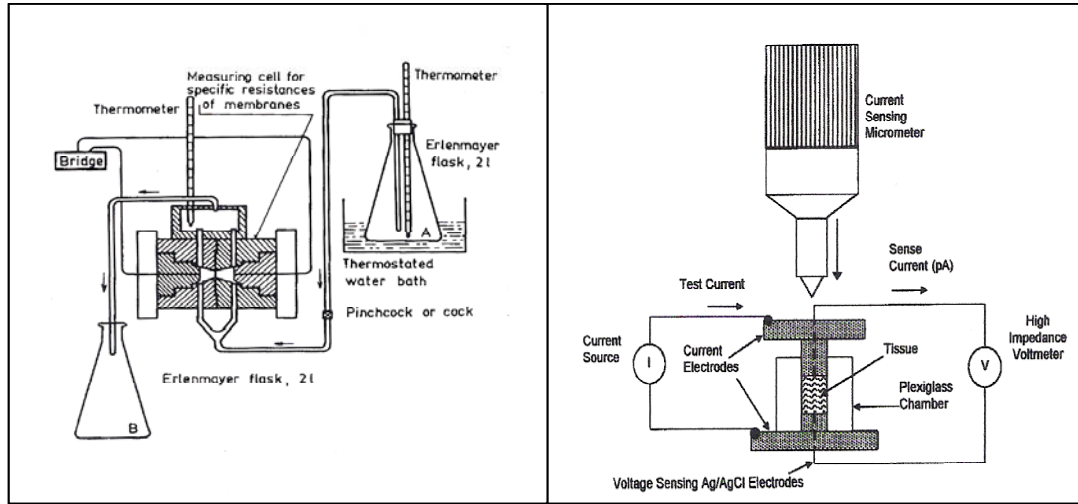
2.3.2 Electrical properties of hydrogels

The response of polymers to an electric field can be divided into two main categories [31]. The first group is composed of dielectric properties and its two fundamental parameters are dielectric constant and tangent of dielectric loss angle. These two parameters represent the polarization and relaxation phenomena

respectively. The second group is composed of the bulk conductive properties and its two fundamental parameters are dielectric strength and conductivity. Both parameters represent the breakdown phenomena and electrical conduction respectively.

Electrical studies performed on synthetic hydrogels revealed that their electrical conductivity can be related to the ionic mobility in water swollen gels [32, 33]. Electrical conductivity of hydrogels has also been attributed to be dominated by the presence of water and how the topologies of its conducting paths are altered as function of water contents [34]. Temperature has also been shown to affect the conductivity of hydrogels suggesting that their conductivity is governed by the motion of the polymeric chains [34]. Hydrogels conductivity has also been shown to be pH dependent as a result of hydration-dependent changes in both the concentration and mobility of charge carriers within the hydrogel [35]. Finally, increases in water content in hydrogels have been related to an increase in molecular mobility, similar to an increase in temperature [36].

Electrical studies performed on hydrogels over the years have used experimental setups similar to those shown below. Figure 9A presents a schematic of the setup used by Vacik and Kopecek on their electrical studies of hydrogels on 1975 [32], while Figure 9B shows a schematic of a sophisticated apparatus developed by Gu and Justiz to perform their electrical studies on 2002 [37]. Both of these reference setups shared some basic features including a cell to place membranes under study and current and voltage sensing equipment.



(A)

(B)

Figure 9: Apparatus for measuring specific resistances of membranes, (A) Vacik and Kopecek 1975 [32], (B) Gu and Justiz 2002 [37].

Independent of the experimental setup used to perform electrical studies on hydrogels, equation 2 has been used classically to describe the specific resistance of the membranes under evaluation.

$$\rho_M = (R_t - R_s) \frac{A}{D} \quad (2)$$

where, ρ_M is the specific resistance of the membrane ($\Omega \times \text{cm}$), R_t is the resistance of the solution plus the membrane (Ω), R_s is the resistance of the solution (ohms), A is the measured membrane area (cm^2) and D is the membrane thickness (cm) [32, 33, 37]. Finally, equation 3 has been used to estimate analytically the electrical conductivity of hydrogels [23, 38]

$$\sigma_{gel} = \sum_{i=1}^{\#ions} |z_i| F c_i \mu_i \quad (3)$$

where z_i is the valence of the i^{th} ion, F is the Faraday constant, and c_i and μ_i are the concentration and mobility of the i^{th} ion, respectively.

2.3.3 Electrical conductivity studies in hydrogels

Sheppard and co-workers [27] (1991) measured the electrical conductivity of hydrogels made of 2-hydroxyethyl methacrylate (HEMA), dimethylaminoethyl methacrylate (DMAEMA) crosslink with tetra(ethyleneglycol) dimethacrylate (TEGDMA) with a molar ratio of 90:10:3. They found that gel conductivity decreased in an exponential manner with respect to the pH of buffer solution with pH values ranging from 6-10. Decrease in gel conductivity in relation to the buffer solution they were equilibrated was associated to the water contents of the gel. Gels at pH 6 had a water content of 51% while those at pH 10 had a water content of 38%. Given this hydration dependent electrical conductivity and the biocompatibility of hydrogels, Sheppard and co-workers developed a method for the design of a conductometric micro-sensor for potential in vivo use [28]

Schwartz et al. (1998) studied the electrical characteristics of glucose-sensitive hydrogels [23]. Specifically they studied the swelling mechanism of the glucose-responsive hydrogels and its relationship to protonation in order to estimate hydrogel swelling by measuring electrical conductivity. Their results showed that electrical impedance of the hydrogels (as function of frequency) almost tripled when hydrogel diameter was doubled. Electrical impedance values appeared to be frequency independent for excitation input signal values greater than 3 KHz. This behavior was related to the parasitic capacitance in the electrode-medium membrane interface. Phase studies were performed to study

the reversibility range of the membrane and showed an almost constant value for all voltage and frequency range values tested. Both magnitude and phase responses are shown in Figure 10.

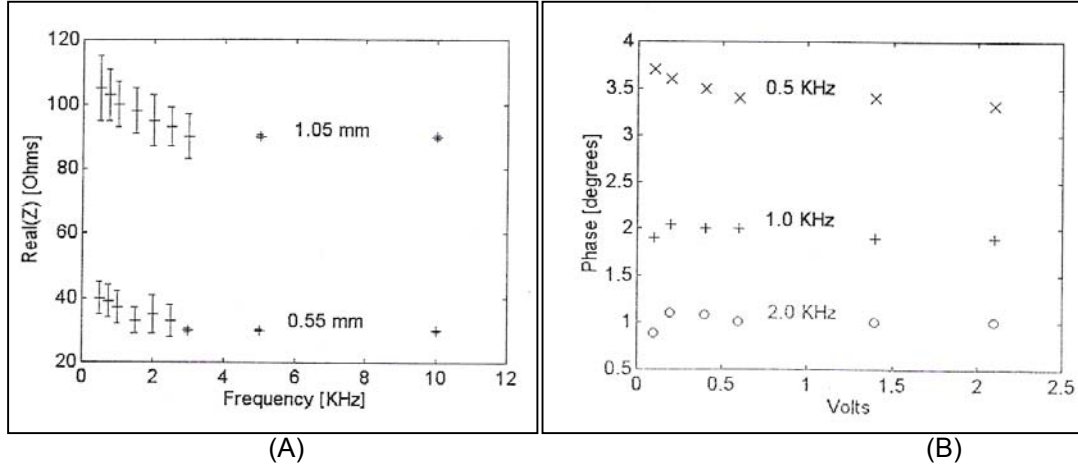


Figure 10: (A) Hydrogel Impedance as a function of the excitation frequency. Numbers on the plots denote the diameter of the membranes. Error bars represent ± 2 SD. (B) Hydrogel phase as function of the excitation voltage. Numbers denote the excitation frequency [23].

Water uptake percentages at different times were calculated using the following relationship:

$$WU = \frac{W_w(t) - W_w(T_0)}{DW} \times 100 \quad (4)$$

where $W_w(t)$, $W_w(T_0)$ and DW are the wet weight, the wet weight at equilibrium and the dry weight, respectively.

A model for the conductivity measurements as function of time of the form

$$\sigma(t) = at^2 + bt + c \quad (5)$$

was proposed and the following relation between conductivity and swelling was obtained:

$$WU(t) = k[\sigma(t) - \sigma(0)] \quad (6)$$

where k is a scale factor and $\sigma(0)$ is the initial conductivity. The proposed model fitted with high accuracy the experimental data as shown in Figure 11.

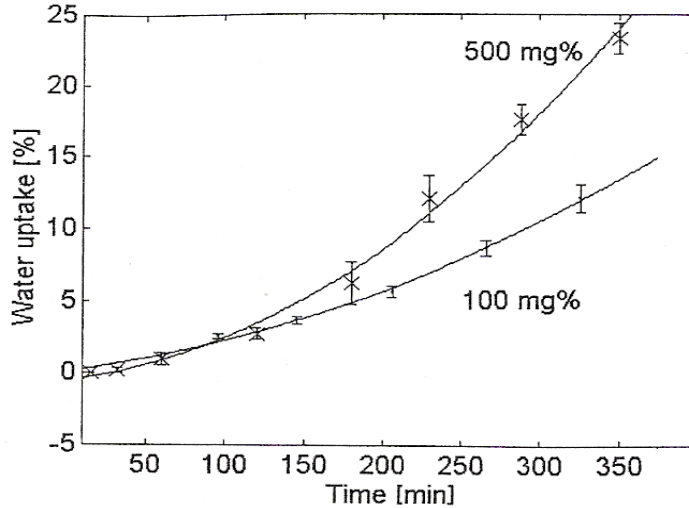


Figure 11: Swelling kinetics of hydrogels with immobilized glucose oxidase measured (bars) and estimated from conductivity measurements (straight lines) at several glucose concentrations. Error bars represent ± 3 SD [23].

An in depth study of electrical conductivity in hydrogels was performed by Pissis and Kyritsis [36] (1997). Their work focused on studying the electrical properties of poly(hydroxyethyl acrylate) PHEA hydrogels by means of dielectric relaxation spectroscopy (DRS) as function of frequency, temperature and hydrogel water content. Tests were performed over a wide range of frequency values (5 Hz – 2 GHz), temperature (173 – 363K) and water contents (0.065 – 0.46 grams water/grams dry material). An increase in water contents at constant temperature showed the same effect as an increase of temperature at constant water contents or an overall increase in molecular mobility, more noticeable at lower frequencies.

For water contents less than or equal to 0.21 the temperature dependence of the conductivity was described by the Vogel-Tamman-Fulcher (VTF) equation:

$$\sigma_{dc} = \sigma_{dc0} \exp\left(\frac{-B}{T - T_0}\right) \quad (7)$$

where σ_{dc0} and B are constants and T_0 the ideal glass temperature. At water contents greater than 0.29 the temperature dependence of the conductivity changed from the VTF type to Arrhenius type.

$$\sigma_{dc} = \sigma_{dc0} \exp\left(\frac{-W}{kT}\right) \quad (8)$$

Where W is the apparent activation energy and k is the Boltzmann's constant.

2.3.4 Electrical studies of molecularly imprinted polymers

The interaction of a substrate with an enzyme immobilized in a polymeric membrane produces conformational changes in the enzyme. These variations have been associated to modifications in the electrochemical properties of the polymeric membranes. Similar electrochemical behavior has been observed in sensor response of imprinted polymers upon the interaction of template molecules with imprinted cavities [39]. These electrochemical properties variations are the foundation for numerous biosensor applications based on molecularly imprinted polymers [3].

Several researchers have investigated the use of molecularly imprinted membranes for sensing applications using electrical conductivity as the transduction mechanism [39, 40]. Karube and co-workers [39] (1995) were able to

develop a mechanism based on MIP's to detect atrazine concentration by means of membrane electrical resistance measurements. Several combinations of the monomers methacrylic acid (MAA) and diethylaminoethylmetacrylate (DEAEM) along with the cross-linker agent ethyleneglycol dimethacrylate (EGDMA) were studied to determine the optimum sensor response. Electrical resistance of the membranes showed an increase in value with increasing concentration of atrazine but tended to saturate at higher concentration levels (Figure 12). This saturation in the response of the sensor was related to the filling of the selective cavities in the polymer by adsorption of the template molecules. A sensor deviation response of 20-30% for different membranes with the same composition was observed. Selectivity studies of the imprinted membranes were performed by utilizing substances with similar molecular structure to that of atrazine. The sensor response to these analog template molecules was much lower to that of atrazine response which suggested high sensor selectivity.

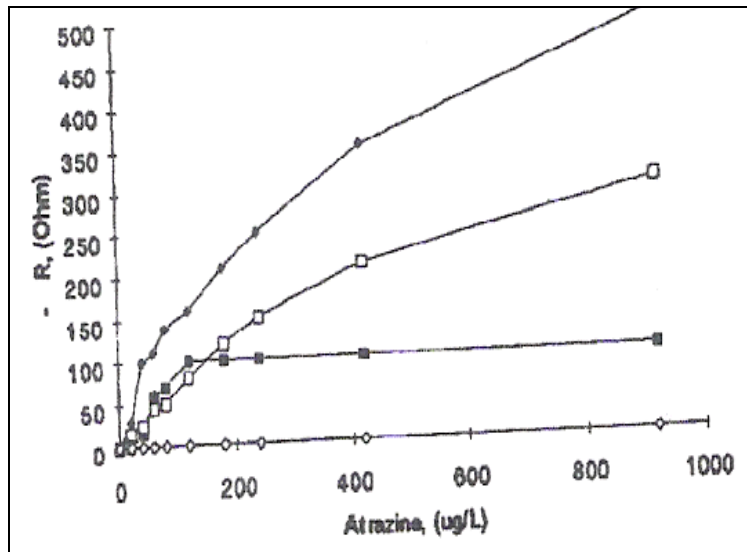


Figure 12: Influence of the herbicide concentration in solution of the sensor response. ■ triazine, □ simazine, ◆ atrazine [39]

Kriz and co-workers [41] (1996) developed a MIP based conductometric sensor for the detection of benzyltriphenylphosphonium ion. MIP's were synthesized using methacrylic acid (MAA), ethylene glycol dimethacrylate (EDMA) and benzyltriphenylphosphonium chloride as template. Conductivity measurements were performed on reference and imprinted polymers using a standard conductometer at 1 KHz. The measurements were made for increasing amounts of benzyltriphenylphosphonium chloride (0 - 2000 μg) once the conductivity value had reached a steady state value. At higher loadings of the template (0 - 200 μg) the MIP's showed a significantly higher conductivity value than those of the reference polymers. This was not the case at lower levels in which the template binding was non specific in nature and reported a conductometric response similar to non imprinting sensor. One severe problem identified by Kriz et al was the long response time involved in the measurements

Figure 13A and 13B present the conductivity difference between the imprinted polymers and its reference polymers as function of template loading and sensor response time respectively.

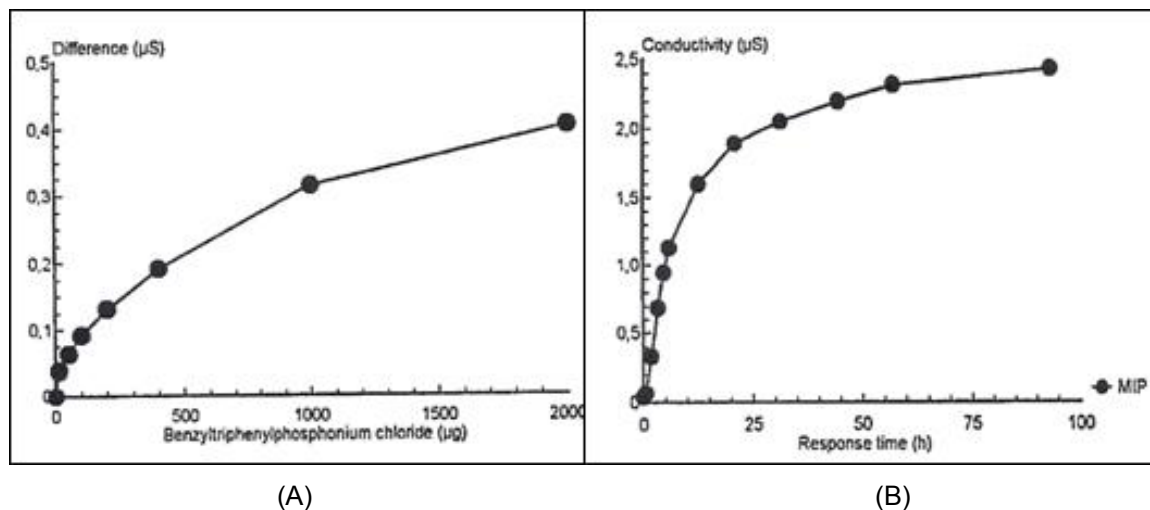


Figure 13: (A) The difference in the responses (MIP and ref-MIP based) of the conductometric sensors as function of the mass of benzyltriphenylphosphonium chloride added. (B) The response time of a MIP based conductometric sensor. The response was recorded after the addition of 2000 µg of benzyltriphenylphosphonium chloride [41]

Sergeyeva and co-workers [40] (1999) were able to develop a MIP based sensor for the detection of atrazine with high degree of sensitivity and selectivity. The synthesized MIP's were prepared using atrazine as template, methacrylic acid (MAA) as functional monomer, tri(ethylene glycol) dimethacrylate (TEDMA) as cross-linker and Oligourethane acrylate (OUA) that aided in obtaining thin, flexible and mechanically stable membranes. Several factors demonstrated to affect the sensor response including the fraction of cross-linker and solvent used to prepare the MIP's. It was shown that a higher fraction of cross-linker agent resulted in a greater sensor response up to a cross-linker fraction optimum value of 85%. At higher TEDMA fractions the response was adversely affected mainly to an

excessive rigid polymer structure that did not allow proper interaction with the template (Figure 14A). Fraction of solvent (chloroform) used in MIP preparation was a crucial factor that affected sensor response. In this case the difference between optimal and discrete sensor response as function of fraction of solvent was a small range, being the optimal value a 30%. At higher values of solvent fraction sensor degradation response was observed which was attributed to membranes being too porous (Figure 14B). Finally, the measured changes in the membrane electrical conductivity as function of atrazine concentration increased as its concentration in solution increased.

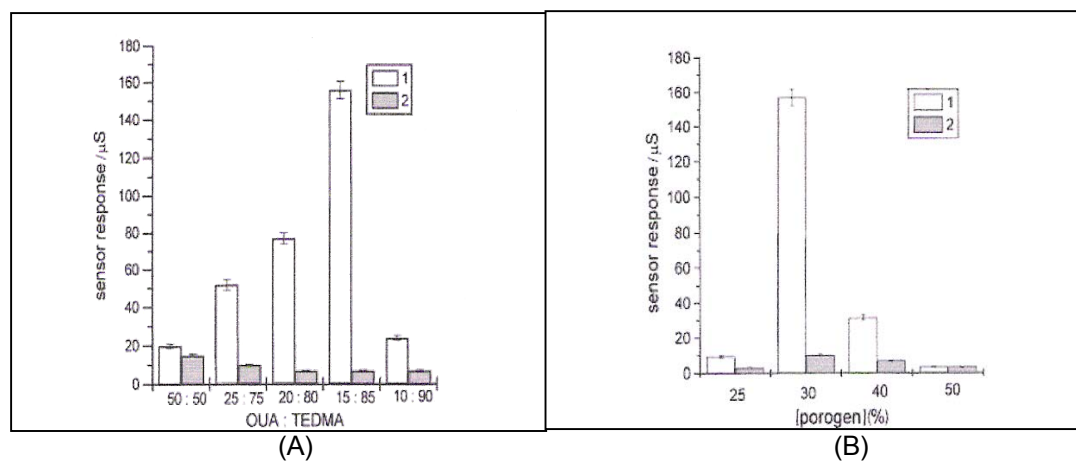


Figure 14: (A): Responses to atrazine as function of the cross-linking agent (TEDMA) concentration: (1) MIP Membrane; (2) Reference membrane. Measurements were carried out in 25 mmol dm^{-3} potassium phosphate buffer (pH 7.5) containing 35 mmol dm^{-3} NaCl. (B): Responses to atrazine as a function of porogen (Chloroform) concentration [40]

Summarizing the discussion of the abovementioned, multiple research efforts have focused in the study of the electrical properties of hydrogels. These works have been the basis for several successful applications of molecularly imprinted polymers developed using a conductometric transduction principle among others. These studies have provided insights on how the electrical

conductivity of hydrogels is altered as function of several factors (pH, temperature, morphology, frequency, etc) and trends have been identified that have allowed the successful development of molecularly imprinted polymer applications. Nevertheless, it is still unclear how much significance each of these factors and/or interactions between them have in the electrical response of these complex systems.

2.4 Factor Analysis

Molecularly imprinting experiments often include a large number of measured variables, and sometimes those variables overlap in the sense that groups of them may be dependent. Factor analysis is a method to fit a model to multivariable data to estimate the interdependence between groups. In the factor analysis model, the measured variables depend on a smaller number of unobserved factors. Each of these factors may affect several common variables. Each variable is assumed to depend on a linear combination of the common factors and the coefficients. Variables also include a component due to independent random variability, known as specific variance because it is specific to one variable [42]:

A model can represent the observations or results from a factorial experiment. One of the most common models for this type of the experiment is the effects model. In the general case of a two-factor experiment the effects model is given by:

$$Y_{ijk} = \mu + \tau_i + \beta_j + (\tau\beta)_{ij} + \epsilon_{ijk} \quad \begin{cases} i = 1, 2, \dots, a \\ j = 1, 2, \dots, b \\ k = 1, 2, \dots, n \end{cases} \quad (9)$$

Where:

Y_{ijk} = Observed response when factor A is at the i^{th} level ($i = 1, 2 \dots a$) and factor B is at the j^{th} level ($j = 1, 2 \dots n$) for the k^{th} replicate ($k = 1, 2 \dots n$)

μ = Overall mean effect

τ_i = Effect of the i^{th} level of factor A

β_j = Effect of the j^{th} level of factor B

$(\tau\beta)_{ij}$ = Effect of the interaction between τ_i and β_j

ϵ_{ijk} = Random error component

Both factors A and B are assumed to be fixed and the effects contribution are defined as deviations from the overall mean, as consequence $\sum_{i=1}^a \tau_i = 0$

and $\sum_{j=1}^b \beta_j = 0$. The interactions effects similarly are fixed and are defined such

that $\sum_{i=1}^a (\tau\beta)_{ij} = \sum_{j=1}^b (\tau\beta)_{ij} = 0$. Since there are n replicates of the experiment there

are a total of abn observations. In order to be able to determine a sum of squares due to the error at least two replicates (n) are necessary if all interactions are to be included in the model. Table 3 presents a general representation of a two factor factorial design.

Table 3: General arrangement for a two factor factorial design [42]

		Factor B			
		1	2	...	b
Factor A	1	Y ₁₁₁ , Y ₁₁₂ , ... Y _{11n}	Y ₁₂₁ , Y ₁₂₂ , ... Y _{12n}		Y _{1b1} , Y _{1b2} , ... Y _{1bn}
	2	Y ₂₁₁ , Y ₂₁₂ , ... Y _{21n}	Y ₂₂₁ , Y ₂₂₂ , ... Y _{22n}		Y _{2b1} , Y _{2b2} , ... Y _{2bn}
	...				
	A	Y _{a11} , Y _{a12} , ... Y _{a1n}	Y _{a21} , Y _{a22} , ... Y _{a2n}		Y _{ab1} , Y _{ab2} , ... Y _{abn}

The total corrected sum of squares can be written symbolically as:

$$SS_T = SS_A + SS_B + SS_{AB} + SS_E \quad (10)$$

Where:

SS_A = Sum of squares due to factor A with a levels

SS_B = Sum of squares due to factor B with b levels

SS_{AB} = Sum of squares due to the interaction of factors A and B

SS_E = Sum of squares due to error

Table 4 shows a typical representation of a two factor fixed effects model.

Table 4: Analysis of variance for a general two factor fixed effects model

Source of variation	Sum of squares	Degrees of freedom	Mean Square	Expected mean square	F ₀
A	SS _A	a-1	MS _A	$\sigma^2 + \frac{bn \sum_{i=1}^a \tau_i^2}{a-1}$	$\frac{MS_A}{MS_E}$
B	SS _B	b-1	MS _B	$\sigma^2 + \frac{an \sum_{j=1}^b \beta_j^2}{b-1}$	$\frac{MS_B}{MS_E}$
AB	SS _{AB}	(a-1)(b-1)	MS _{AB}	$\sigma^2 + \frac{n \sum_{i=1}^a \sum_{j=1}^b (\tau\beta)_{ij}^2}{(a-1)(b-1)}$	$\frac{MS_{AB}}{MS_E}$
Error	SS _E	ab(n-1)	MS _E	σ^2	***
Total	SS _T	abn-1	***	***	***

3. Objectives

The main purpose of this research is to perform an electrical characterization of cross-linked methacrylic acid hydrogels molecularly imprinted with hydrocortisone as a basis for future biosensor development. Specifically, estimates of the electrical resistance of the hydrogels as function of their morphology, solution pH and frequency in the presence (molecularly imprinted) and absence of a template molecule (hydrocortisone) are evaluated, as well as how this electrical property is affected by using template molecule analogs under steady state operating conditions. A factorial analysis technique will be employed to identify a possible optimum operating range for the biosensor candidate. A correlation analysis of the electrical resistance of studied hydrogels as function of system variables and counterpart chemical responses will be performed. Finally, an evaluation of how the electrical resistance of these hydrogel networks could be used as the transduction principle for a future biosensor development is investigated.

4. Materials and Methods

4.1 Experimental Design

4.1.1 Electrical resistance of MAA-TEGDMA hydrogels

A factorial design method was followed in order to study the effect of several measurable factors on the electrical resistance of MAA-TEGDMA hydrogels. This method is useful when investigating systems in which more than one variable contributes asymmetrically in the outcome of the parameter(s) of interest and it is necessary when interactions between variables may be present [42]. The method offers several advantages such as: (a) more efficient than one factor at a time experiments, (b) allows the effects of a factor to be estimated at several levels of other factors and (c) yields conclusions that are valid over a wide range of experimental conditions.

Five factors at a total of fifty nine levels were identified in the development of the design for the first stage of experiments. Table 5 presents the factors and their corresponding levels considered in the first stage of experiments that served as basis for posterior analysis of variance of the electrical resistance of MAA-TEGDMA hydrogels. Preliminary trials included two additional factors that were not included in the final design of experiment due to their noticeable minimal effect on the variability of the response. These two discarded factors were that of input voltage and hydrogel disk sample position in regards to the geometrical center of polymerized membrane.

Table 5: Factors and levels taken into consideration during first stage of experiments for the electrical characterization of MAA-TEGDMA hydrogels.

Factors	Levels	Identifier
Hydrogel Variant	2	Reference and MIPs
Hydrogel Composition	2	17:1 and 39:1
Glutaric acid hydroxide buffer pH	3	3.2, 4.8 and 5.4
Glutaric acid hydroxide buffer saturated in hydrocortisone	2	Yes and No
Input signal frequency	50	100Hz -5kHz , $\Delta f = 100\text{Hz}$

The factors and levels from Table 5 can be classified as: (a) hydrogel variant and its two levels (reference and MIP) that represent MAA-TEGDMA hydrogels (non-imprinted) and molecularly imprinted MAA-TEGDMA hydrogels with hydrocortisone (b) hydrogel composition and its two levels (17:1 and 39:1) that represent the molar ratio of the functional monomer (MAA) to cross-linker (TEGDMA) used in the synthesis of the hydrogels, (c) glutaric acid hydroxide buffer and the three tested pH values of 3.2, 4.8 and 5.4, (d) glutaric acid hydroxide buffer saturated in hydrocortisone (Yes and No) and (e) input signal frequency and its fifty frequency values starting at 100 Hz with increments of 100 Hz. Each complete trial in the experiments had all possible combinations of factors and levels investigated which are presented schematically in Figure 15. Even though hydrogel variant was classified as a factor, it was necessary due to the nature of the experiment to separate the factorial analysis for the non-imprinted and molecularly imprinted hydrogels since no interaction between them occurred during experimentation.

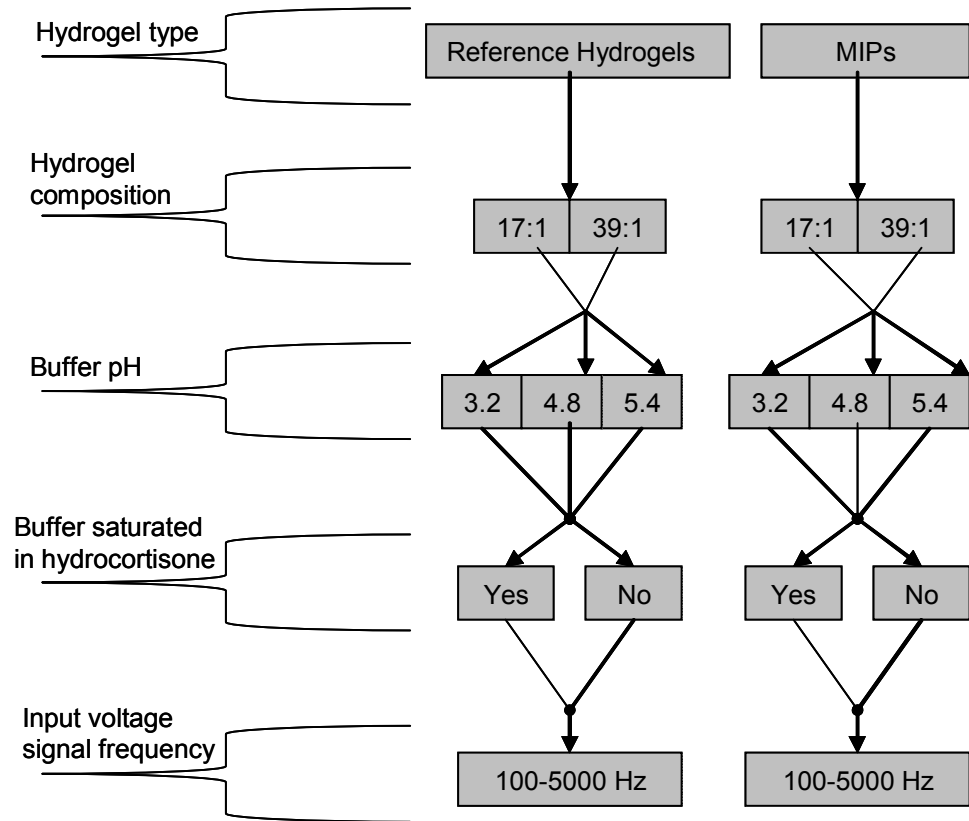


Figure 15: Design of experiment used in first stage of experiments to analyze the contribution of the identified factors in the electrical conductivity of MAA-TEGDMA hydrogels.

4.1.2 Electrical resistance of MIP's as function of hydrocortisone concentration

A second stage of experiments was designed in order to determine an empirical relation between the electrical resistance of molecularly imprinted hydrogels as function of their template molecule. The first stage of experiments served as a guide for the design of the second set of experiments since a similar structure was followed. The main differences between experiments were the exclusive use of MAA-TEGDMA (17:1 molar ratio) molecularly imprinted hydrogels, the incorporation of two new levels in the concentration of the template

molecule in solution and the reduction to one pH level (3.2). Table 6 and Figure 16 present the structure used in the second stage of experiments

Table 6: Factors and levels taken into consideration during second stage of experiments for the electrical characterization of MAA-TEGDMA hydrogels

Factors	Levels	Identifier
Concentration of hydrocortisone in glutaric acid hydroxide buffer	3	None, $\frac{1}{4}$ saturated, $\frac{1}{2}$ saturated,
Input signal frequency	50	100Hz -5kHz , $\Delta f = 100\text{Hz}$

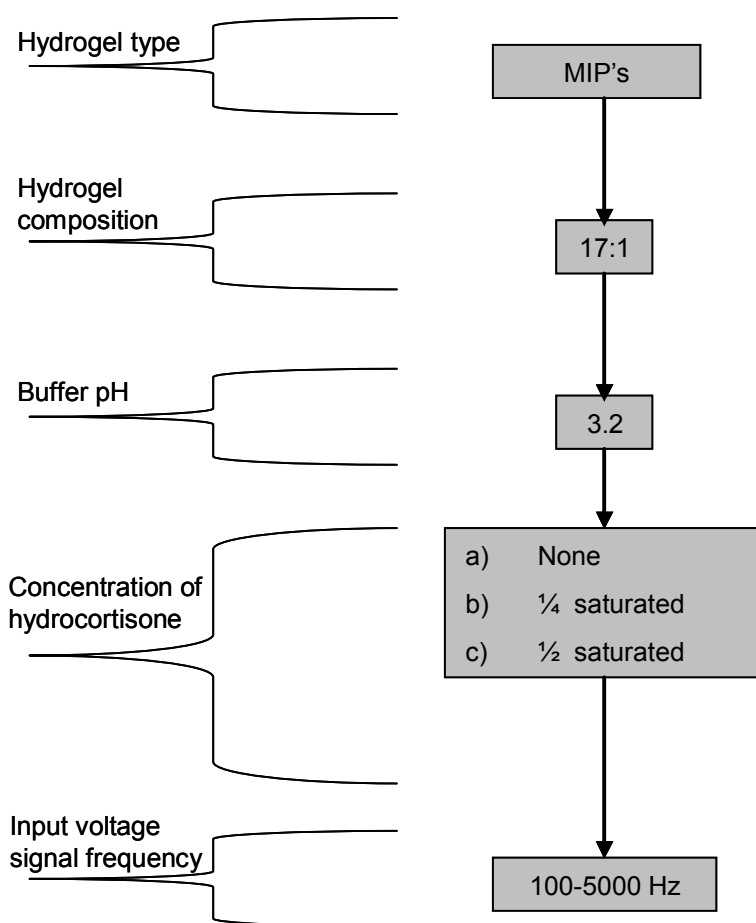


Figure 16: Design of experiment used in second stage of experiments to assess the relation between the electrical resistance of MIP's and template molecule concentration.

4.1.3 Selectivity of MIP's to an analog template molecule

A final experiment was designed to study the selectivity of molecularly imprinted MAA-TEGDMA hydrogels with hydrocortisone to an analog molecule. For this a similar design structure from that of the second stage of experiments was followed being the only modification the use of fluorescein sodium salt instead of hydrocortisone. Table 7 and Figure 17 present the structure used in the final stage of experiments.

Table 7: Factors and levels taken into consideration during third stage of experiments for the electrical characterization of MAA-TEGDMA hydrogels

Factors	Levels	Identifier
Concentration of Fluorescein sodium salt in glutaric acid hydroxide buffer	3	0.0, 0.06, 0.12 mg/ml
Input signal frequency	50	100Hz -5kHz , $\Delta f = 100\text{Hz}$

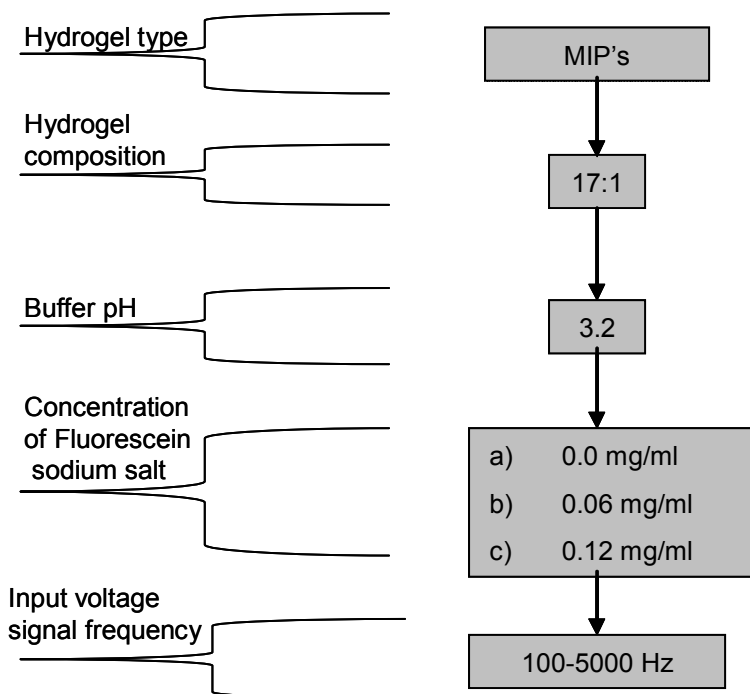


Figure 17: Design of experiment used in final stage of experiments to assess the selectivity of MIP's to an analog template molecule.

4.2 Experimental components and setup

4.2.1 Silver/Silver Chloride (Ag/AgCl) Electrodes

The Silver/Silver Chloride electrode is a practical electrode with characteristics similar to that of a perfectly non-polarizable electrode. Ideally, these electrodes are characterized by having an electrode-electrolyte interface in which current passes freely, thus no over-potentials exist [2]. When used with sinusoidal signals, the terminal characteristics of the electrode are frequency dependent and exhibit both a resistive and reactive component. This frequency dependent behavior can be characterized with the equivalent circuit of Figure 18. In addition to its non-polarizable behavior, Ag/AgCl electrodes exhibit less electric noise than similar metallic Ag electrodes. In terms of impedance, Ag/AgCl electrodes possess a lower magnitude value than that of metallic Ag electrodes. This deviation is a function of both input frequency and current density used in the preparation of the Ag/AgCl electrode and it is more noticeable at lower frequencies. This behavior is presented in Figure 19.

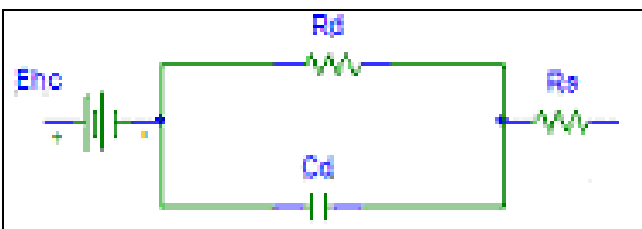


Figure 18: Equivalent electrode circuit in contact with an electrolyte. E_{hc} is the half cell potential, R_d and C_d make up the impedance associated with the electrode-electrolyte interface and polarization effects, and R_s is the series resistance associated with interface effects and due to resistance in the electrolyte [2].

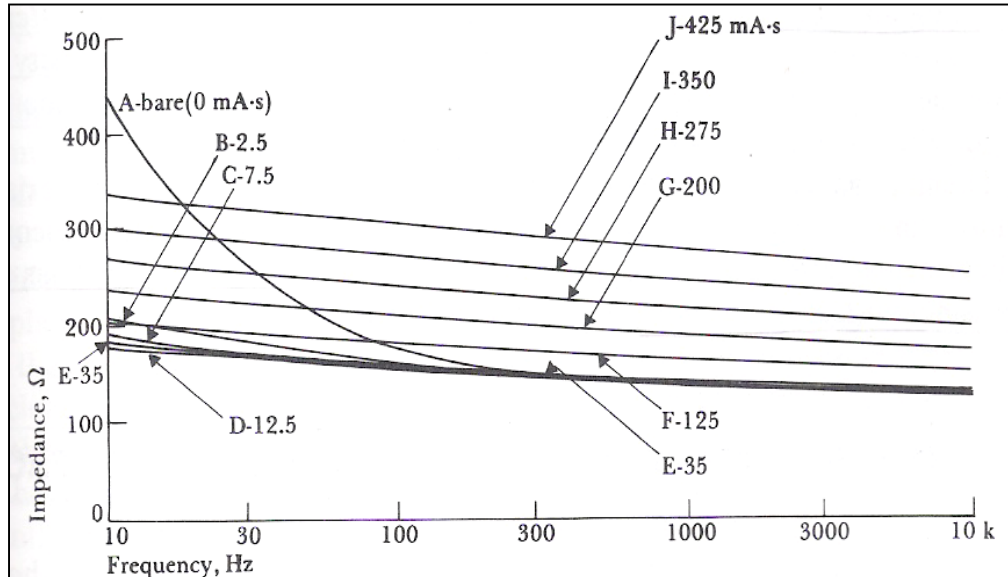


Figure 19: Impedance as function of frequency for A_g electrodes coated with an electrolytically deposited A_gCl layer. The electrodes area is 0.25 cm^2 . Numbers attached to curves indicate number of $\text{mA}\cdot\text{s}$ for each deposit [2].

Based on their stability two pair of custom made Ag/AgCl electrodes were chosen to perform the experiments. One pair served as the interface between the signal generator (Agilent 33120A) and the system, thus acting as a current source for the excitation of the system. A second pair was used as a voltage sensing element in the measurements of the potential differential across MAA-TEGDMA hydrogel samples. A four wire method was chosen to perform the experiments to isolate the voltage sensing electrodes from the electrical circuit under evaluation, hence minimizing any impedance contribution these could have had on the system overall response.

Following procedures similar to those described in literature [2, 43], Ag/AgCl electrode fabrication was performed using an electrolytic process. This process improves electrodes electrochemical stability and reduces their impedance contribution to the system, which results in signals with less electrical

noise. The electrolytic process consisted of an electrochemical cell made up of a 99.99% Ag electrode (Alfa Aesar, Ward Hill, MA), in which an AgCl layer was deposited and second piece of Ag wire whose surface area was much greater than that of the Ag electrode. Figure 20 presents the two sets of electrodes used in the experiments.

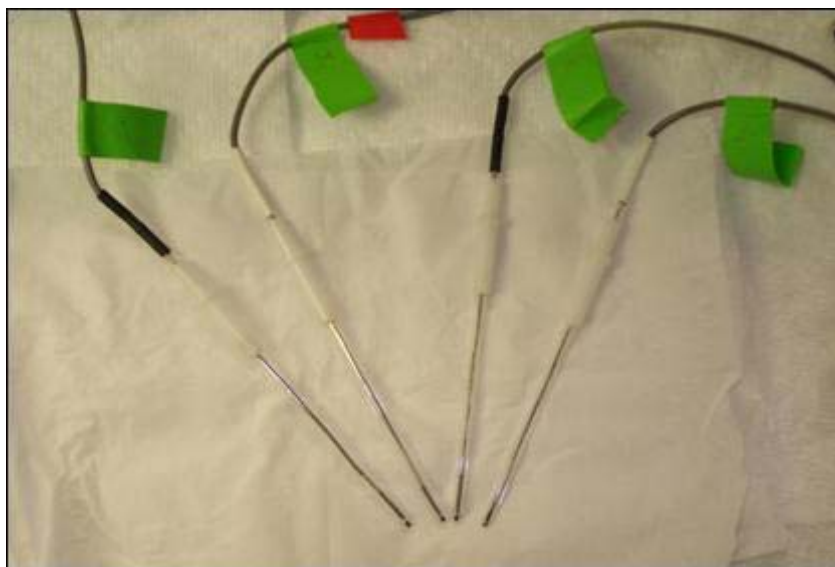


Figure 20: Ag/AgCl electrodes used in experiments of the electrical characterization of MAA-TEGDMA hydrogels.

4.2.2 Instrumentation amplifier development

A two channel instrumentation amplifier was developed in order to augment the difference in potential at the terminals of a resistor of known value (channel 1) and across the hydrogel samples through the voltage sensing electrodes (channel 2). Instrumentation amplifier AD620 (Analog Devices) was chosen for the circuit implementation, due to its low cost, high accuracy and high input impedance. Another advantage of the AD620 is that it only requires an external resistor to set

gains between 1 and 1000. Figure 21 shows a top view and connection diagram for the AD620.

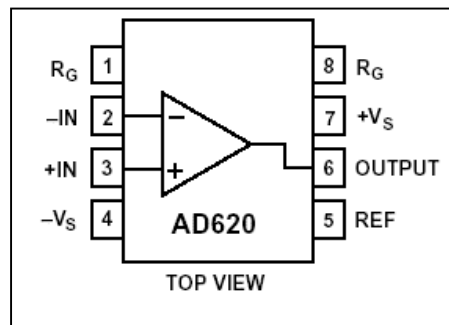
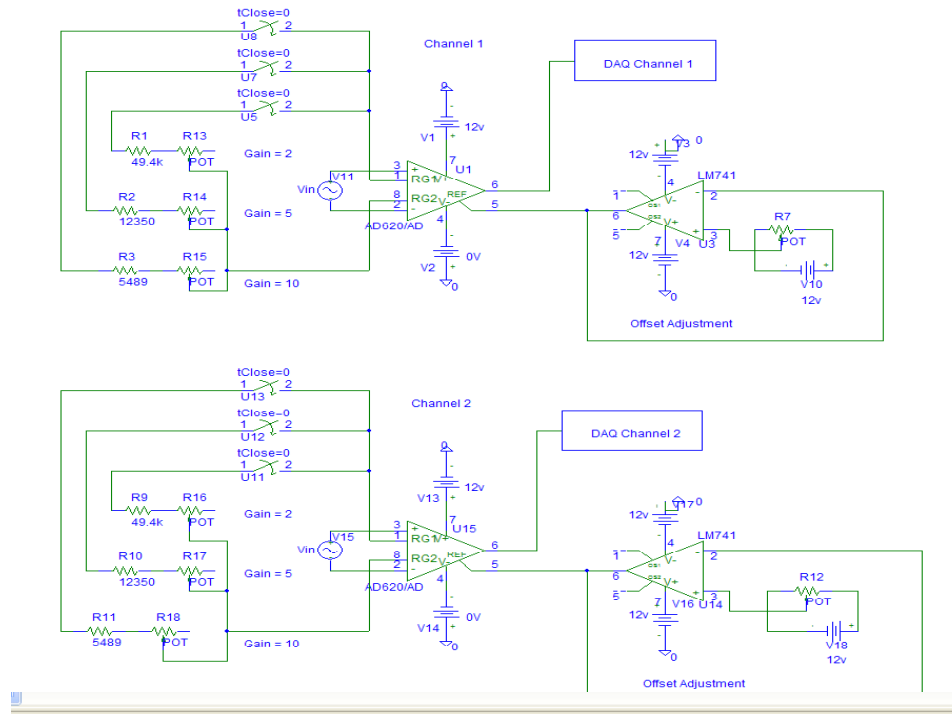
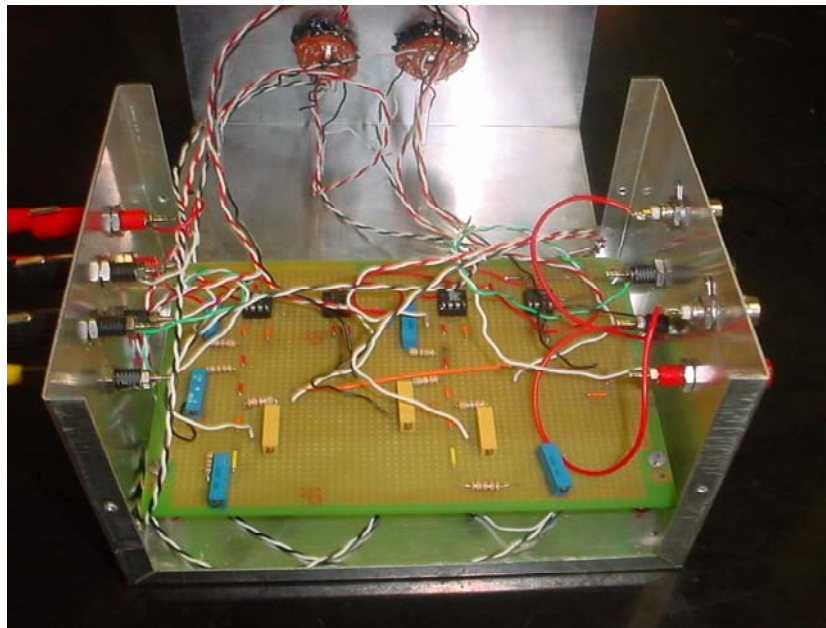


Figure 21: Analog Devices instrumentation amplifier AD620 connection diagram [44].

The high input impedance characteristic of the AD620 with respect to the impedance of the Ag/AgCl electrode and glutaric acid hydroxide buffer interface was required in order to avoid circuit loading due to possible current entering the input terminals of the differential amplifier. The development of the instrumentation amplifier consisted of variable voltage gains of 1, 2, 5 and 10 V/V and DC offset compensation for both channels (Figure 22).



(A)



(B)

Figure 22: (A) Circuit schematic of instrumentation amplifier used in the experiments. Voltage gains of 1, 2, 5 and 10 V/V and DC offset compensation. (B) Actual instrumentation amplifier used in the experiments.

4.2.3 Graphical user interface development

An user interface was developed using software package LabView 6.1 by National Instruments (Texas, USA). The user interface permitted an automation of data acquisition and processing for all the experiments performed. Some of the characteristics of the user interface were a control panel in which the user set the desired conditions for the particular experiment to be performed. The user was able to choose the initial, final and increment values for the magnitude and frequency of the excitation signal used as input to the system provided by a function generator (Agilent 33120A) which was controlled remotely through a serial port. The capability of being able to control the function generator remotely and having an automatic data acquisition system was invaluable for the completion of this work. Over 11,000 samples were recorded during the different experimental phases of this work (~ 5 minutes/replicate = 150 samples) that permitted the study of a representative range of the system variables. Figures 23 and 24 show several snapshots of the different features and signals from the developed graphical user interface.

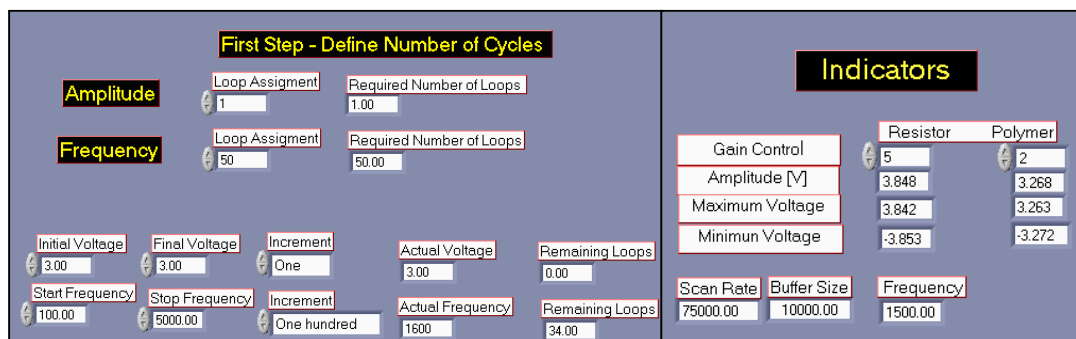


Figure 23: User interface controls and indicators used to setup and monitor the experiments respectively

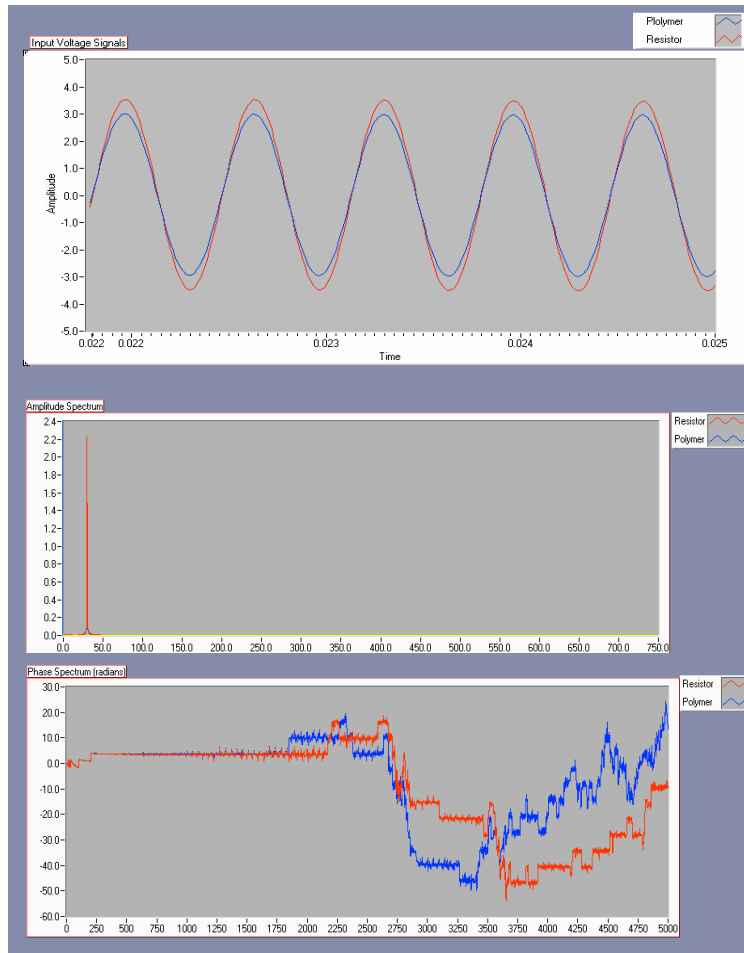


Figure 24: From top to bottom, time domain acquired voltage signals across control resistance and sample membrane, amplitude and phase spectrum of acquired signals.

4.2.4 Experimental setup

The electrical resistance of hydrogels networks was estimated by using procedures similar to the ones described in the literature [27, 28, 37, 40]. An experimental setup diagram of the apparatus that was used to perform the electrical resistance estimates of MAA-TEGDMA hydrogels is shown in Figure 25. It consisted of a side by side diffusion chamber with an external water inlet that was used to control the temperature of the system. The temperature of the system

in the experiments was held constant at 37° C using a water heater with temperature control capabilities. A function generator (Agilent 33120A) was used to stimulate the system with sinusoidal input waves. Two pairs of Ag/AgCl electrodes were used along a custom made dual channel instrumentation amplifier to acquire the voltage signals from the system. A data acquisition board (National Instruments PCI-6052-E) allowed the conversion from analog to digital voltage signals that were processed, monitored and recorded with the software package LabView 6.1 (National Instruments, Texas) in a personal computer.

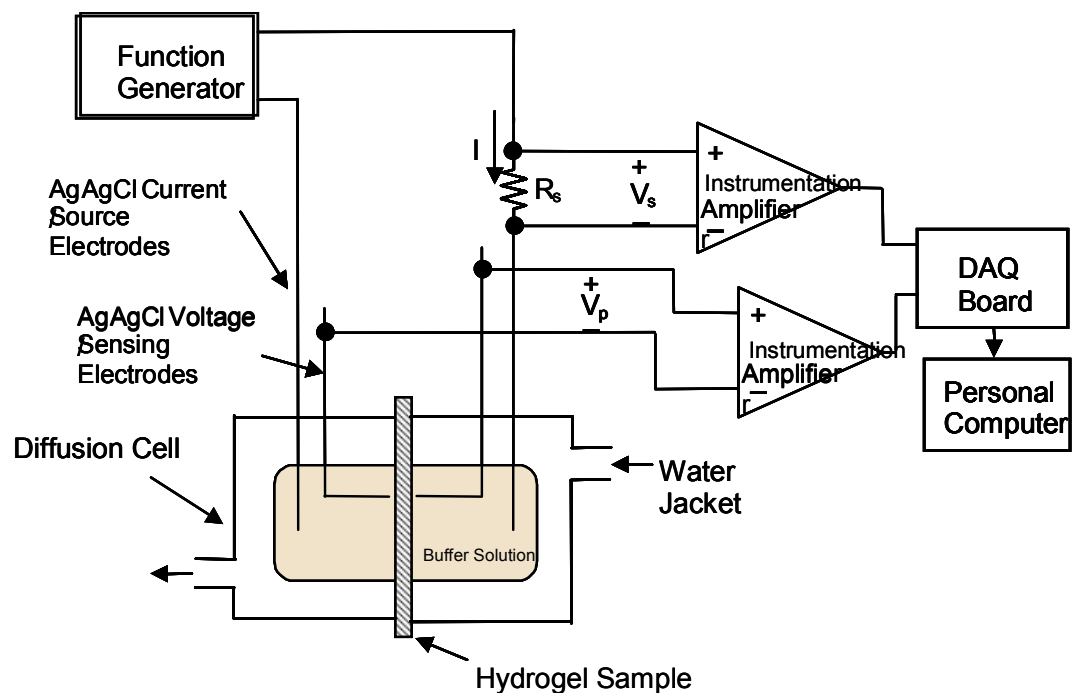


Figure 25: Experimental setup diagram.

Figure 26 presents the actual experimental setup used in the laboratory to estimate the electrical resistance of hydrogels for posterior electrical characterization.

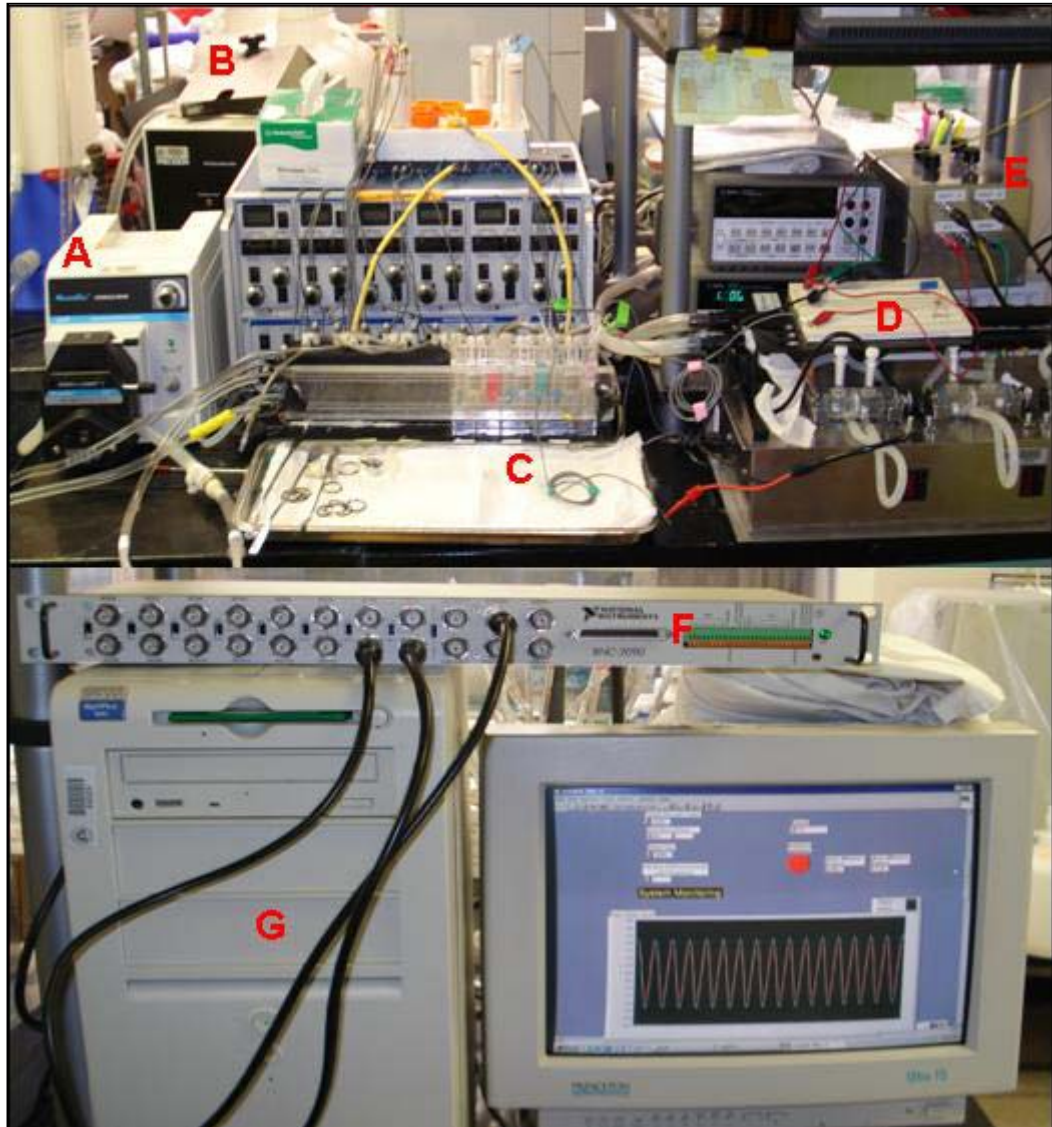


Figure 26: Actual experimental setup used to perform the experiments. (A) Water pump (Master Flex – Cole-Parmer Instrument Company), (B) Heater (Precision 180 Series Water Bath), (C) Electrodes and Diffusion Cells, (D) Electric circuit board with current control resistance, (E) Custom made differential amplifier, (F) Data acquisition board (National Instruments BNC-2090), (G) Personal Computer.

4.3 Hydrogel synthesis

Hydrogels were synthesized by free radical solution polymerization. The pre-polymeric mixture was purged with nitrogen for 20 minutes to remove dissolved oxygen that would act as reaction inhibitor. The mixture was placed between microscope slides (75 x 50 x 1 mm) that were 0.381mm apart to control the resulting hydrogel thickness. Teflon[®] spacers were placed between the slides to provide this separation. Microscope slides with the mixture were exposed to ultraviolet light (EFOS Acticure[®], Ontario, Canada) at 28 ± 2 mW/cm² to perform the polymerization for a period of time that varied with mixture composition.

Two different morphologies were used in the synthesis of the hydrogels. These were a 39:1 and 17:1 monomer (purified methacrylic acid) to crosslinker (tetra-ethylene glycol dimethacrylate) molar ratio. Both the monomer and crosslinker were purchased from Polyscience, Inc (Warrington, Pa, USA). A 1:1 mass ratio of ethanol and de-ionized water was employed as solvent with a 50% w/w dilution ratio. The photo-initiator used was 1-hydroxyphenyl ketone (Sigma Aldrich, Co. St. Louis, MO, USA). Similar protocols were reproduced to synthesized imprinted polymer by incorporating the template molecule hydrocortisone (Sigma Chemical Co. St. Louis, MO, USA) at the pre-polymeric mixture.

4.4 Hydrogel swelling procedure

Reference hydrogels films were washed daily in de-ionized water for a week to remove any un-reacted monomer from the synthesis procedure. Molecularly imprinted hydrogels were washed in a solution of 9:1 methanol to

acetic acid for three days to remove the template molecule in the polymer receptor sites. After this, MIP's were washed in de-ionized water for four additional days. Films were then cut in disks of 1.5 cm in diameter and equilibrated in a glutaric acid hydroxide buffer solution (0.1M) with pH values of 3.2, 4.8 and 5.4 (Figure 27).



Figure 27: Hydrogels after circular disks have been sliced in order to equilibrate them in glutaric acid hydroxide buffer at several pH values.

The following procedure was used to prepare the buffer in which the hydrogels were equilibrated: (a) 0.1 M solution of diethyl glutaric acid (Sigma Aldrich, Co. St. Louis, MO, USA) was prepared by mixing 16.02 grams with 1000 mL de-ionized water stirred until homogeneity was observed; (b) 0.2 N sodium hydroxide solution was prepared by mixing 8.0 grams with 1000 mL de-ionized water stirred until homogeneity was observed. To have the desired pH solution with a 0.1 M ionic strength 100 mL of dimethyl glutaric acid solution was mixed with 5.844g of Sodium Chloride (NaCl) plus the amount of sodium hydroxide solution from Table 8.

Table 8: Glutaric acid hydroxide buffer guide

pH	Sodium hydroxide (mL)
3.2	14.4
4.8	48.3
5.4	58.2

Hydrogels were considered to have reached equilibrium and be ready for electrical experiments when consecutive weight measurements did not change by more than $\pm 5\%$, which approximately was observed in a twenty four hour time period.

4.5 Electrical studies of MAA crosslinked hydrogels

4.5.1 Electrical characterization experiments

The first step in estimating the electrical impedance of (MAA-TEGDMA) hydrogels was to examine the impedance contribution of the aqueous solution glutaric acid hydroxide buffer in which the hydrogels were equilibrated. The electrical impedance of the solution was estimated for frequencies ranging from 100 Hz to 5 kHz at 100 Hz intervals with a constant input voltage of 5 Volts. For each frequency interval, three electrical impedance estimates (magnitude and phase) were performed. The mean and standard deviation of the impedance estimates were calculated offline. This procedure was repeated for each frequency interval, and plots showing the mean value of magnitude and phase angle were generated. To perform the experiments, the buffer solution was placed inside a chamber of a diffusion cell and a sinusoidal stimulating current was generated using a function generator controlled by a virtual instrument (LabView 6.1) through a serial port. Voltage drop V_s across a resistor R_s of known value in series with the system were recorded using input channel 1 of the custom built instrumentation

amplifier and the total current (I_T) in the system was estimated by means of Ohm's Law

$$I_T = \frac{V_s}{R_s} \quad (11)$$

Voltage sensing electrodes were used to measure the voltage drop V_m across the aqueous buffer solution and recorded using input channel 2 of the instrumentation amplifier. Impedance contribution of the medium was then estimated by means of Ohm's Law

$$Z_m = \frac{V_m}{I_T} \quad (12)$$

The output voltages of the instrumentation amplifier were stored in a computer using a data acquisition board in conjunction with the software package LabView 6.1. The software permitted (a) signal generation, (b) acquisition, filtering and processing of signals, (c) data storage as well as a (d) graphical user interface in a complete automatic process.

Once all the experiments were completed it was possible to perform an analysis of variance and posterior characterization of the electrical resistance of hydrogels as function of the factors and levels previously identified. Figure 28 presents a flowchart that summarizes the steps performed during the first stage of experiments.

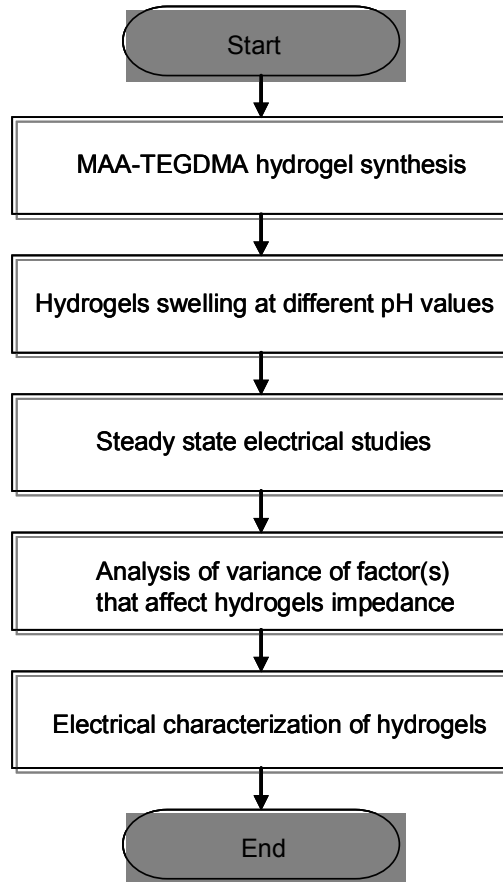


Figure 28: Flowchart of electrical characterization of hydrogels experiments.

4.5.2 MIP's sensitivity experiments

Following similar experimental procedures from those of the first stage of experiments (electrical characterization of hydrogels) MIP's sensitivity experiments were performed. MIP's were equilibrated in glutaric acid hydroxide buffer at pH 3.2 with 3 different concentrations (Table 9) of template molecule hydrocortisone. This constant buffer pH value was identified to be the optimal in regards to resistivity magnitude levels (ohms*cm) during the first stage of experiments when MIP's were tested at extreme concentrations (none and saturated) of hydrocortisone.

Table 9: Concentration of hydrocortisone in buffer solution for MIP's sensitivity experiments

Trial	Concentration of hydrocortisone (mg/ml)	Concentration Identifier
1	0.0	None
2	0.06	$\frac{1}{4}$ Saturated
3	0.12	$\frac{1}{2}$ Saturated

After the second stage of experiments were completed it was possible to analyze the relation between the electrical resistance of molecularly imprinted MAA-TEGDMA hydrogels as function of the concentration of their template molecule (hydrocortisone). Figure 29 presents a flowchart that summarizes the steps performed during the second stage of experiments.

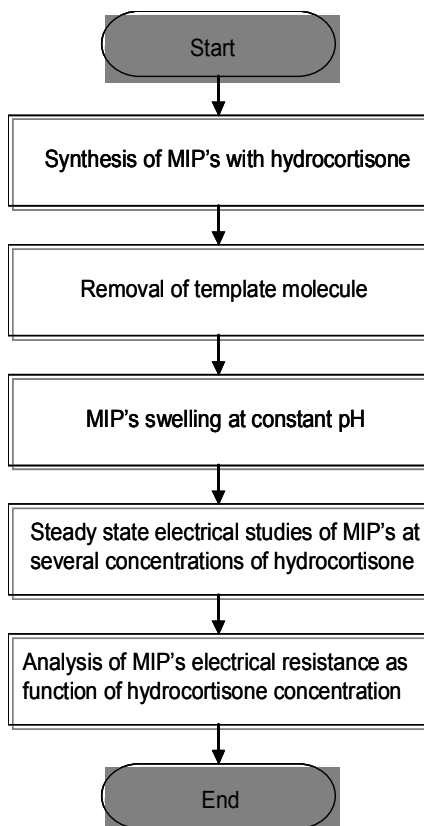


Figure 29: Flowchart of sensitivity experiments performed on MIP's as function of template molecule concentration under equilibrium conditions.

4.5.3 MIP's selectivity experiments

Following similar experimental procedures from those of the previous two stages of experiments (electrical characterization of hydrogels and molecularly imprinted hydrogels sensitivity studies) molecularly imprinted hydrogels selectivity experiments were performed. Molecularly imprinted hydrogels were equilibrated in glutaric acid hydroxide buffer at pH 3.2 with 3 different concentrations (Table 10) of template molecule analog fluorescein sodium salt (Sigma Aldrich, Co. St. Louis, MO, USA). The solutions had the same concentration levels as the one used during sensitivity experiments with hydrocortisone.

Table 10: Concentration of fluorescein sodium salt in buffer solution for MIP's selectivity experiments

Trial	Concentration of fluorescein sodium salt (mg/ml)
1	0.0
2	0.06
3	0.12

After the third stage of experiments was completed it was possible to make an assessment of the selectivity of the studied MIP's to an analog template molecule. Figure 30 presents a flowchart that summarizes the steps performed during the third stage of experiments.

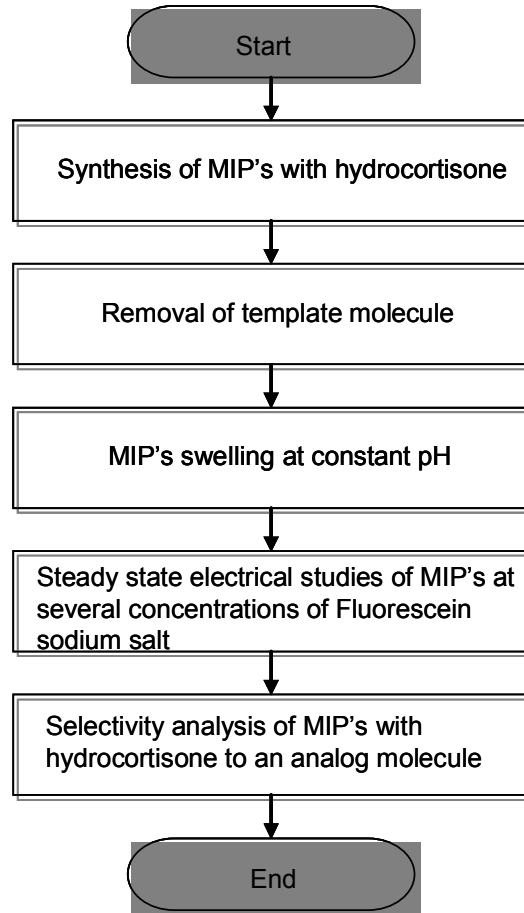


Figure 30: Flowchart of selectivity experiments performed on MIP's with hydrocortisone to analog molecule fluorescein sodium salt under equilibrium conditions.

5. Results and Discussion

5.1 Virtual Instrument Validation

Electrical impedance estimates were the basis of the characterization performed on MAA-TEGDMA hydrogels (non-imprinted and molecularly imprinted) on this work. As consequence it was necessary to validate the certainty of the estimation system. A preliminary experiment was designed to determine the error induced by the instrumentation and virtual instrument in the impedance estimation process. Instrumentation for this experiment represented a custom built instrumentation amplifier, data acquisition board and personal computer running the virtual instrument. The experimental setup consisted of two resistors of known value (R_1 and $R_2 \pm 1\%$ in Figure 31) measured using a digital multimeter (Agilent 34401A) to three significant figures. This test simulated posterior experimental setups in a controlled environment in which the resistance to be estimated (R_2) was known *a priori*. Figures 31 and 32 below illustrate the similarity between the validation and posterior experimental setup. In both setups the input voltage and control resistance (R_1 and R_{control} in Figures 31 and 32 respectively) were known *a priori* but differed in the context that the resistance to be estimated (R_2 in Figure 31) was known *a priori* in the validation experiment in contrast to the hydrogels resistance (R_{hydrogel} in Figure 32) which were estimated in real time as function of the factors and levels previously discussed.

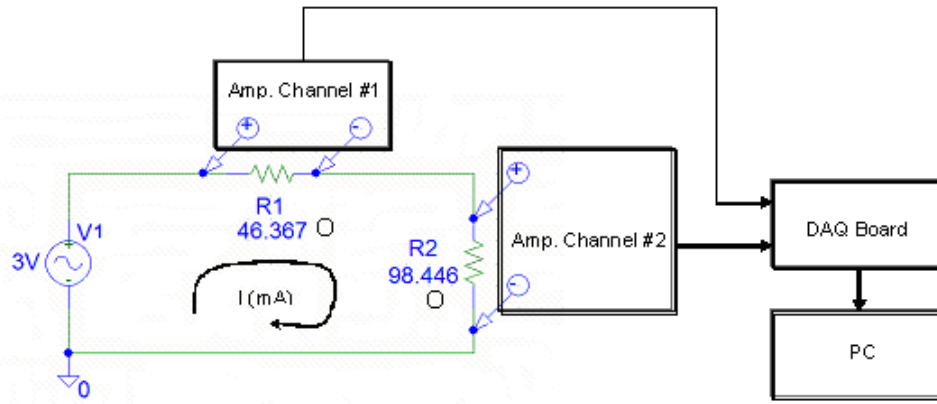


Figure 31: Experimental setup used to determined error induced by the instrumentation and virtual instrument.

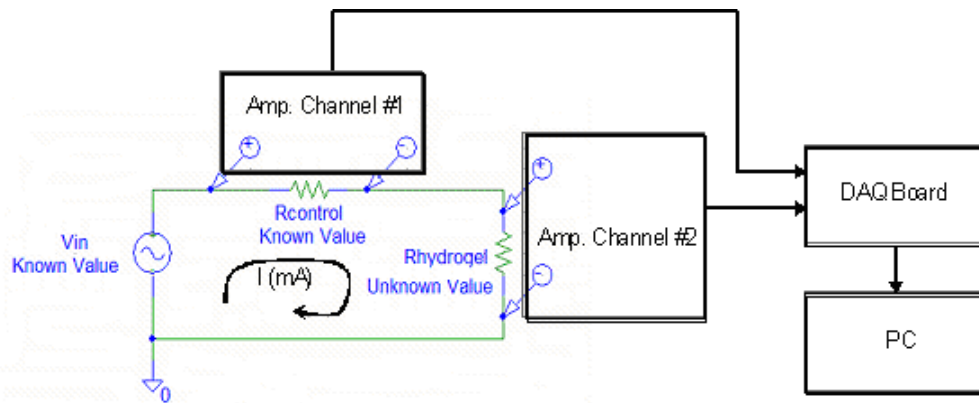


Figure 32: Experimental setup used to estimate MAA-TEGDMA hydrogels resistance.

Three replicates of the validation experiment were performed taking three samples of the voltage drop across R_1 and R_2 at each input signal frequency. A total of fifty input frequency values were tested with a frequency range from 100 to 5000 Hz with step changes of 100 Hz between sampling periods for a total of 150 estimated electrical resistance values per replicate or 450 in total. The average values for each set of estimated resistances along their standard deviation were then calculated offline. An approximate resistance magnitude estimate error of

0.4% was generated by the system in the validation process. Table 11 and Figure 33 present the validation results summary as well as the actual resistance estimates.

Table 11: Summary of validation results of virtual instrument using a controlled setup in which resistance values were known *a priori*.

Virtual Instrument Validation					
Run	Theoretical resistance (Ω)	Average estimated resistance (Ω)	Standard Deviation	Average Error	Average Deviation
1	98.446	98.18	0.453	0.40%	0.36%
2	98.446	98.1955	0.435	0.39%	0.36%
3	98.446	98.1936	0.449	0.39%	0.37%
Total		98.1897	0.445	0.39%	0.36%

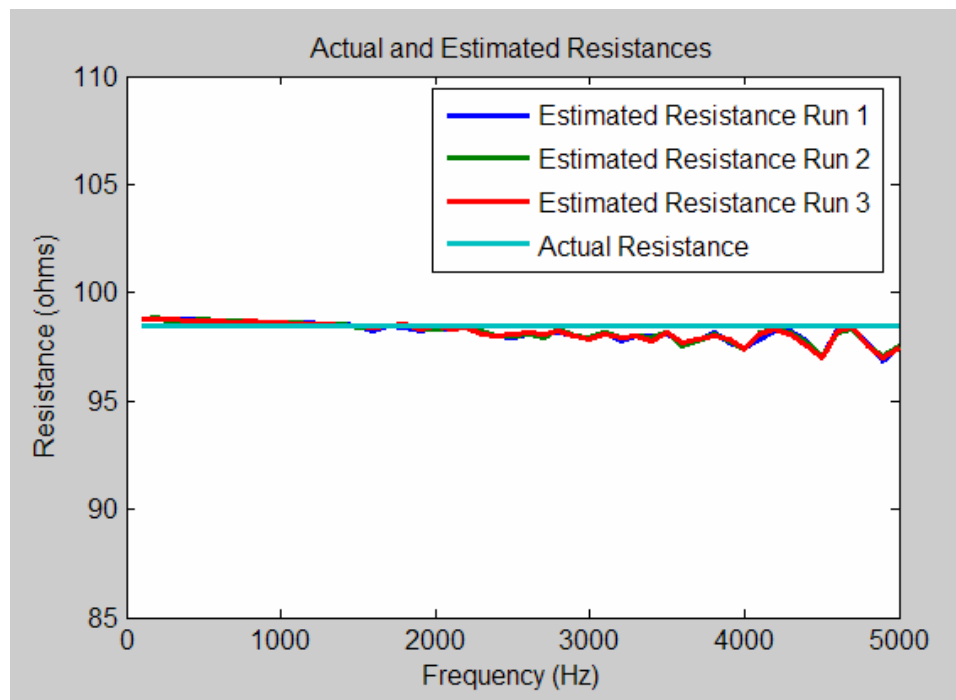


Figure 33: Estimated resistances from a simulation run in order to determine the error induced by the virtual instrument and instrumentation. Three replicates were performed taking three samples at each frequency interval (100 – 5kHz, $\Delta f = 100\text{Hz}$). Each of the values plotted represents an average of three sampled data points.

5.2 MAA-TEGDMA hydrogels electrical studies

5.2.1 Experimental protocol

Two hydrogels morphologies were used in the experiments at several experimental conditions to study a representative spectrum with the goal of identifying and optimal operating point. The hydrogel morphologies were defined as a control or non-molecularly imprinted and those molecularly imprinted with hydrocortisone. The experimental conditions for each of the MAA-TEGDMA hydrogel variants were defined as their composition (17:1 and 39:1 molar ratio), medium pH (3.2, 4.8 and 5.4), hydrocortisone concentration (0 mg/ml and 0.24 mg/ml) and input signal frequency (0 – 5000 Hz). The main focus of this study was to: (a) characterize the electrical behavior of these hydrogels as function of studied variables, (b) compare the electrical response of control hydrogels to molecularly imprinted ones, and (c) determine a possible optimum operation region of molecularly imprinted hydrogels with hydrocortisone as the basis for future biosensor development. To achieve this goal an analysis of variance of the electrical properties of MAA-TEGDMA hydrogels as function of the experimental conditions was performed and the results are presented in the following sections.

As reference for all trials performed during this experimental stage figures 34 to 36 present a chronological sequence for one of the experimental conditions tested. A similar sequence was followed for all of the other tested combinations. The trial selected for this walkthrough is that of non-imprinted MAA-TEGDMA hydrogels variant at a 17:1 monomer to cross-linker molar ratio, medium pH of 3.2, hydrocortisone concentration of 0.0 mg/ml and an input signal frequency sweep

from (0 to 5 KHz, with a delta of 100Hz). The first part of the trial consisted of estimating the electrical impedance of the buffer medium. This was done by estimating the current in the system by measuring the voltage drop across a control resistor of known value. A similar procedure was followed afterwards with a hydrogel sample in the center of the diffusion cell. Estimated currents for both of these cases are shown in figure 34.

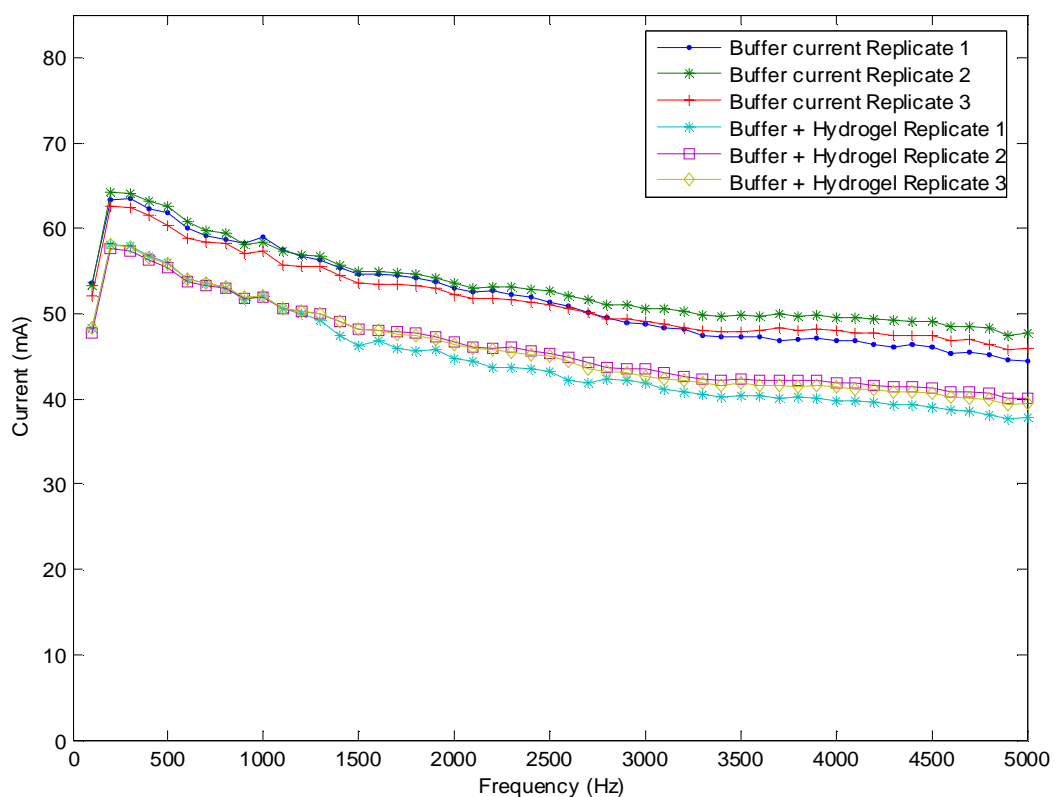


Figure 34: Estimated currents (mA) for glutaric acid sodium hydroxide buffer pH 3.2 and buffer + non-MIP MAA-TEGDMA (17:1) hydrogels. Buffer + hydrogel trials produced a lower net current in the system than that of the buffer trials.

During the real time data acquisition and processing of the samples it was possible to estimate the electrical impedance contribution of the buffer medium by dividing the acquired voltage drop across the buffer solution by the previously estimated

current in the same data acquisition cycle. Similar procedure was performed to estimate the electrical impedance contribution of the buffer solution plus a hydrogel sample. The last phase in the process of estimating the electrical impedance of the hydrogels was to subtract offline the curves of the buffer plus hydrogel estimated impedance and the buffer impedance.

After all trials were completed for all the different combinations it was observed that the electrical response of hydrogels was not significantly affected by signal frequency. As consequence of this it was decided to convert the magnitude of the impedance in ohms to a material specific resistivity value in ohms*cm by using the geometrical features of the studied samples using equation 13.

$$\rho = (R_{total} - R_{solution}) * \frac{A}{D} \quad (13)$$

Where,

R_{total} = Estimated hydrogel + solution resistance (ohms)

$R_{solution}$ = Estimated solution resistance (ohms)

A = Hydrogel Area = $\pi * (0.6035)^2 = 1.14$ (cm²)

D = Hydrogel thickness = 0.0381 (cm)

This frequency independent response when compared to other system variables will be discussed in detail in section 5.3.1. A sample of this frequency independency behavior is presented in figures 35 and 36 with the impedance magnitude and phase responses of these hydrogels. For the remaining of the discussion phase estimates are going to be discarded as well as the impedance term and the analysis will concentrate in the electrical resistivity of MAA-TEGDMA hydrogels (non-imprinted and molecularly imprinted).

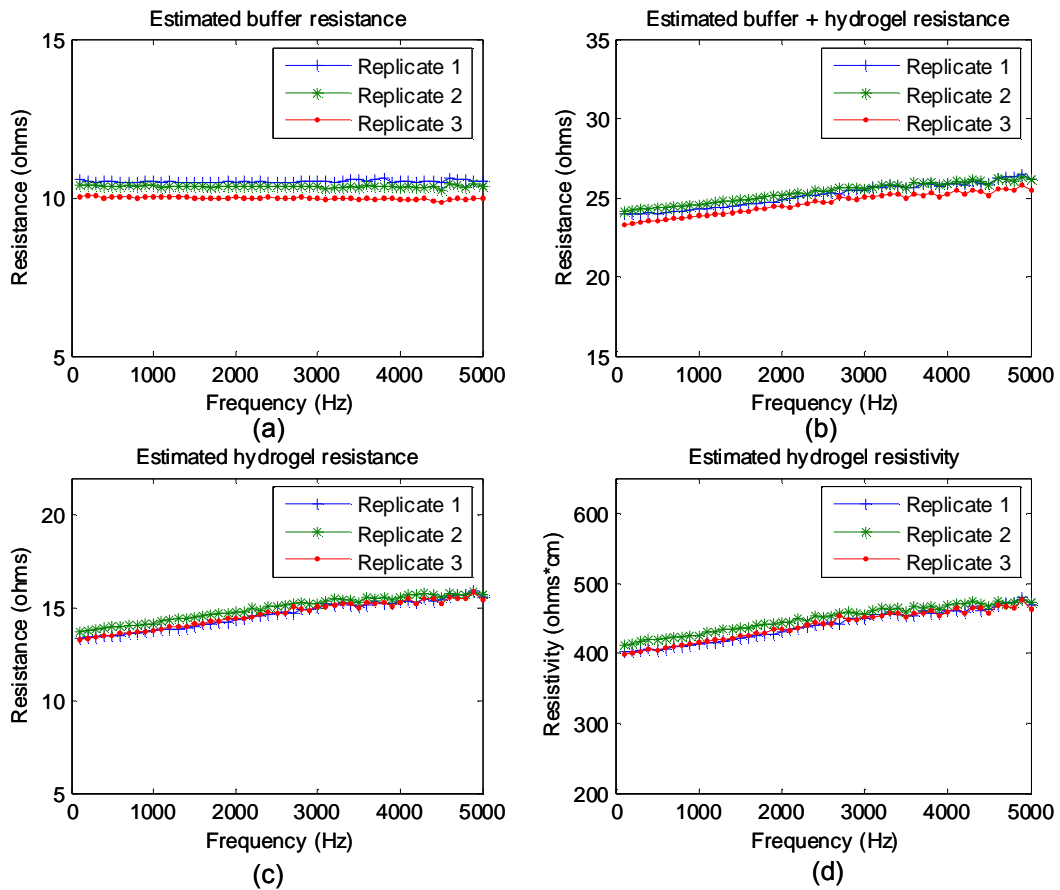


Figure 35: Sample replicates of MAA-TEGDMA electrical studies. From top to bottom, left to right: (a) estimated electrical resistance of glutaric acid sodium hydroxide buffer pH 3.2; (b) estimated electrical resistance of buffer + hydrogel samples; (c) estimated electrical resistance of hydrogels calculated offline; (d) estimated hydrogels resistivity calculated offline. Each data point represents the mean value of 3 samples for a total of 150 samples per replicate.

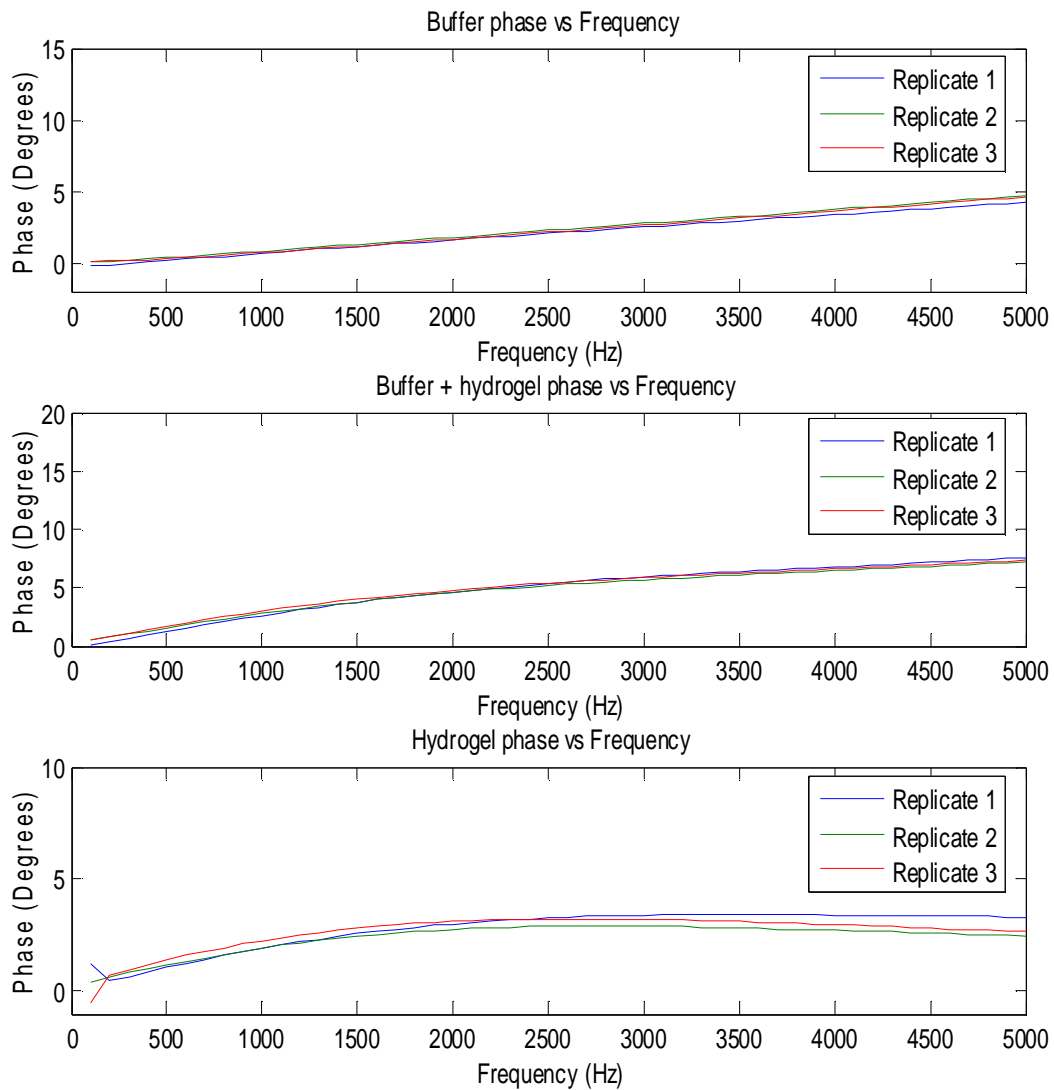


Figure 36: Sample plot of electrical studies on MAA-TEGDMA (17:1) hydrogels equilibrated at pH 3.2. (Top) Buffer phase as function of frequency, (Middle) Buffer + Hydrogel phase as function of frequency, (Bottom) estimated hydrogel phase calculated offline as the difference between curves Middle and Top. Each data point represents the average from 3 replicates ($n = 9$), error bars do not show in plot due to their small magnitude compared to the scale.

5.2.2 Non-molecularly imprinted MAA-TEGDMA hydrogels

Once all specified combinations were tested on reference hydrogels, it was possible to identify several trends in their electrical response. Combinations in this experiment are defined as the product of the identified levels, replicates and samples taken at each unique combination. In this experiment the number of samples was equal to 5,400. As mentioned earlier one of the identified trends was the weak dependency of the response as function of input signal frequency. It was observed that hydrogel morphology, buffer pH and to some extent the concentration of hydrocortisone had an effect in the electrical resistivity of non-imprinted MAA-TEGDMA hydrogels.

The 17:1 morphology and 3.2 pH levels produced the greatest difference in response when examined within the same group. This noticeable difference in the electrical resistivity of non-molecularly imprinted hydrogels at these two levels was related to the water contents inside the hydrogels. Water contents in hydrogels have been attributed to be a factor in their electrical conductivity. The greater the water contents within a hydrogel the largest its expected conductivity. At higher cross-linker values (17:1) and lower pH value (3.2) the swelling ratio of MAA-TEGDMA hydrogels was at a minimum in this tested population (Section 5.6). Being this the case it was expected that their electrical conductivity will be the lowest when compared to rest of population which is analogous to the greatest magnitude in electrical resistivity obtained in this experiment. The trend of decreasing resistivity of 39:1 hydrogels as function of increasing pH was also observed but to a lesser degree at higher pH values. The electrical resistivity response of non-imprinted MAA-TEGDMA hydrogels was for the most part non-

specific as function of hydrocortisone concentration. The only deviation to this lack of significance as function of a buffer saturated in hydrocortisone (0.24 mg/ml) was for the case of 17:1 hydrogel composition and buffer pH's of 3.2. Figure 37 presents a summary of the electrical resistivity of non-imprinted hydrogels as function of the factors and levels studied.

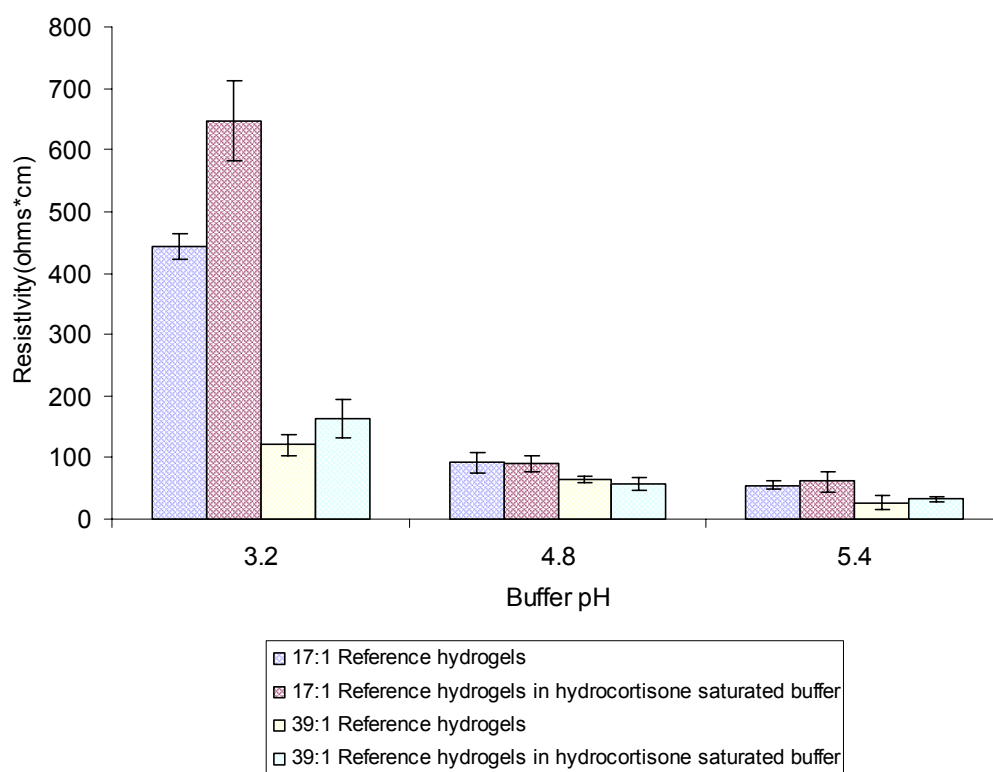


Figure 37: Estimated electrical resistivity as function of pH and hydrocortisone concentration for MAA-TEGMA non-imprinted. Vertical bars represent the average value from 3 replicates (n = 450) while error bars represent the mean standard deviation.

5.2.3 Molecularly imprinted MAA-TEGDMA hydrogels

A similar testing procedure as with the control group was followed for the study of molecularly imprinted MAA-TEGDMA hydrogels with hydrocortisone. All factors and their corresponding levels remained fixed to compare the response of the control variant (non-imprinted hydrogels) and the biosensor prospect (molecularly imprinted hydrogels). As before several trends were identified in the response of the molecularly imprinted hydrogels as function of the studied variables. In terms of morphology and pH, similar trends to the control group were observed. Higher cross-linker ratio in the hydrogels (17:1) and lower pH values yielded a greater electrical resistivity response in the studied samples. A significant difference in regards to the control group was the response of molecularly imprinted hydrogels when equilibrated in a buffer saturated (0.24 mg/ml) with hydrocortisone. As in the case of the control group the greater magnitude response was obtained with the 17:1 morphology. Molecularly imprinted hydrogels also exhibited a significant difference as function of hydrocortisone at two pH values (3.2 and 4.8) and two morphologies (17:1 and 39:1). At 17:1 and pH 3.2 the response was doubled while at 17:1 and pH 4.8 the response was more than tripled when comparing at high and low levels of hydrocortisone. This is attributed to the interaction between the model molecule and specific binding cavities that were created during the synthesis and posterior washing of the molecularly imprinted hydrogels. At the higher pH value of 5.4 there was not any significant difference in the response of the MIP's as function of concentration. It is believed that this behavior is due to the significant amount of swelling at higher pH values for the two morphologies under study. Is worth highlighting that even though the

control group (non-imprinted) reported some degree of interaction at 17:1 and pH 3.2 with the model molecule that the response of this same combination for the molecularly imprinted case was significantly greater. Figure 38 presents a summary of the responses of molecularly imprinted hydrogels as function of studied variables. Figure 39 presents a summary of the response of the non-imprinted and molecularly imprinted hydrogels in a normalized version of the electrical resistivity response for visualization purposes.

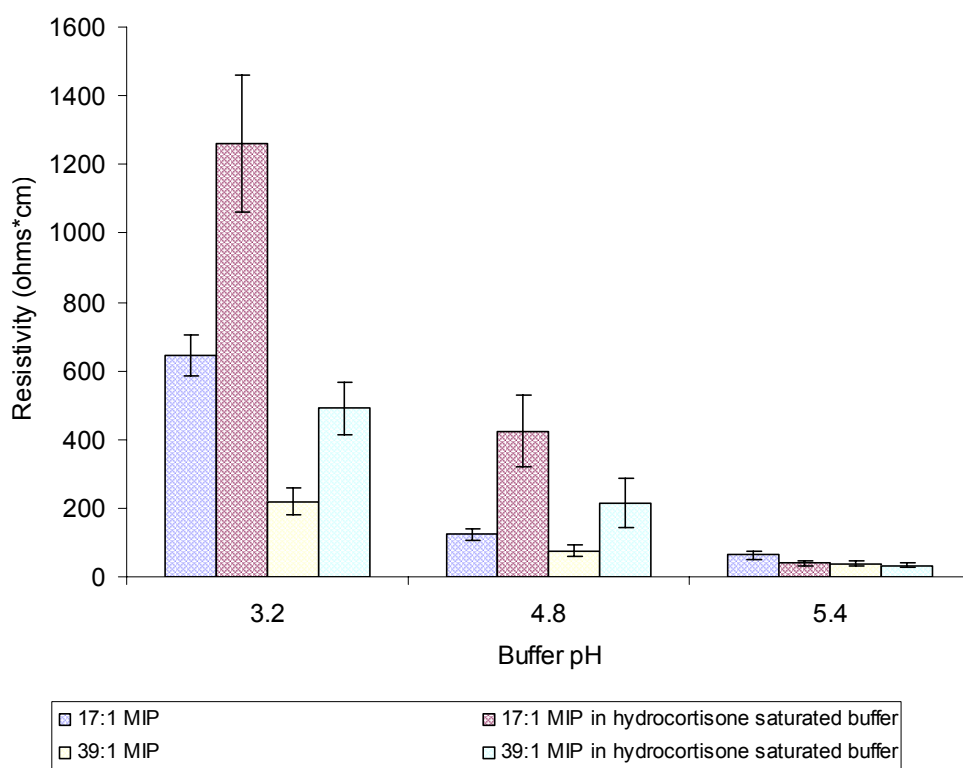


Figure 38: Estimated electrical resistivity as function pH and hydrocortisone concentration for MIP MAA-TEGDMA hydrogels. Vertical bars represent the average value from 3 replicates ($n = 450$) while error bars represent the mean standard deviation.

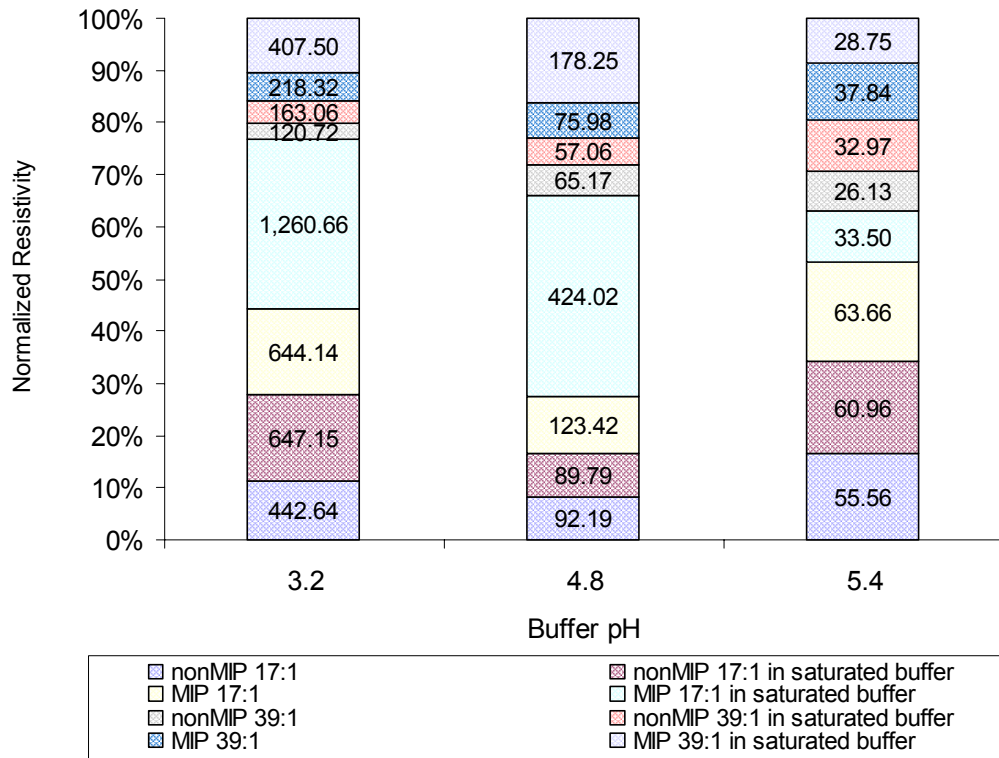


Figure 39: Normalized estimated resistivity of MAA-TEGDMA non-imprinted and imprinted with hydrocortisone as function of buffer pH (3.2, 4.8 and 5.4), hydrogel composition (17:1 and 39:1), hydrocortisone concentration (0 mg/ml and 24 mg/ml) and input signal frequency (100 – 5000 Hz). Each block represents the mean value (3 replicates, n = 450) for each of the 24 combinations studied stacked in a normalized resistivity value per pH tested.

5.3 Factor analysis of electrical resistivity of MAA-TEGDMA hydrogels

5.3.1 Analysis of variance: MAA-TEGDMA Reference hydrogels resistivity versus composition, pH, concentration and frequency

A factor analysis was performed to determine the factors that had a significant effect in hydrogel resistivity by developing a general linear model in Minitab. The factors and levels for this analysis are presented in Table 12. For each combination the corresponding electrical resistivity value obtained in the experiments was used as the response.

Table 12: General linear model: hydrogels resistivity versus hydrogel composition, solution pH, concentration and frequency

Factor	Type	Levels	Values
Hydrogel Composition (MAA-TEGDMA)	fixed	2	80:20, 90:10 (by weight)
Solution pH	fixed	3	3.2, 4.8, 5.4
Saturated in hydrocortisone	fixed	2	No, Yes
Frequency	fixed	50	100, 200, 300, 400, 500, 600, 700, 800, 900, 1000, 1100, 1200, 1300, 1400, 1500, 1600, 1700, 1800, 1900, 2000, 2100, 2200, 2300, 2400, 2500, 2600, 2700, 2800, 2900, 3000, 3100, 3200, 3300, 3400, 3500, 3600, 3700, 3800, 3900, 4000, 4100, 4200, 4300, 4400, 4500, 4600, 4700, 4800, 4900, 5000

The generated model was able to explain the variability of the data to a 98.48% value and the main effects and interaction effects (Figures 40 and 41) agreed with the expected results but did not meet the required assumptions for an analysis of variance model (Figures 42 and 43). These assumptions are that the error terms given by the residuals comply with: (a) the variance of the observed value should

be equal across all factor levels, (b) errors should be normally distributed ($AD < 0.75$ or 1), and (c) errors should be structure less.

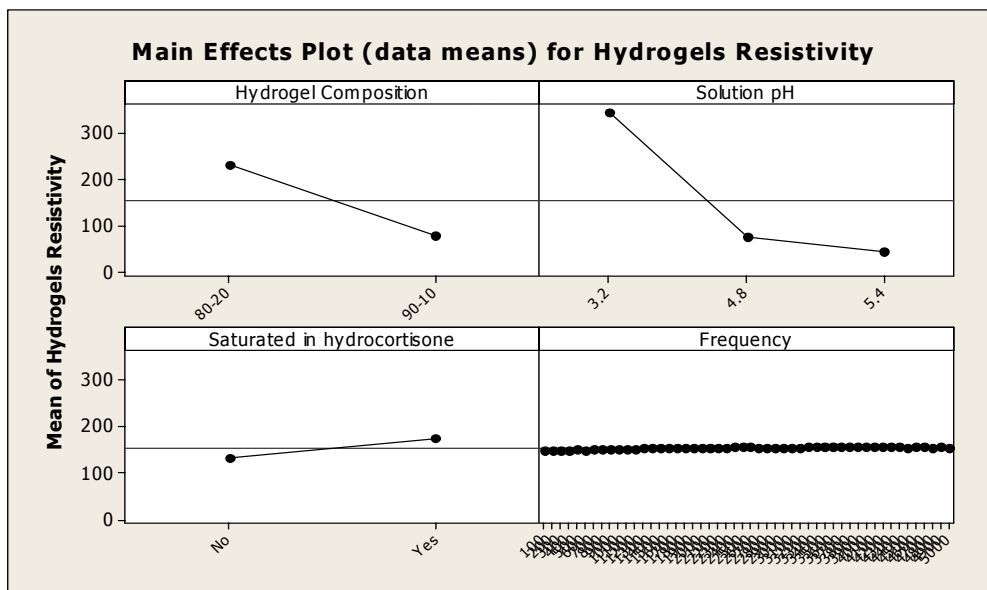


Figure 40: Main effects plot of the factors taken into consideration during electrical studies of reference MAA-TEGDMA hydrogels. Data points represent the mean value for each of the levels studied within the main factors.

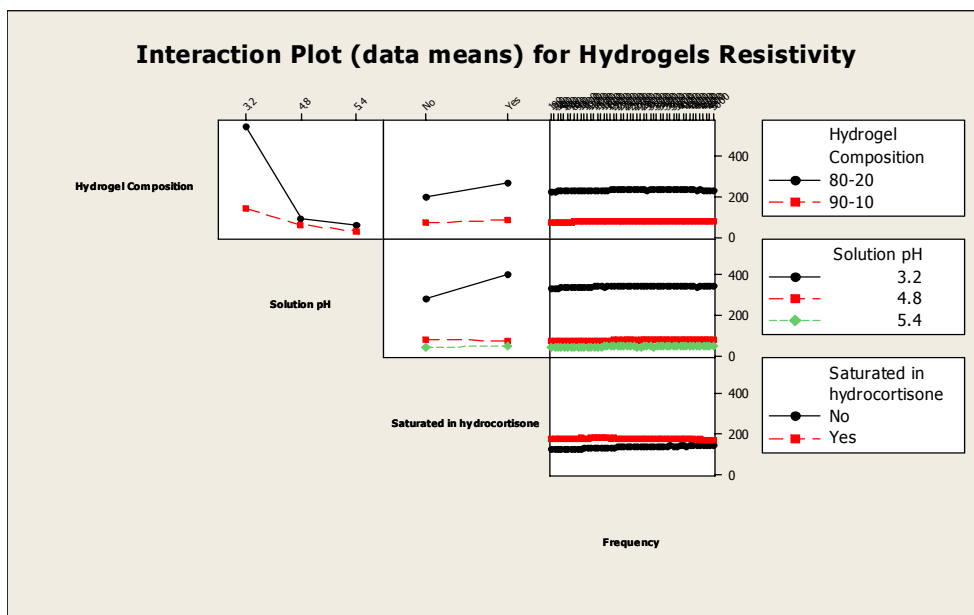


Figure 41: Interactions plot of the factors and levels taken into consideration during electrical studies of reference MAA-TEGDMA hydrogels. Data points represent the mean value for each of the combinations studied.

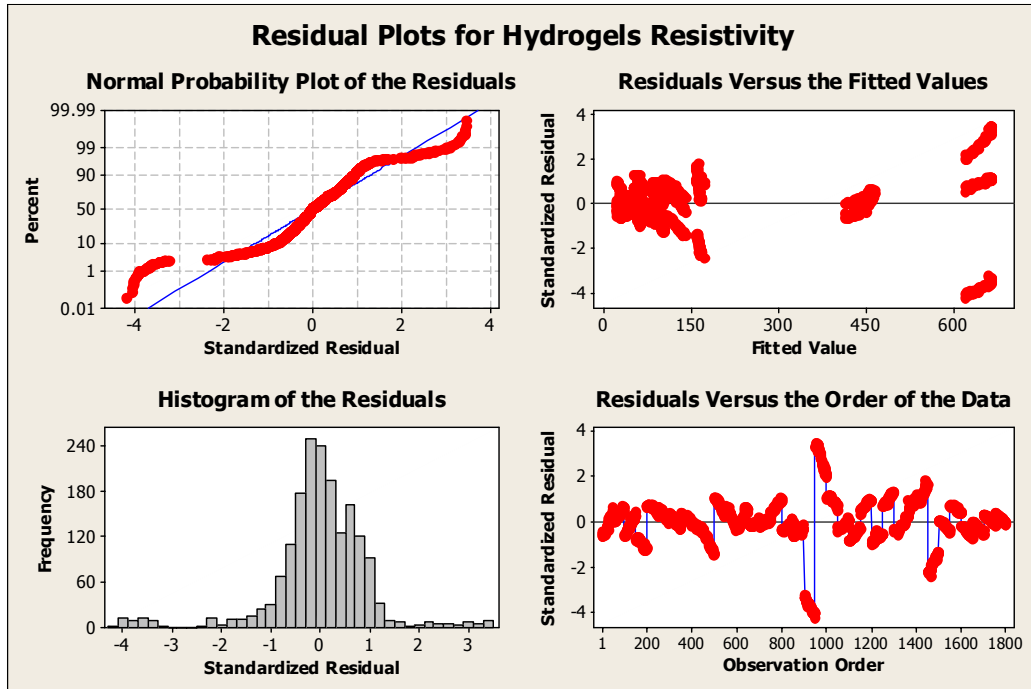


Figure 42: Four in one plot of residuals of analysis of variance of the electrical resistivity of reference MAA-TEGDMA hydrogels, n = 1800.

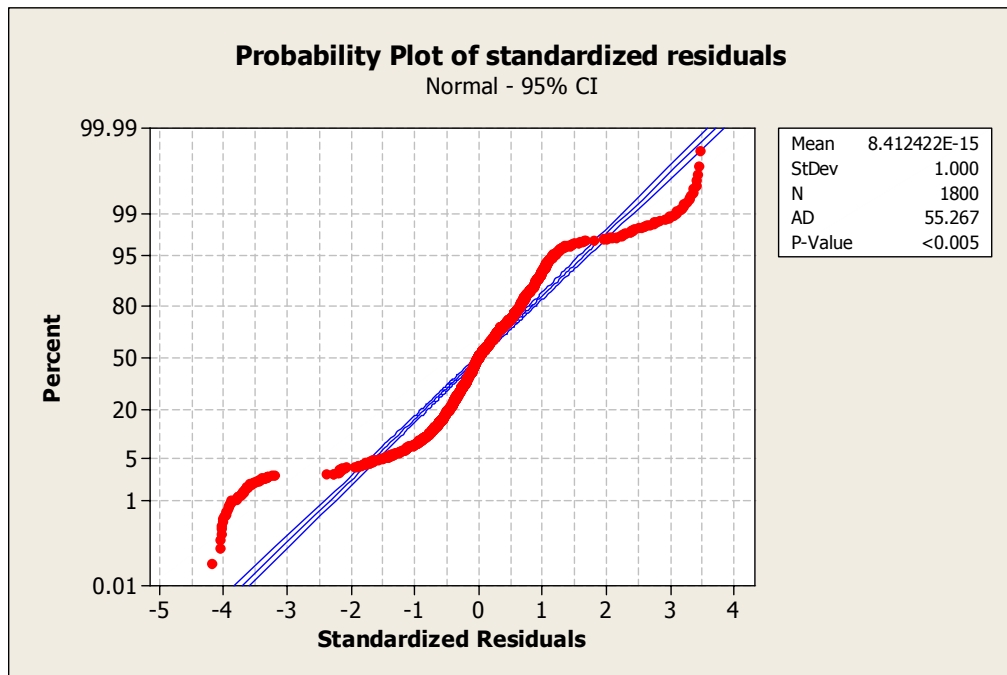


Figure 43: Normal probability plot at 95% confidence interval of standardized residuals of analysis of variance of reference MAA-TEGDMA hydrogels.

At this point it was decided to reduce the complexity of the model by using some of the information from the main effects and interaction plots. From these plots and corresponding factors P values it was concluded that frequency did not have any significant effect on the response of the system. It was decided to use the frequency factor as a repetitive term in the sampling; therefore the mean was calculated for each replicate of 150 points. A final adjustment was made by removing the pH 5.4 level in order to have a balance structure of two levels per factor since this level was also insignificant to the variability of the response. Table A1 in the appendix section shows the reduced set used in order to try to comply with the required model assumptions.

A second analysis was performed, this time with the reduced data set. The effects were similar as before but this time the model assumptions were met while using a second order interaction model. The numerical output from this fit is presented in Table A2 and Table **A3** in the appendix. From this output it can be concluded that all factors and interactions between them had a significant effect in the response ($P \text{ value} < 0.05$). This can be seen in graphical form in Figure 44 in which the standardized effects have been plotted in a Pareto and all effects are greater than the calculated significance value. It is also evident that the main effects have more significance in the response than two way interactions by looking at their F statistic (161.29 and 53.93 respectively). The F statistic is a ratio of the amount of variability explained by the treatment effect compared to the amount of natural variability. This can be viewed as a signal to noise ratio figure. The more variability that can be explained by the treatments (factor levels), the larger the F statistic becomes. If there is a large F statistic, the probability that we

just happened to see much variability accounted for by our treatment effect, simply due to a random chance would be small.

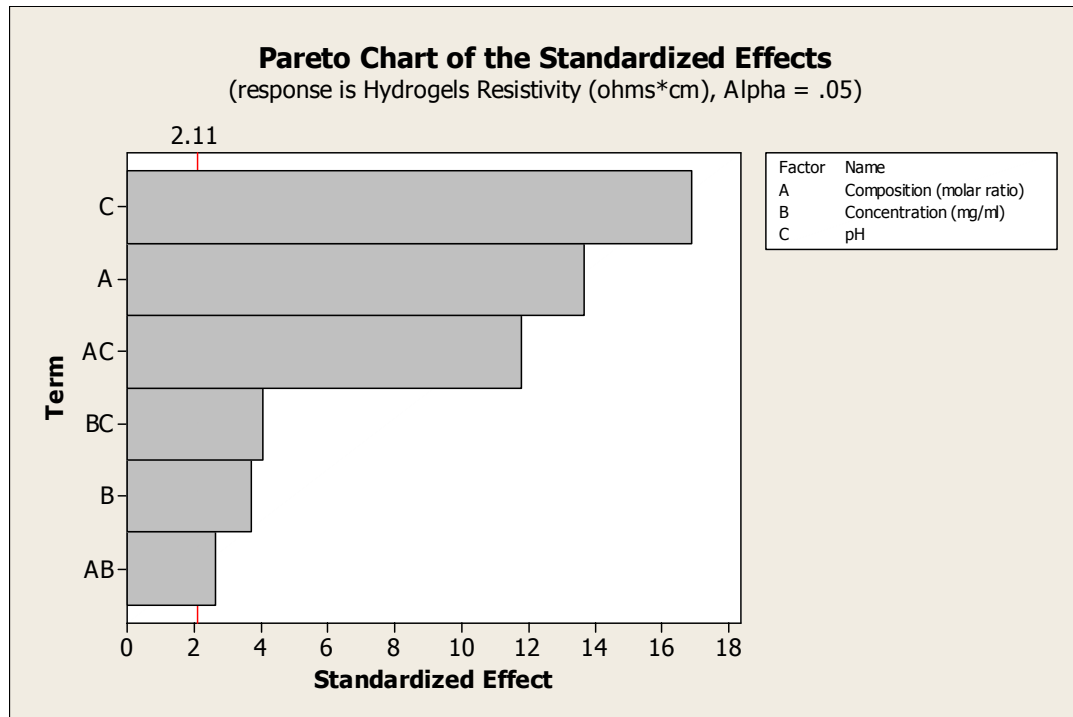


Figure 44: Pareto chart of standardized effects up to two way interactions for non-MIP MAA-TEGDMA hydrogels. Effects to the right of vertical line are considered statically significant.

Figures 45 and 46 present the main effects and interactions. It can be seen in graphical form on these two plots what the ANOVA table provided in numerical format with respect to the greater significance of the main effects when compared with the interactions. Main effects have a considerable change (slope) when moving from low to a high level, while interactions between factors showed a somewhat weak relation noted by the lack of intersection (parallelism) of the lines.

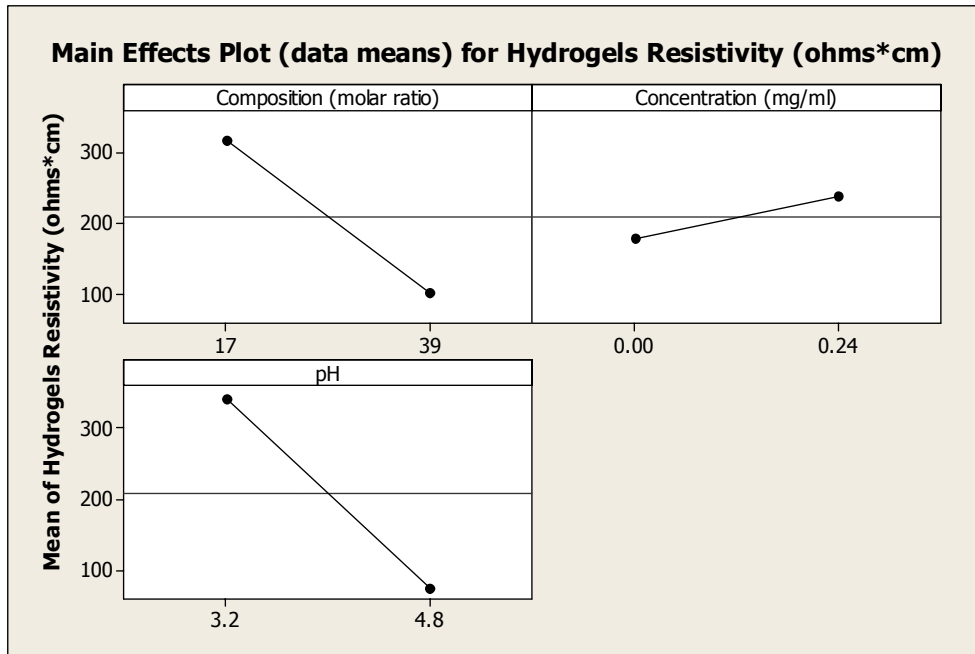


Figure 45: Modified (frequency less) main effects plot of the factors taken into consideration during electrical studies of reference MAA-TEGDMA hydrogels. Data points represent the mean value for each of the levels studied within the main factors.

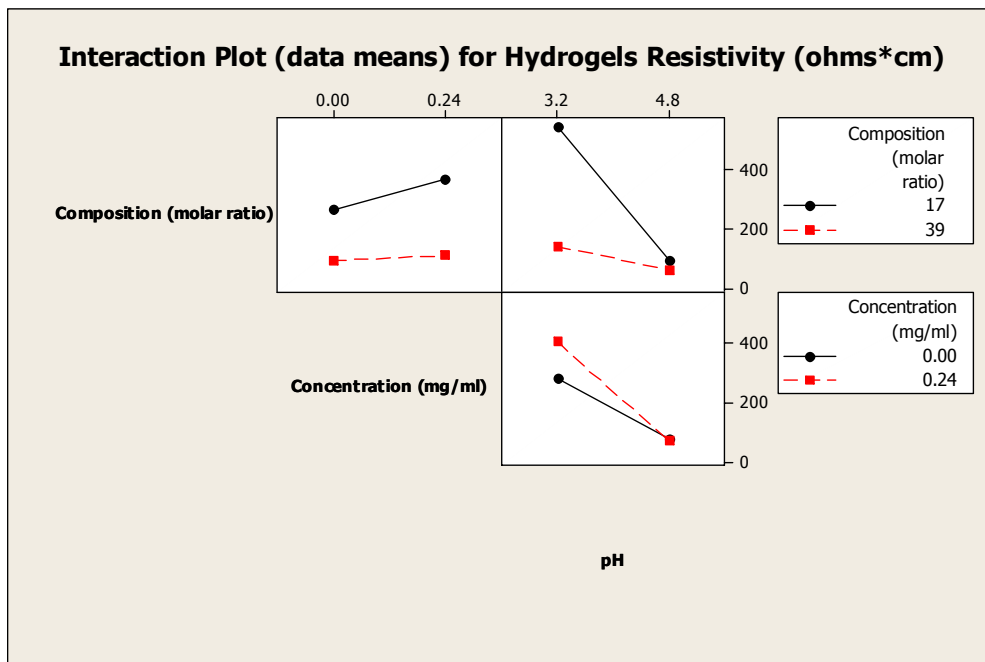


Figure 46: Modified (frequency less) interaction plot of the factors and levels taken into consideration during electrical studies of reference MAA-TEGDMA hydrogels. Data points represent the mean value for each of the combinations studied.

Model adequacy was verified (Figures 47 and 48) and it is evident it complies with all the residuals assumptions presented earlier.

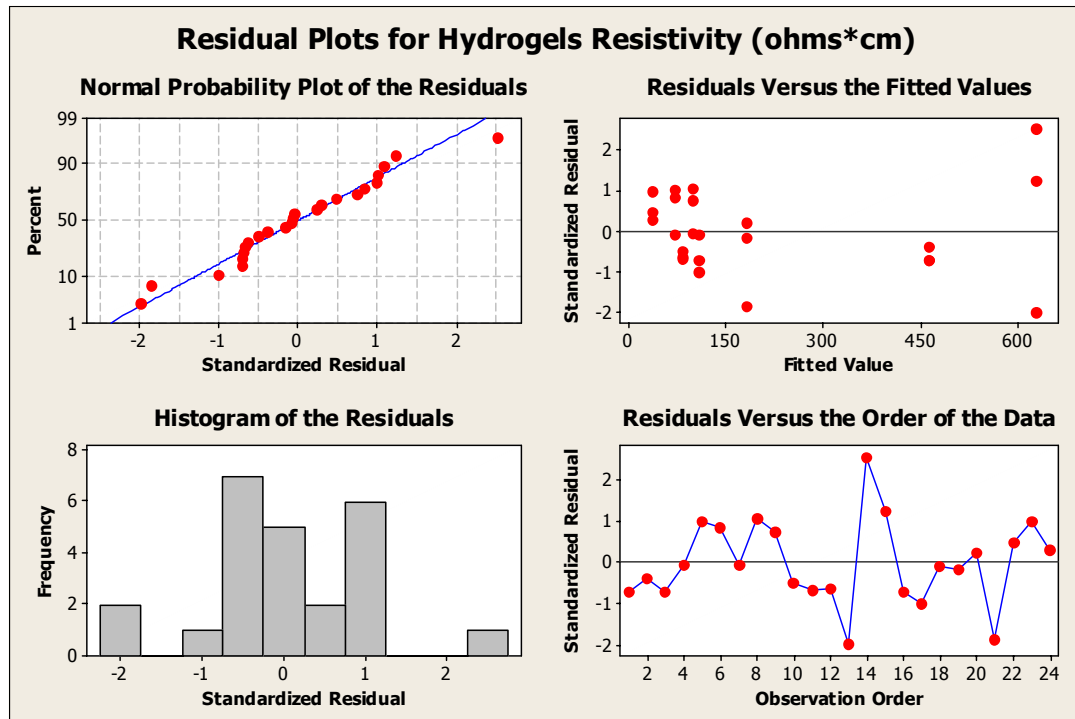


Figure 47: Four in one plot of residuals of analysis of variance of the electrical resistivity of reference MAA-TEGDMA hydrogels without frequency as a factor, $n = 24$.

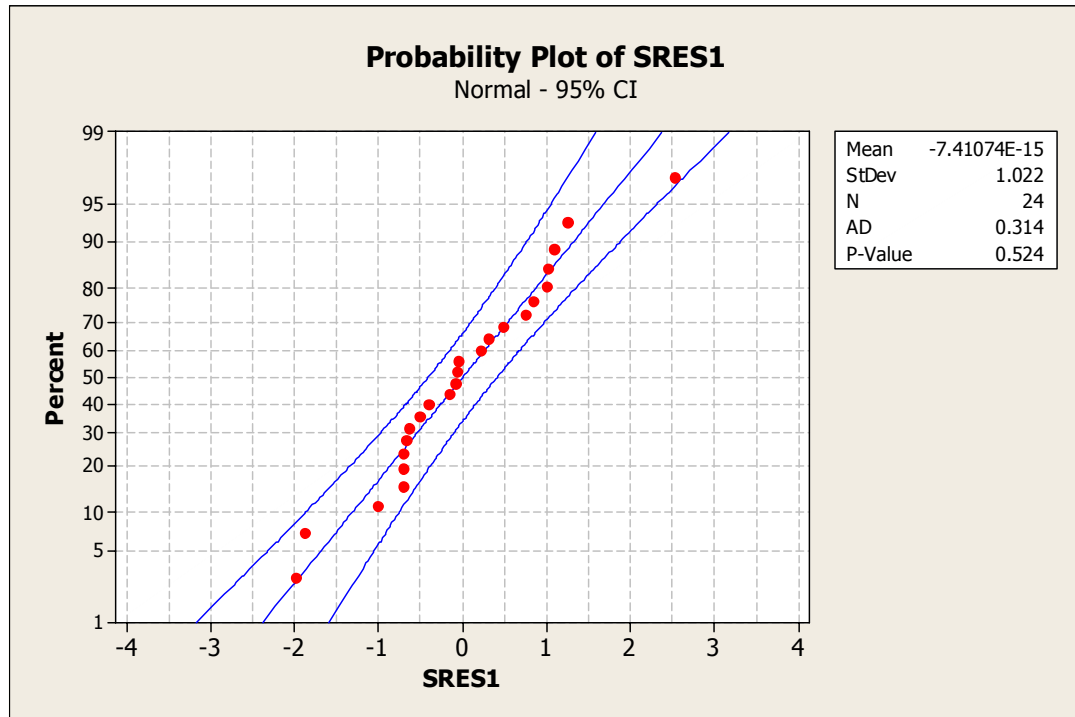


Figure 48: Normal probability plot at 95% confidence interval of standardized residuals of analysis of variance of reference MAA-TEGDMA hydrogels (frequency less).

Finally, the estimated second order interaction model coefficients are presented in Table A4 in the appendix.

5.3.2 Analysis of variance: MAA-TEGDMA molecularly imprinted hydrogels resistivity versus composition, pH and concentration

A similar approach of a reduced data set was used to develop a factorial fit of the electrical resistivity of MAA-TEGDMA molecularly imprinted hydrogels.

Table 13 presents the factors and levels used in the analysis.

Table 13: Factors and levels used in analysis of variance of molecularly imprinted MAA-TEGDMA hydrogels resistivity.

Factor	Type	Levels	Values
Hydrogel Composition (MAA-TEGDMA)	Fixed	2	80:20, 90:20 (weight ratio)
Saturated in hydrocortisone	Fixed	2	No, Yes
Solution pH	fixed	3	3.2,4.8,5.4

As in the case of non-imprinted hydrogels, all factors and their combinations were statically significant in the electrical resistivity of MIP's yielding P values < 0.05. The factorial fit is presented in Table A5 and Table **A6** in the appendix section. As in the case of non-imprinted MAA-TEGDMA hydrogels the main effects had more significance than the interactions between factors but again the two of them were statically significant. The pH factor was also the most significant in the response of molecularly imprinted hydrogels as was the case with the non-imprinted hydrogels (Figure 49). Figures 50 and 51 present a summary of the main and interaction effects. Model adequacy was again verified against the required assumptions, which were all met (Figures 52 and 53).

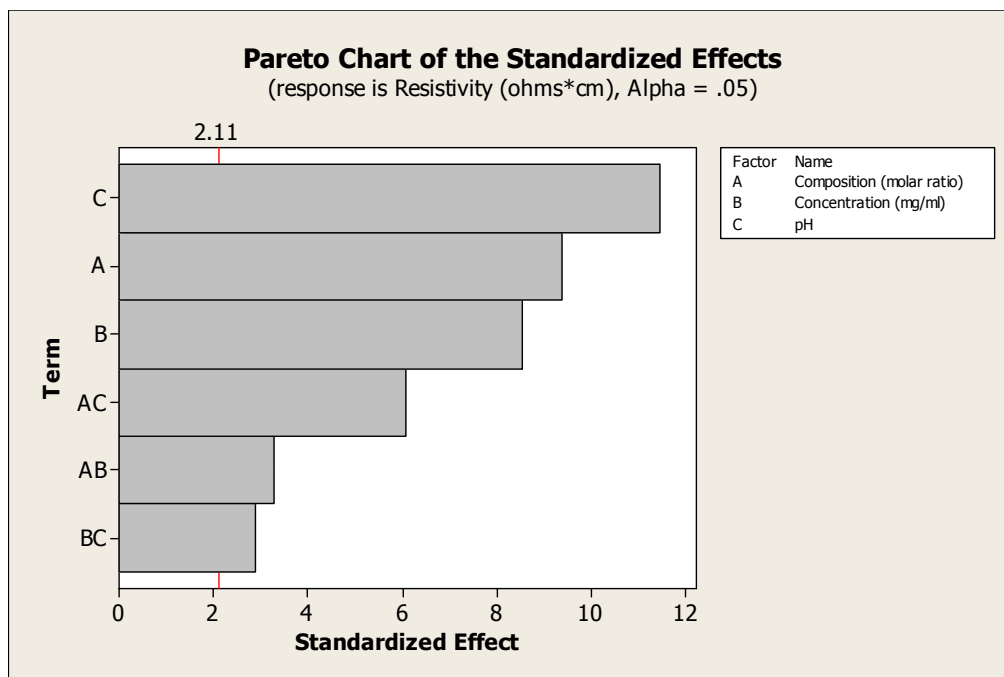


Figure 49: Pareto chart of standardized effects up to two way interactions for MIP MAA-TEGDMA hydrogels. Effects to the right of vertical line are considered statically significant.

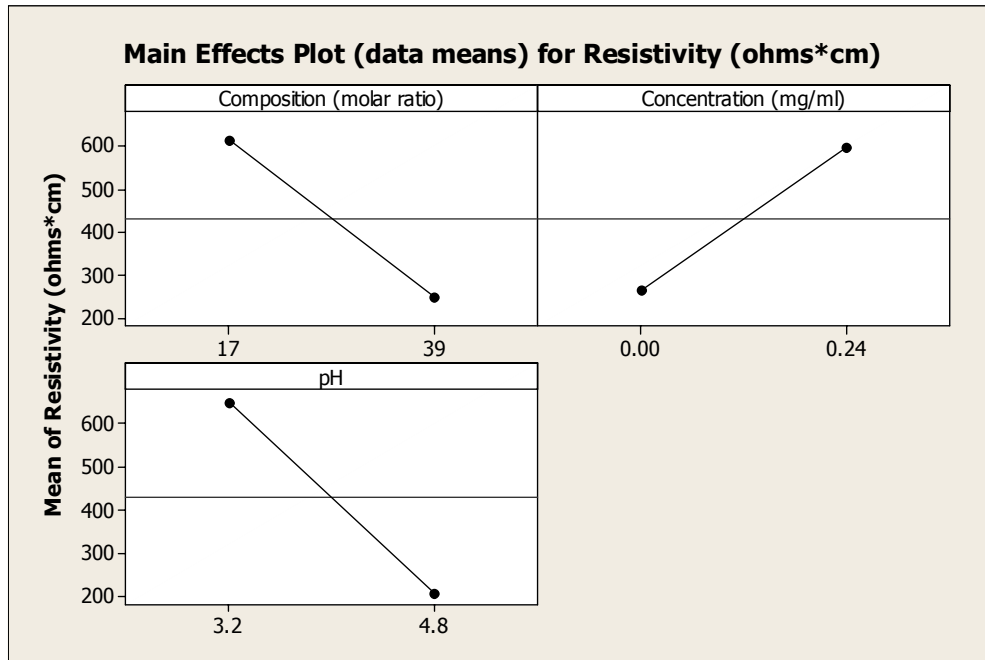


Figure 50: Modified (frequency less) main effects plot of the factors taken into consideration during electrical studies of molecularly imprinted MAA-TEGDMA hydrogels. Data points represent the mean value for each of the levels studied within the main factors.

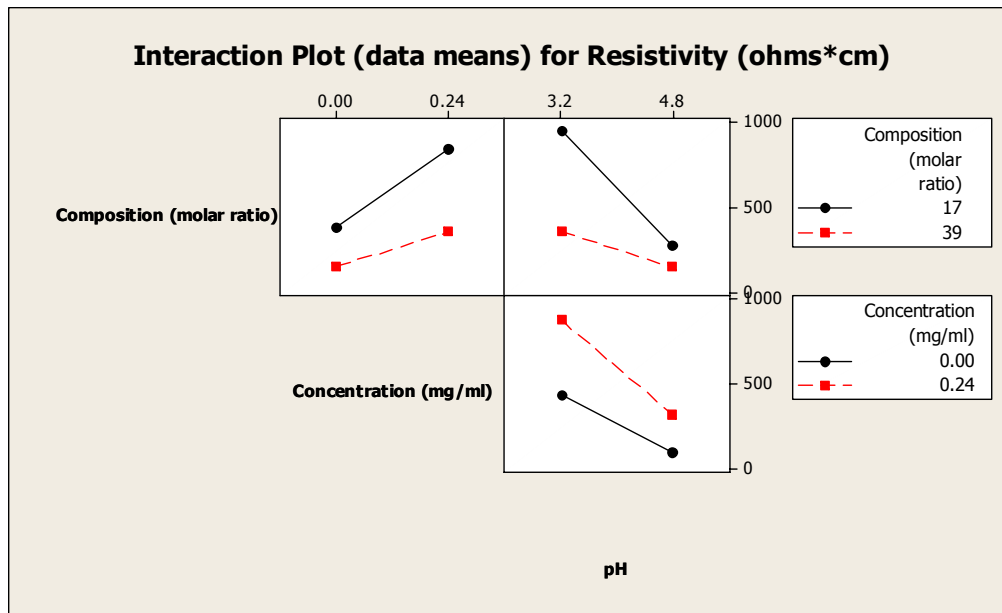


Figure 51: Modified (frequency less) interaction plot of the factors and levels taken into consideration during electrical studies of molecularly imprinted MAA-TEGDMA hydrogels. Data points represent the mean value for each of the combinations studied.

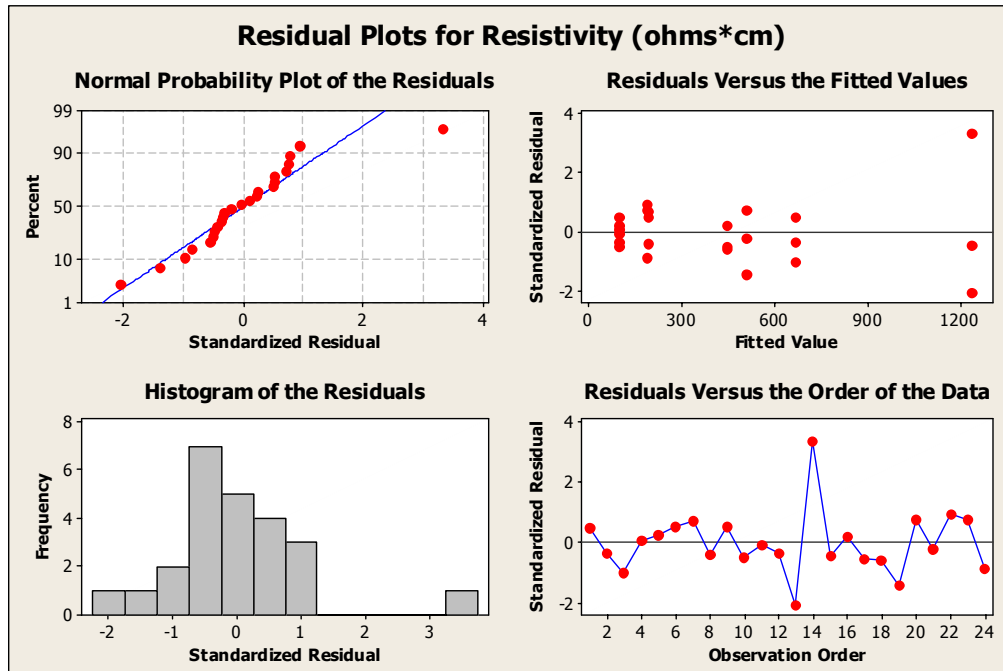


Figure 52: Four in one plot of residuals of analysis of variance of the electrical resistivity of molecularly imprinted MAA-TEGDMA hydrogels without frequency as a factor, n = 24.

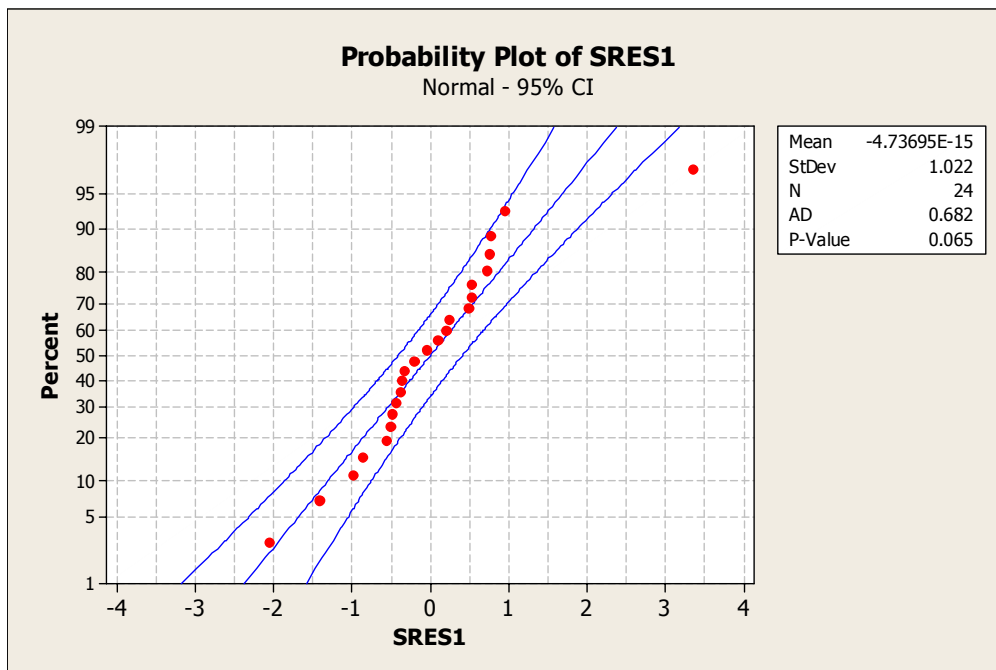


Figure 53: Normal probability plot at 95% confidence interval of standardized residuals of analysis of variance of molecularly imprinted MAA-TEGDMA hydrogels (frequency less).

Finally, the estimated second order interaction model coefficients are presented in Table A7 in the appendix.

5.3.3 Comparison of non-imprinted and molecularly imprinted hydrogels resistivity as function of composition, pH and template concentration

Examining the least squared means data from the factorial fit for non-imprinted and molecularly imprinted MAA-TEGDMA hydrogels (Table 14) it can be concluded that average response of molecularly imprinted hydrogels as well as their variance was greater to that of non-imprinted hydrogels under the same operating conditions.

Table 14: Least Squares Means for Hydrogels Resistivity (ohms*cm)

	non-MIP		MIP	
	Mean	SE Mean	Mean	SE Mean
Composition				
17:1	317.84	11.21	613.09	27.42
39:1	101.53	11.21	249.47	27.42
Concentration (mg/ml)				
0.00	180.15	11.21	265.47	27.42
0.24	239.21	11.21	597.10	27.42
pH				
3.2	343.32	11.21	653.15	27.42
4.8	76.05	11.21	209.41	27.42
Composition*Concentration				
17:1, 0.00	267.32	15.86	383.83	38.78
39:1, 0.00	92.99	15.86	147.10	38.78
17:1, 0.24	368.37	15.86	842.34	38.78
39:1, 0.24	110.06	15.86	351.85	38.78
Composition*pH				
17:1, 3.2	544.74	15.86	952.45	38.78
39:1, 3.2	141.89	15.86	353.85	38.78
17:1, 4.8	90.94	15.86	273.72	38.78
39:1, 4.8	61.16	15.86	145.09	38.78
Concentration*pH				
0.00, 3.2	281.63	15.86	431.23	38.78
0.24, 3.2	405.00	15.86	875.07	38.78
0.00, 4.80	78.68	15.86	99.70	38.78
0.24, 4.80	73.42	15.86	319.12	38.78

The most significant and encouraging figures in regards to molecularly imprinted hydrogels when compared to non-imprinted is their larger resistivity magnitude (more than double) for each of the combinations that contained a saturated level of hydrocortisone (0.24 mg/ml) which suggest a greater affinity to their target molecule. This difference is not only in overall magnitude which can be somewhat misleading due to the heterogeneity of the samples but also in the deltas between lower and higher levels. A closer look at this difference is presented in Figure 54 in which the resistivity delta between the high level (0.24 mg/ml) and low level (0.00 mg/ml) of hydrocortisone concentration was calculated for each of the evaluated groups.

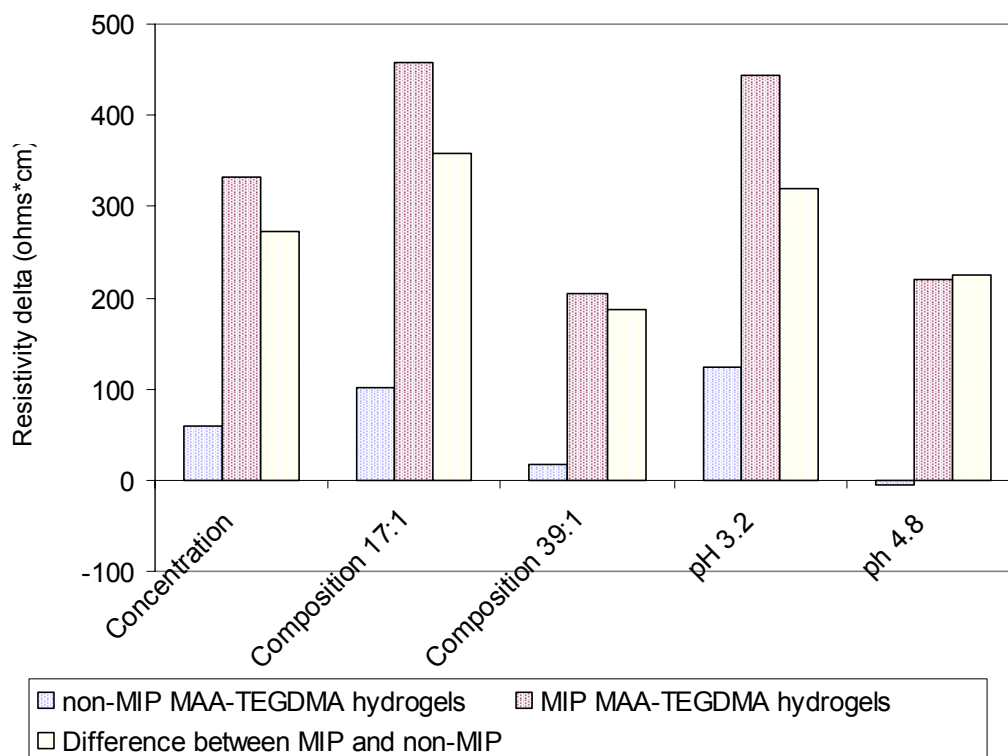


Figure 54: Least squares mean resistivity delta between high level (0.24 mg/ml) and low level (0.0 mg/ml) concentration of hydrocortisone in solution per tested group and level.

5.4 Sensitivity studies of molecularly imprinted MAA-TEGDMA hydrogels

Having obtained a better understanding of how the different studied factors and their levels affect the electrical resistivity of MAA-TEGDMA molecularly imprinted hydrogels a second experiment was developed. The intent for this experiment was to determine the sensitivity of molecularly imprinted hydrogels to concentration of hydrocortisone. For this, a simple experiment was conducted in which the electrical resistivity of non-imprinted and molecularly imprinted hydrogels was estimated at three concentrations levels of hydrocortisone different from saturation. Electrical resistivity estimates were taken at 24 hour intervals to allow the hydrogels to reach equilibrium at each ascendant concentration level. The concentration levels were defined as 0.0, 0.06 and 0.12 mg/ml of hydrocortisone in glutaric acid sodium hydroxide buffer.

Using as input the results obtained from the first stage of experiments it was decided to perform this experiment at the combination of levels identified as optimum earlier in regards to resistivity magnitude levels. The tests were performed using MAA-TEGDMA hydrogels (non-imprinted and molecularly imprinted) with a 17:1 monomer to cross-linker molar ratio, glutaric acid sodium hydroxide buffer at a pH value of 3.2 and the concentration levels of hydrocortisone specified earlier. Finally, it was decided to also use the same frequency sweep approach from those of the electrical characterization studies to avoid discarding any effect frequency may had in the response. As in the previous experiment this factor came out to be negligible. As consequence the results are

presented at a fixed frequency value of 2.5 KHz for simplicity and redundancy avoidance.

Another important feature from this test that differed from previous runs was to discard the estimation of the electrical resistance of the buffer solution previous to estimating the resistance for the hydrogels samples. As result of this, performed trials only estimated the electrical resistance of the buffer + hydrogel and offline subtracted the average buffer resistance (10.77 ohms) obtained from the electrical characterization experiment. The reason for this change in the experimental protocol was due to the fact that concentration measurements were being performed in parallel to the electrical estimates. In order to augment the resolution of the concentrations measurements (every 24 hours) it was necessary to reduce the buffer volume the hydrogels were equilibrated in to the minimum, in this case the volume of the diffusion cell of 20 milliliters. Figure 55 presents the 3.2 pH buffer resistance distribution from electrical characterization experiments.

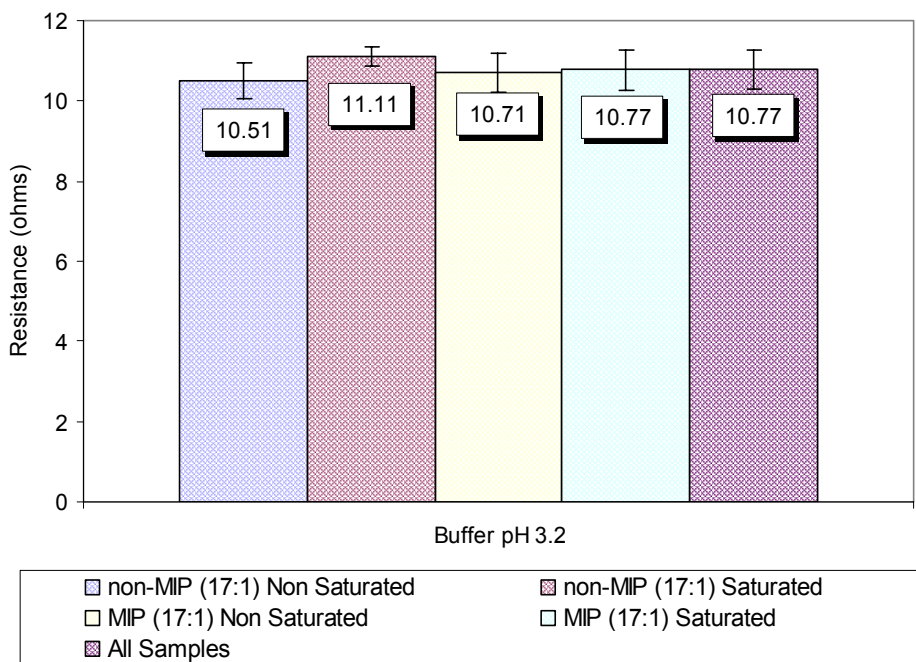


Figure 55: Distribution of estimated resistance of glutaric acid sodium hydroxide buffer at pH 3.2 for all tested combinations of 17:1 hydrogels during first stage of experiments. Bars 1 - 4 from left to right represent the average resistance value for each of the sample (n = 450) while 5th bar is the average of all samples (n = 1800). Error bars represent the mean standard deviation.

Once the electrical estimates were completed as function of hydrocortisone concentration it was possible to observe some patterns in the hydrogels electrical response. The electrical resistivity of the control group (non-imprinted) was non specific to increasing concentration of hydrocortisone concentration. In the case of molecularly imprinted hydrogels mixed results in regards to their electrical response were observed. One of the samples showed a similar response as the one from the non-imprinted group while the other sample showed a significant increase in response as function of increasing hydrocortisone concentration (Figure 56). This deviation in the response of the molecularly imprinted hydrogels

is attributed to their heterogeneity in which there can be a significant difference between available cavities for interaction with the target molecule from sample to sample.

A closer inspection to the obtained responses is presented in Figure 57 in which the more specific response from the non-imprinted and molecularly imprinted groups are compared. In order to compare the actual sensitivities of the samples to the concentration of hydrocortisone the responses are presented in terms of a delta resistivity value. This electrical resistivity delta was defined as:

$$\rho_n = \rho_n - \rho_0 \quad (14)$$

Where

ρ_n = resistivity at concentration C_n

ρ_0 = resistivity at baseline concentration C_0 of 0.0 mg/ml

for $n = 0 \dots k$

This delta allowed the comparison of both responses with a common starting point which clearly shows the greater sensitivity value obtained from the best response of a molecularly imprinted hydrogels versus the best response obtained from the non-imprinted group as function of increasing hydrocortisone concentration.

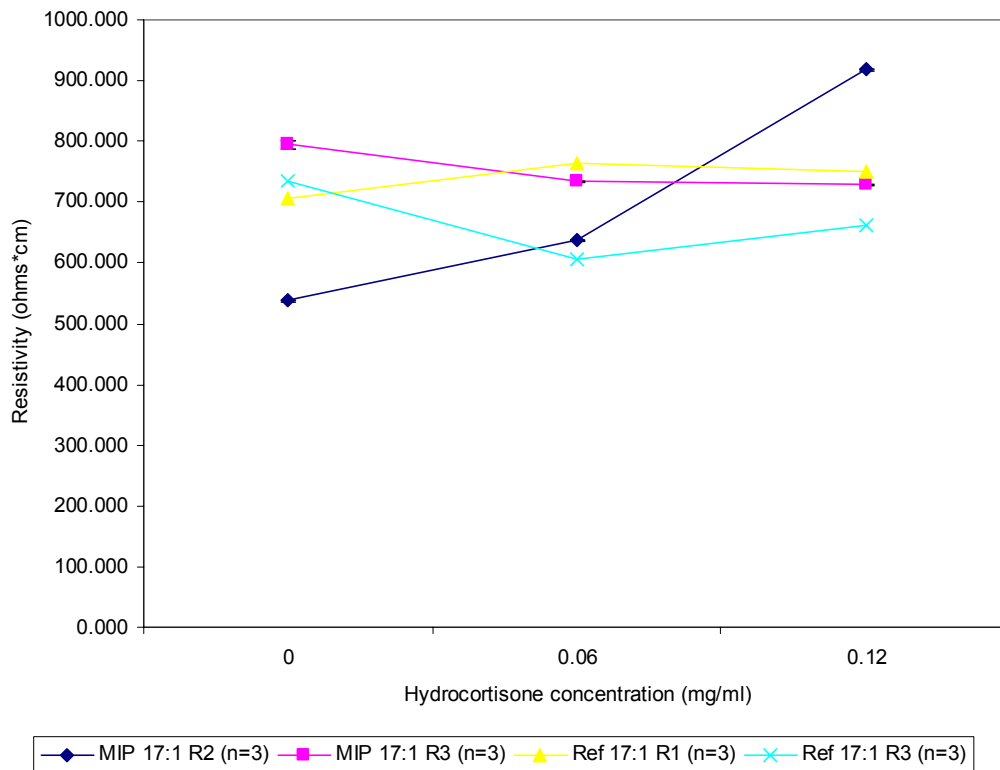


Figure 56: Estimated electrical resistivity for MAA-TEGDMA (17:1 molar ratio) non-imprinted and molecularly imprinted as function of hydrocortisone concentration. Data points represent mean value for each replicate (n = 3) at an excitation signal frequency of 2.5 KHz in a glutaric acid sodium hydroxide buffer pH 3.2.

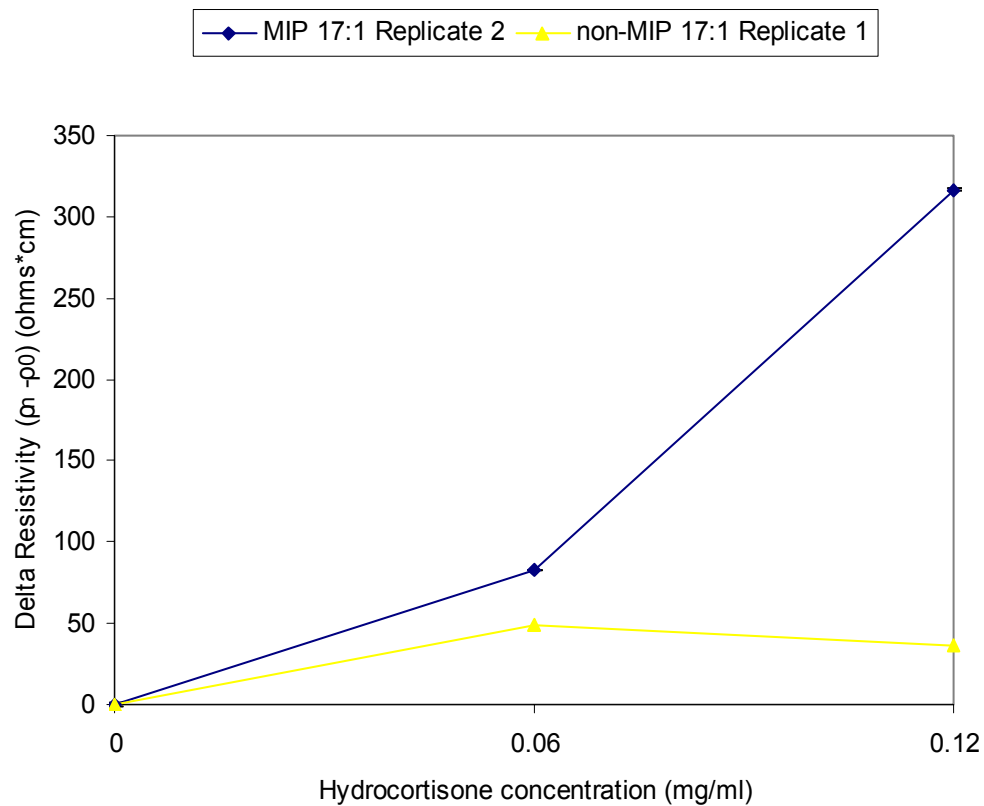


Figure 57: Evaluation of change in electrical resistivity of MAA-TEGDMA (17:1 molar ratio) non-imprinted and molecularly imprinted as function of hydrocortisone concentration. Delta values were calculated as the difference in electrical resistivity at each concentration value and the baseline value of resistivity $C_0 = 0$ mg/ml. Data points represent mean value ($n = 3$) at an excitation signal frequency of 2.5 KHz in a glutaric acid sodium hydroxide buffer pH 3.2.

5.5 Selectivity studies of molecularly imprinted MAA-TEGDMA hydrogels

A final experiment was performed in order to study the selectivity of molecularly imprinted hydrogels with hydrocortisone to an analog molecule. Initial trials were attempted by using Estradiol but due to its extreme low solubility it was not possible to conduct the experiments with this molecule at the required concentration levels (0.0, 0.06 and 0.12 mg/ml). Instead a second trial was performed with Fluorescein sodium salt and on this attempt it was possible to dilute in solution at the required concentrations. Besides the use of Fluorescein sodium salt instead of hydrocortisone all remaining system parameters remained fixed in comparison to the sensitivity experiments. These parameters were: (a) glutaric acid sodium hydroxide buffer pH 3.2, (b) concentration in solution of 0.0, 0.06 and 0.12 mg/ml, and (c) molecularly imprinted MAA-TEGDMA (17:1) hydrogels,

As in the sensitivity experiments the electrical estimates were performed for the buffer + hydrogel combination only and offline the mean buffer resistance value from electrical characterization experiments was subtracted (10.77 ohms). Figure 58 presents the estimated resistivity as function of fluorescein sodium salt. Both tested samples showed a negative correlation between electrical resistivity and Fluorescein sodium salt concentration, in contrast with the previously seen positive correlation with hydrocortisone in solution. Figure 59 shows the resistivity delta of the tested samples using the same approach as before of a common baseline resistivity value between samples to identify the greater rate in response as function of increasing concentration.

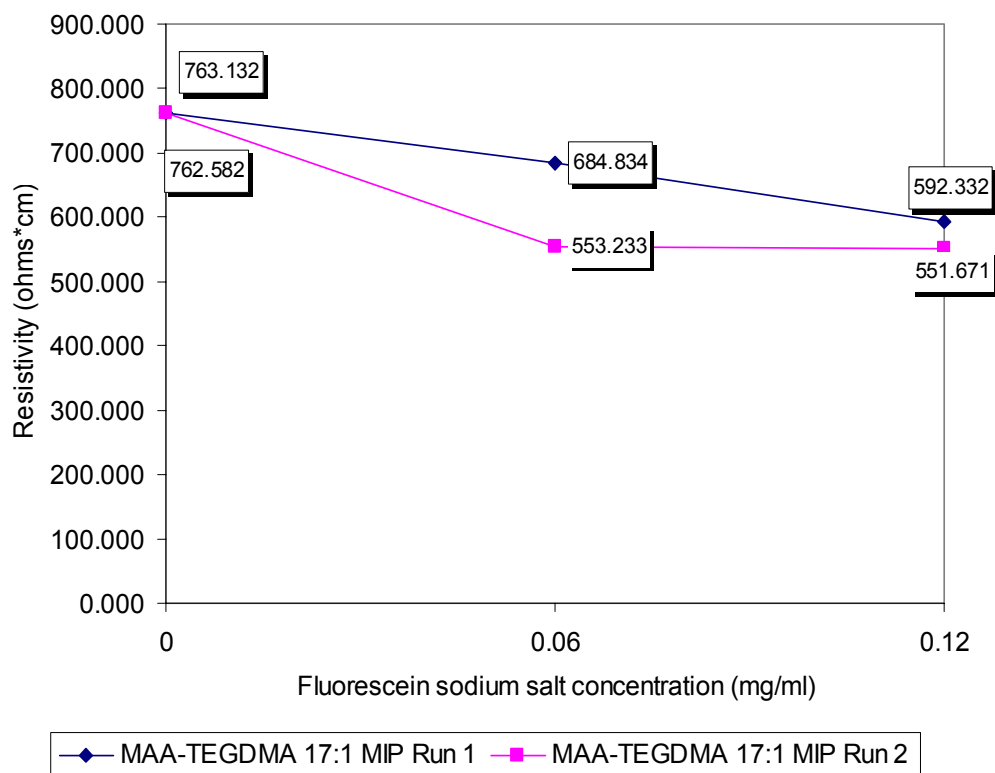


Figure 58: Estimated electrical resistivity for MAA-TEGDMA (17:1) molecularly imprinted with hydrocortisone as function of Fluorescein Sodium Salt concentration. Data points represent mean value for each replicate (n = 3) at an excitation signal frequency of 2.5 KHz in a glutaric acid sodium hydroxide buffer pH 3.2.

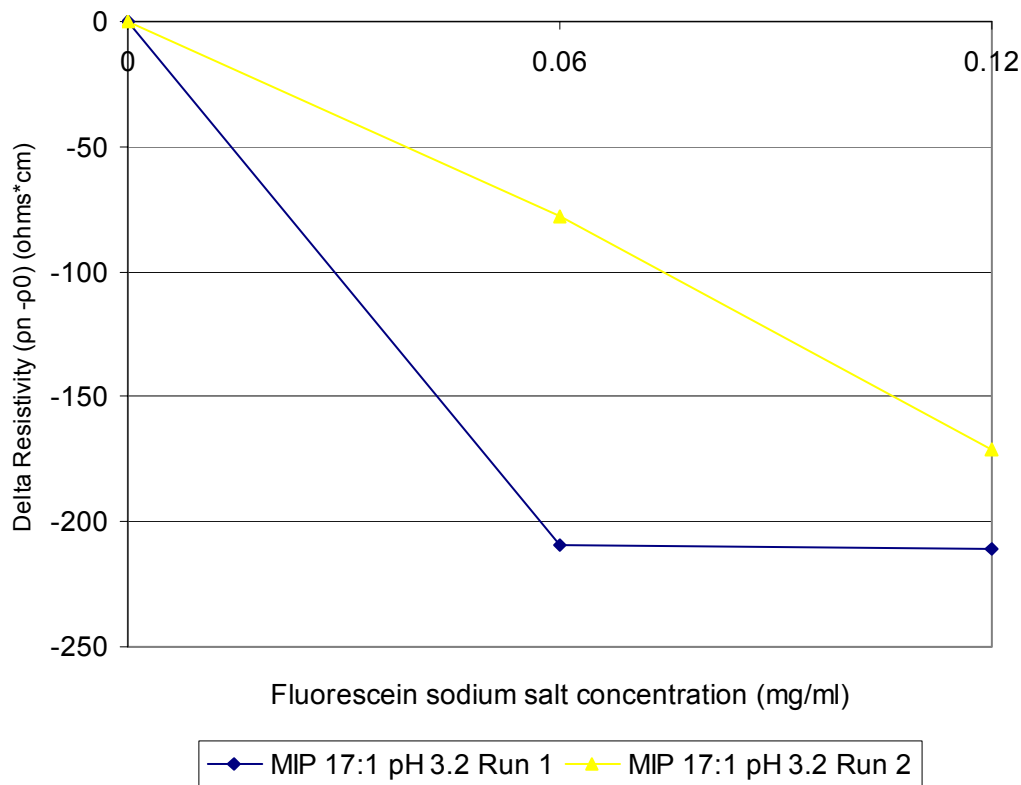


Figure 59: Evaluation of change in electrical resistivity of MAA-TEGDMA (17:1) molecularly imprinted with Hydrocortisone as function of Fluorescein Sodium Salt concentration. Delta values were calculated as the difference in electrical resistivity at each concentration value and the baseline value of resistivity at $C_0 = 0$ mg/ml. Data points represent mean value ($n = 3$) at an excitation signal frequency of 2.5 KHz in a glutaric acid sodium hydroxide buffer pH 3.2.

Finally, a comparison of the tested responses of the molecularly imprinted hydrogels with the greater rate of change in resistivity for solutions at different concentrations of hydrocortisone and fluorescein sodium salt is presented in Figure 60. Taking the magnitude of the mean delta resistivity responses the results suggest a favorable selectivity of molecularly imprinted hydrogels with hydrocortisone at higher concentration values (0.12 mg/ml), where at a lower

concentration (0.06 mg/ml) this was not the case as the absolute rate of change in response for the hydrocortisone and fluorescein sodium salt were almost identical.

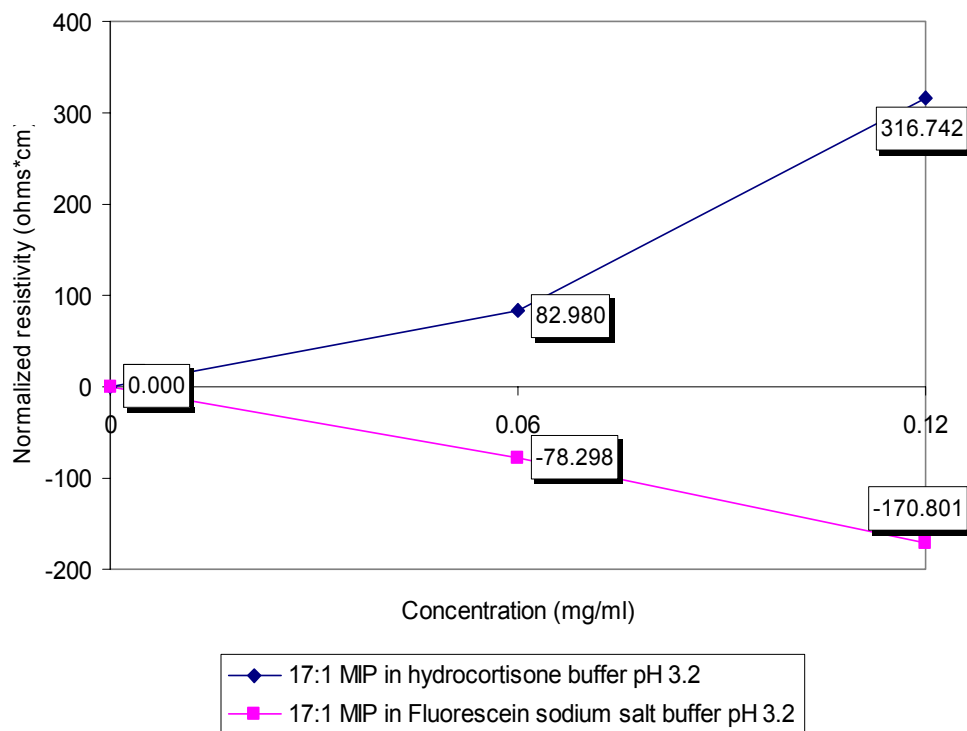


Figure 60: Evaluation of change in electrical resistivity of MAA-TEGDMA (17:1) molecularly imprinted with hydrocortisone as function of Hydrocortisone and Fluorescein Sodium Salt concentration. Delta values were calculated as the difference in electrical resistivity at each concentration value and the baseline value of resistivity at $C_0 = 0$ mg/ml. Data points represent mean value ($n = 3$) at an excitation signal frequency of 2.5 KHz in a glutaric acid sodium hydroxide buffer pH 3.2.

5.6 Swelling and electrical resistivity correlation of MAA-TEGDMA hydrogels

The electrical resistivity of MAA-TEGDMA hydrogels (non-imprinted and molecularly imprinted) has been shown to be affected by factors such as their composition and pH as discussed in previous sections. In order to get a better insight on how the composition and pH affect the electrical resistivity of hydrogels a correlation analysis was performed to validate the apparent dependency between these variables. The correlation analysis was performed between the

electrical resistivity of hydrogels and their swelling ratio, which is a function of composition and pH. The factors and levels used for this analysis are the same as the ones used for the electrical characterization experiments. They are defined as: (a) two MAA-TEGDMA hydrogel variants (non-imprinted and molecularly imprinted), (b) two molar ratios of monomer to cross-linker (17:1 and 39:1) and (c) three pH buffer values (3.2, 4.8 and 5.4). Figures 61 and 62 presents the resistivity and swelling responses as function of pH for all the combinations studied. It can be seen that there is an apparent negative correlation between the resistivity and swelling of hydrogels as function of increasing pH.

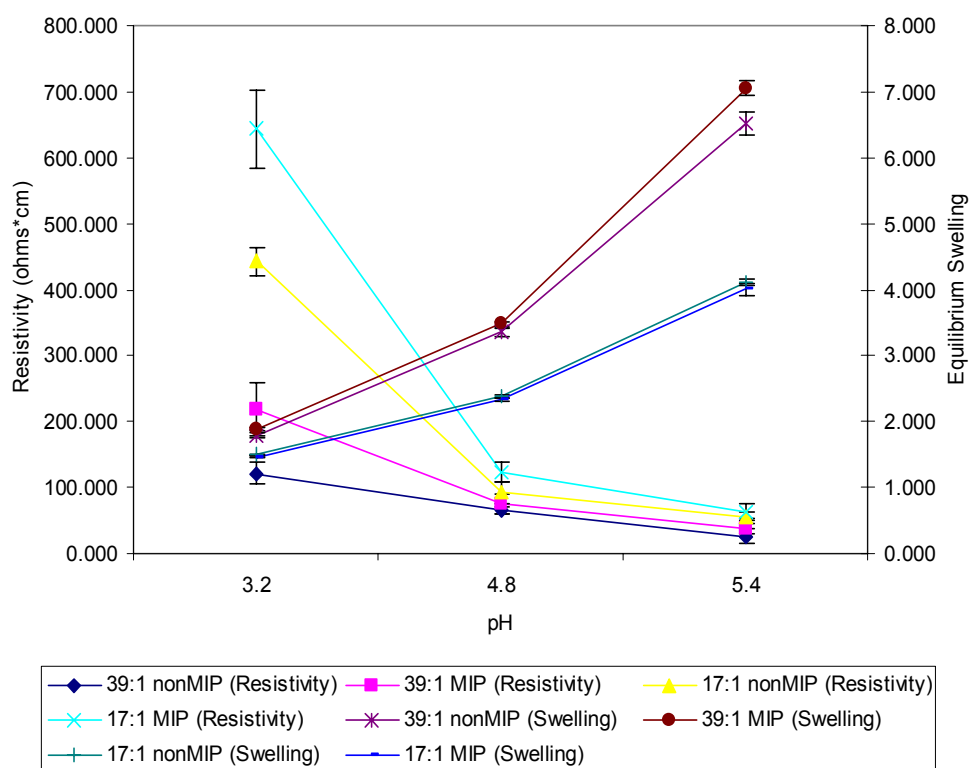


Figure 61: Estimated resistivity and equilibrium swelling [45] of MAA-TEGDMA non-imprinted and imprinted with hydrocortisone as function of glutaric acid sodium hydroxide buffer pH value. Resistivity data points represent the average value from 3 replicates (n = 450) while swelling value represent the average value from 3 replicates. Errors bars represent the mean standard deviation.

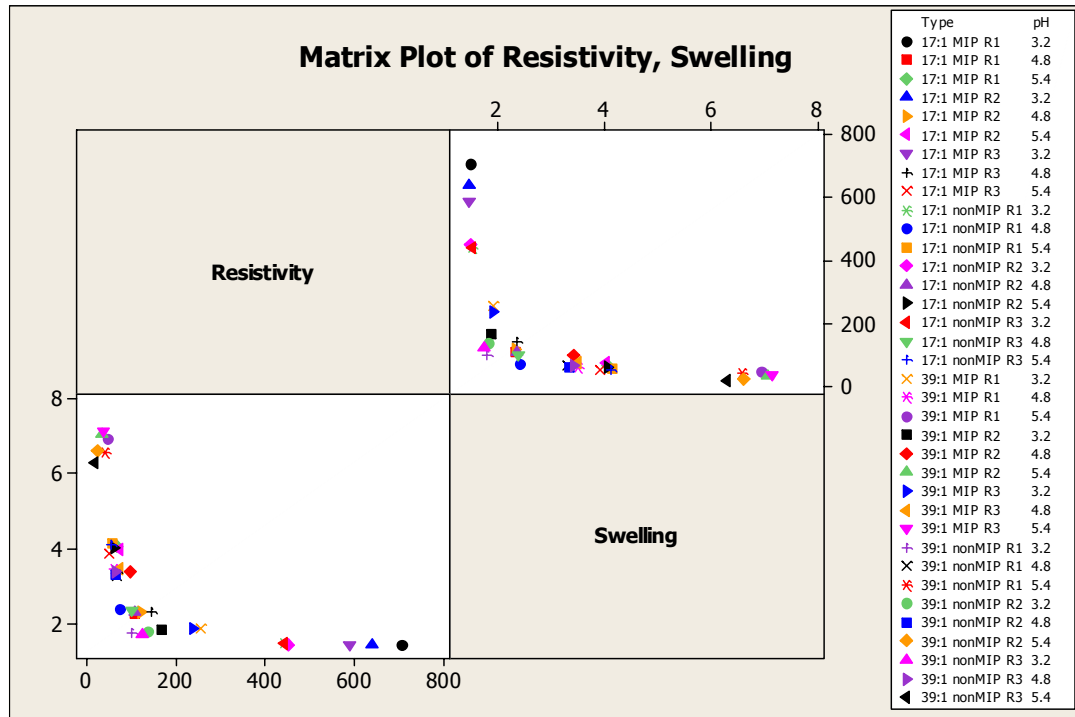


Figure 62: Scatter plot of electrical resistivity and swelling of reference and molecularly imprinted MAA-TEGDMA (17:1 and 39:1 molar ratio) hydrogels at three different glutaric acid sodium hydroxide buffer pH values (3.2, 4.8 and 5.4). Electrical resistivity data points correspond to average of 3 samples taken at an input signal frequency of 2.5 KHz for each replicate.

A correlation analysis was performed in Minitab between the electrical resistivity and swelling of MAA-TEGDMA hydrogels (non-imprinted and molecularly imprinted) by pH levels. Three Pearson correlation coefficients were obtained from this analysis (Table 15) that confirmed the hypothesis of a strong negative correlation (< -0.65) between these variables under the same operating conditions. Figure 63 shows a scatter plot of MAA-TEGDMA hydrogels electrical resistivity and swelling grouped by solution pH.

Table 15: Pearson correlation coefficients – electrical resistivity and swelling of MAA-TEGDMA hydrogels (non-imprinted and molecularly imprinted) by pH levels.

pH	Pearson correlation coefficient	P-Value
3.2	-0.869	0.000
4.8	-0.742	0.006
5.4	-0.774	0.003

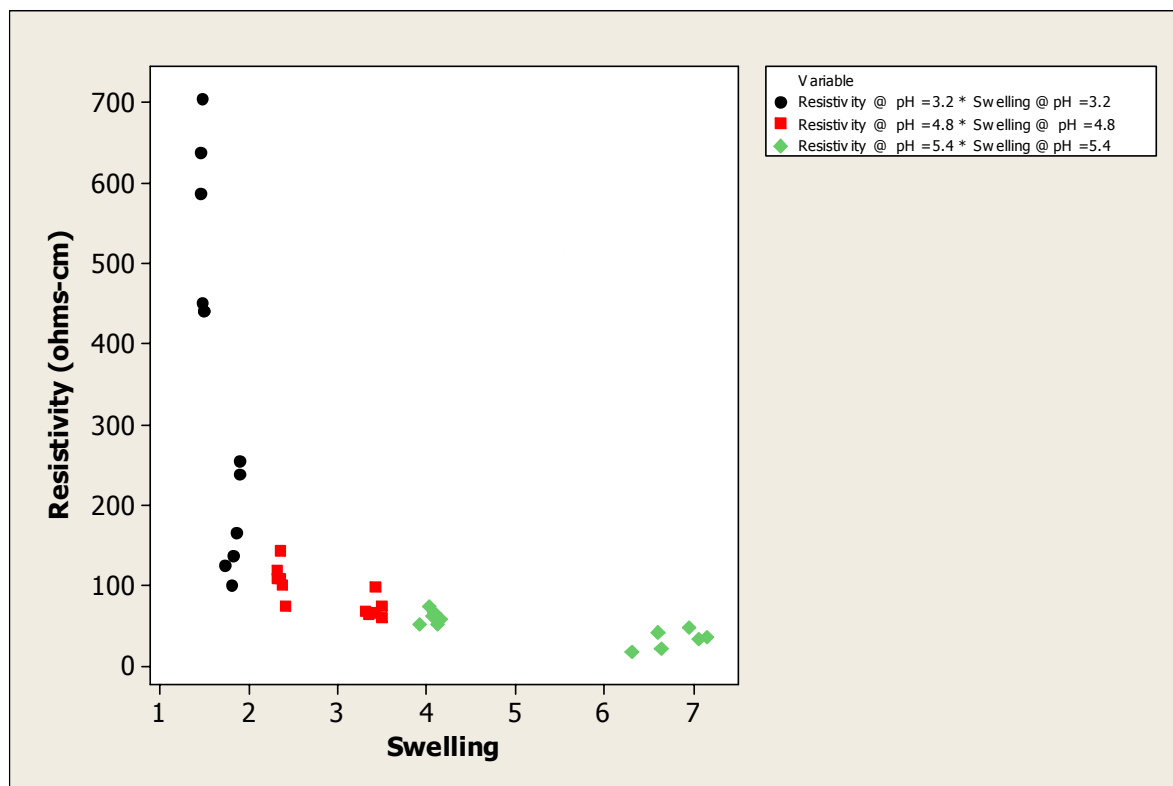


Figure 63: Scatter plot of MAA-TEGDMA hydrogels (non-MIP and MIP) resistivity versus swelling grouped by pH.

6. Conclusions

It was possible to characterize electrically the response of crosslinked methacrylic acid hydrogels as function of their monomer to crosslinker molar ratio, solution pH, concentration of hydrocortisone and signal frequency using a conductometric transduction principle. A factorial experimental design was the basis for this characterization. The output from this study suggests that pH, hydrogel composition, concentration of hydrocortisone and two way interactions between them were significant in the electrical response of non-molecularly imprinted and molecularly imprinted hydrogels. From these factors, pH came out to be the most significant and at the lowest tested levels of 3.2 and 4.8 it was possible to observe the largest responses in magnitude and rate of change between levels. Hydrocortisone concentration had a greater effect on molecularly imprinted hydrogels to that of the control group which suggests a greater affinity between the molecularly imprinted hydrogels and their target molecule. Least square means from the performed factorial fit for molecularly imprinted hydrogels in average were significantly greater to that of non-MIP hydrogels under the same operating conditions. Molecularly imprinted hydrogels also exhibited a greater standard error for all combinations studied when compared to the control group. This is attributed to their heterogeneous nature which at the lower levels of crosslinker studied can be further accentuated. Sensitivity and selectivity studies were conducted with favorable outcomes at intermediate concentrations (0.12 mg/ml) levels of hydrocortisone. Further tests can be performed in the future with multiple analog molecules combined with additional chemical tests (concentration

changes, permeability, etc.) in order to have a more complete picture of the system response as well as tests as function of time. Also, it should be interesting to study the outcome of a similar system design to interact with a different molecule that can be diluted in greater quantities in water than hydrocortisone. The low solubility of hydrocortisone resulted in a great challenge in this work and may have limited the possibilities for further interaction with the molecularly imprinted hydrogels. Finally, this work presents a general methodology which can be followed with any other synthetic molecule different from hydrocortisone to study and try to optimize the electrical response of the system.

7. References

- [1] Moore, J, **Biomedical Technology and Devices Handbook** (2003)
- [2] Webster, G. John - **Medical Instrumentation Application and Design**, Third Edition
- [3] Piletsky, Sergey and Turner, Anthony - **Electrochemical Sensors Based on Molecularly Imprinted Polymers**, *Electroanalysis* 2002, Vol.14 No. 5
- [4] Society for Molecular Imprinting - <http://www.smi.tu-berlin.de/story/MIT.htm>
- [5] Piletsky, Sergey A.; Alcock, Susan and Turner, Anthony - **Molecular Imprinting at the edge of the third millennium**, *TRENDS in Biotechnology* Vol. 19 No.1 January 2001
- [6] <http://en.wikipedia.org/wiki/Cortisol>
- [7] **American Institute of Stress** - <http://www.stress.org>
- [8] McEwen Bruce, Ph.D. - **Protective and Damaging effects of stress mediators**, Seminars in Medicine of the Beth Israel Deaconess Medical Center.
- [9] Johnston, A., **Trends in biosensor research and development**. IEEE, 1988: p. 654-657
- [10] Kriz, Dario and Ansell, J. Richard – **Molecularly Imprinted Polymers, Man-Made Mimics of Antibodies and their applications in analytical chemistry**. P. 418-428
- [11] Shwartz, A., Neufeld, T., Rishpon J. – **Electrochemical biosensors for on-site analysis**. Department of Molecular Microbiology and Biotechnology, Tel-Aviv University, Ramat-Aviv 69978
- [12] Patton, Jese – **Overview of Biosensor Design and Fabrication**, Digene Diagnostics Inc, Silver Spring , MD
- [13] Rolfe, P and Martin, P.J. – **Medical Sensors and biosensors**. *Chemistry in Britain*. Vol. 24, No. 10, 1988
- [14] Spegel, Peter; Schweitz, Leif; Nilsson Staffan – **Molecularly imprinted polymers**. *Bioanal Chem* (2002) 372:37-38.
- [15] Edelman G., Peter and Wang, Joseph – **Biosensors and Chemical Sensors, Optimizing Performance through polymeric materials**. ACS Symposium Series 487 1992, American Chemical Society, Washington DC 1992.
- [16] Peppas, Nicholas; Huang, Yanbin; **Polymers and Gels as Molecular Recognition Agents** - *Pharmaceutical Research*, Vol. 19, No. 5, May 2002
- [17] Wulff, Gunter - **Molecular Imprinting - A way to effective mimics of natural antibodies and enzymes**, Institute of Organic and Macromolecular Chemistry - Dusseldorf, Germany
- [18] Byrne, Mark; Park, Kinam; Peppas, Nicholas – **Molecular imprinting within hydrogels**. *Advanced Drug Delivery Reviews*. Vol. 54, No. 1, p. 149-161, 2002.
- [19] Peppas, Nikolaos A. – **Hydrogels in medicine and pharmacy, Volume I Fundamentals**. *Hydrogels in Med and Pharm*, Purdue Univ, West Lafayette, IN, USA, 1986.

- [20] Konsta, A.A., Daoukaki. D., Pissis. P., Vartzelli. K., **Hydration and conductivity studies of polymer-water interactions in polyacrylamide hydrogels**. *Solid State Ionics* 125 (1999) 235-241.
- [21] Rosiack, M. Janusz - **Radiation Formation of Hydrogels for Biomedical Applications**, Institute of Applied Radiation Chemistry, Technical University of Lodz
- [22] Watanabe Junji, Kiritishi Yoshihiro, Woo Kwang, Ishihara Kazuhiko -**Hydrogels** 790-801 *Encyclopedia of Biomaterials and Biomedical Engineering*.
- [23] Schwartz, M.; H. Guterman, and J. Kost - **Electrical Properties of Glucose-Sensitive Hydrogels: Swelling and Conductivity Relationships**. *J. Biomed. Mater. Res*, 1998. 41: p. 65-70.
- [24] Seon Jeong Kim, C.K.L., Young Moo Lee, In Young Kim, Sun I. Kim, **Electrical/pH-Sensitive swelling behavior of polyelectrolyte hydrogels prepared with hyaluronic acid-poly(vinyl alcohol) interpenetrating polymer networks**. Elsevier Science B.V., 2003.
- [25] Andrea Richter, D.K., Steffen Howitz, Thomas Gehring and Karl-Friedrich Arndt **Electronically Controllable Microvalves Based on Smart Hydrogels: Magnitude and Potential Applications**. *Microelectromechanical Systems*, 2003. 12(5): p. October 2003.
- [26] Michael J. Bassetti, J.S.M., David J. Beebe - **Development of electrically triggered hydrogels for microfluid application**. *Annual International IEEE-EMBS Special Topic Conference on Microtechnologies in Medicine & Biology*. 2002. Madison, Wisconsin.
- [27] Sheppard, Norman; Salehi, Samira; Tucker, Robert - **Design of a conductometric microsensor based on pH sensitive polymer hydrogels**. Annual International Conference of the IEEE Engineering in Medicine and Biology Society. 1991.
- [28] Sheppard, N.F. - **Design of a conductometric microsensor based on reversibly swelling polymer hydrogels**. IEEE, 1991: p. 773-776.
- [29] Chatterjee, Aveek N. ; Yu, Qing; Moore, J.S. ; Aluru, N.R. – **Mathematical modeling and simulation of dissolvable hydrogels**. *Journal of Aerospace Engineering*, Vol. 16, No. 2, p. 57-64, 2003.
- [30] Peppas, Nikolaos A. – **Hydrogels in medicine and pharmacy, Volume III Properties and Applications**. Hydrogels in Med and Pharm, Purdue Univ, West Lafayette, IN, USA,
- [31] Ku, Chen C. – **Electrical properties of polymers: chemical principles**. Hanser Publishers, 1987
- [32] Vacik J. and Kopecek J. - **Specific Resistances of Hydrophilic Membranes Containing Ionogenic Groups**, *Applied Polymer Science* 19, p. 3029-3044 (1975)
- [33] Vacik et al. - **The Effect of pH and Temperature on the Electrical Conductivity of Membranes Made of Methacrylic Acid Copolymers**, *Coll. Czech. Chem. Comm.* 48, p. 3071-3078 (1983)
- [34] Pissis, P., Kyritsis, A., Shilov, V.V. – **Molecular mobility and protonic conductivity in polymers; hydrogels and ionomers**. *Solid States Ionics* 125 (1999) 203-212
- [35] Lesho, Matthew J., Sheppard, Norman F. – **A method for studying swelling kinetics based on measurement of electrical conductivity**. *Polymer Gels and Networks* 5 (1997) 503-523.
- [36] Pissis, P. ; Kyritsis, A. - **Electrical Conductivity Studies in hydrogels**. *Solid State Ionics* 97 (1997) p. 105-113

- [37] Gu, W.Y. and Justiz, M.A. – **Apparatus for measuring the swelling dependent electrical conductivity of charged hydrated soft tissues**, Journal of Biomechanical Engineering, Vol. 124, p. 790-793, 2002
- [38] Sheppard Norman, Tucker Robert, Salehi-Had Samira - **Electrical conductivity of pH sensitive hydrogels**. Polymeric Materials Science and Engineering, Proceedings of the ACS Division of Polymeric Materials Science and Engineering, Vol. 66, p. 226-227, 1992
- [39] Karube, I, Piletsky, S.A, Piletskaya, E.V., Elgersma, A.V. - **Atrazine Sensing by Molecularly Imprinted Membranes. Biosensors & Bioelectronics**, 1995. 10: p. 959-964
- [40] T. A. Sergeyeva, a.S.A.P., a A. A. Brovko,b E. A. Slinchenko,b L. M. Sergeeva,b and T.L.P.a.A.V. El'skayaa, **Conductometric sensor for atrazine detection based on molecularly imprinted polymer membranes**. The Analyst, 1999: p. 331-334.
- [41] Kriz, Dario; Kempe, Maria; Mosbach, Claus – **Introduction of molecularly imprinted polymers as recognition elements in conductometric chemical sensors**. Sensors and Actuators B 33 (1996) 178-181
- [42] Montgomery, Douglas C. - **Design and Analysis of Experiments**, 5th Edition
- [43] Simion, A; Mistrianu, M.; Manoiu, A. and Vaireanu D.I. - **The Evaluation of a Silver/Silver Chloride Electrode Stability**, Faculty of Industrial Chemistry , University Politehnica of Bucharest
- [44] Analog Devices – **AD620 data sheet**
- [45] Padro, Lorena – **Into the rational design of molecularly imprinted polymers**, Ph.D. Thesis Dissertation (In progress), University of Puerto Rico – Mayagüez

8. Appendix

Table A1: Factors and levels used in analysis of variance of reference MAA-TEGDMA hydrogels resistivity.

Factor	Type	Levels	Values
Composition	Fixed	2	17:1, 39:1 (molar ratio)
Concentration	Fixed	2	0.0, 0.24 (mg/ml)
pH	fixed	2	3.2,4.8

Table A2: Factorial Fit: non-MIP Hydrogels Resistivity versus Composition, Concentration and pH. Eight combinations 3 replicates (each replicate is the average of 150 samples). Estimated Effects and Coefficients for Hydrogels Resistivity (ohms*cm) (coded units)

Term	Effect	Coef	SE Coef	T	P
Constant		209.7	7.930	26.44	0.000
Composition (molar ratio)	-216.3	-108.2	7.930	-13.64	0.000
Concentration (mg/ml)	59.1	29.5	7.930	3.72	0.002
pH	-267.3	-133.6	7.930	-16.85	0.000
Composition (molar ratio)* Concentration (mg/ml)	-42.0	-21.0	7.930	-2.65	0.017
Composition (molar ratio)*pH	186.5	93.3	7.930	11.76	0.000
Concentration (mg/ml)*pH	-64.3	-32.2	7.930	-4.06	0.001

S = 38.8483 R-Sq = 97.43% R-Sq(adj) = 96.53%

Table A3: Analysis of Variance for non-MIP Hydrogels Resistivity (ohms*cm) (coded units)

Source	DF	Seq SS	Adj SS	Adj MS	F	P
Main Effects	3	730274	730274	243425	161.29	0.000
2-Way Interactions	3	244173	244173	81391	53.93	0.000
Residual Error	17	25656	25656	1509		
Lack of Fit	1	9144	9144	9144	8.86	0.009
Pure Error	16	16512	16512	1032		
Total	23	1000103				

Table A4: Estimated Coefficients for Hydrogels Resistivity (ohms*cm) using data in uncoded units.

Term	Coefficient
Constant	2096.45
Composition (molar ratio)	-50.3185
Concentration (mg/ml)	2031.33
pH	-423.608
Composition (molar ratio)* Concentration (mg/ml)	-15.9060
Composition (molar ratio)*pH	10.5987
Concentration (mg/ml)*pH	-334.970

Table A5: Factorial Fit: MIP Hydrogels Resistivity versus Composition, Concentration and pH. Eight combinations 3 replicates (each replicate is the average of 150 samples). Estimated Effects and Coefficients for Resistivity (ohms*cm) (coded units)

Term	Effect	Coef	SE Coef	T	P
Constant		431.3	19.39	22.24	0.000
Composition (molar ratio)	-363.6	-181.8	19.39	-9.38	0.000
Concentration (mg/ml)	331.6	165.8	19.39	8.55	0.000
pH	-443.7	-221.9	19.39	-11.44	0.000
Composition (molar ratio)* Concentration (mg/ml)	-126.9	-63.4	19.39	-3.27	0.004
Composition (molar ratio)*pH	235.0	117.5	19.39	6.06	0.000
Concentration (mg/ml)*pH	-112.2	-56.1	19.39	-2.89	0.010

S = 94.9943 R-Sq = 95.34% R-Sq(adj) = 93.69%

Table A6: Analysis of Variance for MIP Hydrogels Resistivity (ohms*cm) (coded units)

Source	DF	Seq SS	Adj SS	Adj MS	F	P
Main Effects	3	2634612	2634612	878204	97.32	0.000
2-Way Interactions	3	503443	503443	167814	18.60	0.000
Residual Error	17	153407	153407	9024		
Lack of Fit	1	12529	12529	12529	1.42	0.250
Pure Error	16	140878	140878	8805		
Total	23	3291461				

Table A7: Estimated Coefficients for Resistivity (ohms*cm) using data in uncoded units (MIP's)

Term	Coefficient
Constant	2890.95
Composition (molar ratio)	-64.1664
Concentration (mg/ml)	5065.21
pH	-581.046
Composition (molar ratio)* Concentration (mg/ml)	-48.0594
Composition (molar ratio)*pH	13.3514
Concentration (mg/ml)*pH	-584.438